ACOUSTIC-STRUCTURE INTERACTION FOR FLOATING STRUCTURE UNDER MOVING LOAD

Thesis submitted to
Cochin University of Science and Technology, Kochi
for the award of the degree

of

Doctor of Philosophy

by

Cdr. Nitin Agarwala

under the guidance of

Dr. E. M. Somashekharan Nair

Department of Ship Technology
Cochin University of Science and Technology, Kochi

March 2013

Dedicated

to

My Family

Declaration

I certify that

a. the work contained in this thesis is original and has been done by me under the guidance of my supervisor.

b. the work has not been submitted to any other Institute for any degree or diploma.

c. I have followed the guidelines provided by the University in preparing the thesis.

d. I have conformed to the norms and guidelines given in the Ethical Code of Conduct of the University.

e. whenever I have used materials (data, theoretical analysis, figures, and text) from other sources, I have given due credit to them by citing them in the text of the thesis and giving their details in the references. Further, I have taken permission from the copyright owners of the sources, whenever necessary.

Nitin Agarwala

Department of Ship Technology
Cochin University of Science and Technology
Kochi, India 682 022.

Certificate

This is to certify that the thesis titled **"Acoustic-Structure Interaction for Floating Structure under Moving Load"**, submitted by Cdr. Nitin Agarwala to Cochin University of Science and Technology, Kochi, is a record of bona fide research work under my supervision and is worthy of consideration for the award of the degree of Doctor of Philosophy of the University.

CUSAT, Kochi
March, 2013

Dr. E. M. Somashekharan Nair
Professor (Retd.)
Department of Ship Technology
Cochin University of Science and Technology
India 682 022.

Acknowledgment

Although the completion of a Ph.D is looked upon as an individual accomplishment, it is rarely achieved without the help of many people. The research presented in this thesis is no exception. I would like to express my gratitude to the following people for support and guidance through the process of researching for and writing this thesis:

- Dr. E. M. Somashekharan Nair, my advisor, for making his time and experience available to me, inspiring me and for the ample freedom he allowed me in conducting my research;
- Dr. C. G. Nandakumar, for serving on my committee, supporting me with the correct direction and good literature for this research;
- Dr. K. P. Narayanan, for serving on my committee, and encouraging me to think thoroughly;
- Cdr. P. K. Satheesh Babu, for paving the way for successful completion of my research by giving me adequate time and opportunity and for all the supportive encouragement;
- The Indian Navy, for having given me the time, opportunity and the requisite approvals for pursuing this research;
- Dr. T. Sahoo, of Indian Institute of Technology, Kharagpur, for being my mentor, for being the guiding light for my research and helping me out both morally and technically especially when it mattered most;
- My beloved wife, Indu, for her love, encouragement and understanding. For giving me a free hand at home to do whatever and whenever I wanted to do for my research. For partnering me in all aspects of life and making this work fun and meaningful. Her constant confidence in me helped me push forward and overcome the obstacles and challenges which presented themselves;
- Pratham and Garima, my children, for their smiles and hugs and for being the stress busters of the frustrations due to the blockades in the work;

- My parents, for having faith in me, inspiring me to take up the research, encouraging my curiosity and to "carry on regardless" of the ups and downs during the course of the study;
- My inlaws for their selfless support, blessing and encouragement;
- Finally, I would like to thank GOD, for His great and magnificent creation and giving us a Universe governed by laws, and for providing us with the tools that allow us to discover and learn about them.

Nitin Agarwala

List of Symbols

α_0	Fluid loading factor
$\bar{E}$	Complex Young's Modulus
$\bar{G}$	Complex Shear Modulus
$\bar{I}$	Time averaged sound intensity
$\bar{M}$	Modified Mach number in presence of mean flow
$\dot{U}_s^*(\xi, t)$	Beam surface velocity of conjugation
η	Loss factor or Damping factor
γ	Wavenumber ratio
κ^2	Cross sectional shape factor or the shear correction factor
ν	Poisson's ratio
ω	Angular frequency
Π	Acoustic power radiated per unit width
π	constant, $\pi = 3.14159265....$
ρ_0	Mass density of acoustic structural material
ρ_v	Mass density of material

$\tilde{F}(\xi, t)$ Force function in the wavenumber domain

$\tilde{P}(\xi, y, t)$ Pressure function in the wavenumber domain

$\tilde{U}_s(\xi, t)$ Response (Transverse displacement) function in the wavenumber domain

ξ Wavenumber variable

ζ Non-dimensional wavenumber variable

C_0 Sound speed in the acoustic medium

C_L Longitudinal wave speed

D Non-dimensional variable

D_s Flexural rigidity

E Young's Modulus

$F(\zeta)$ Non-dimensional strength of external force

f_0 Total force strength per unit width

G Shear Modulus

g Acceleration due to gravity , $g = 9.80663\ m/s^2$ (average)

h Height of the structure (beam or plate)

$H(x)$ Heavyside step function

I Second Moment of Inertia

j Unit imaginary number, $j = \sqrt{-1}$

K_0L Acoustic length

K_0 Acoustic wavenumber

K_B Free bending wavenumber

M Mach number

$p(x, y = 0, t)$ Acoustic pressure acting on surface

Q Compressive inplane load

T Tensile inplane load

U Speed of mean flow of the fluid

$u(x, t)$ Transverse displacement of the structure (Beam or Plate)

$U_s(\xi)$ Transverse displacement of structure (Beam or plate) in wave number domain

$U_s(\zeta)$ Non-dimensional transverse displacement of structure (Beam or Plate)

V Subsonic velocity of moving load

W Non-dimensional power per unit width

Z_a Acoustic impedance operator

Z_F Impedance parameter

Z_m Structure (beam or plate) impedance operator

Parameter Values

Parameter	Value	Unit
For Steel		
E	20×10^{10}	N/m^2
ρ_v	7800	kg/m^3
D_s	560	KNm
For Aluminium		
E	7.1×10^{10}	N/m^2
ρ_v	2700	kg/m^3
D_s	237	KNm
Common to all		
h	2.54×10^{-2}	m
ν	0.3	
κ^2	0.85	
C_0	1481	m/s
ρ_0	1000	kg/m^3
Q	Between 5 and 200	MN
T	Between 5 and 200	MN
U	Between -10 and 10	m/s
K_0h	0.05	
K_0L	0.1, π or 2π	
γ	Between 0 and 2.2	

f_0	Unit magnitude

Abstract

A ship at sea responds to the relative force between the surface forces applied and the motion of the fluid it is traveling in. The response (seen as vibration) gets converted to sound if the structure imparts kinetic energy (in the form of pressure waves) to the surrounding fluid. These propagating pressure waves are audible if their speed is greater than the speed of sound. A similar analogy exists for a landing / taking off of an airplane from a floating airport wherein the landing / taking off airplane acts as a moving force. This moving force causes the floating airport to respond and produce sound which gets transmitted to the water below. ***The present study concentrates largely on sound radiation from floating structure due to moving load.***

Accordingly the study is divided into two parts. One valid for a ***ship*** *(by considering a classical beam theory) and the other for a* ***floating airport*** *(by considering a Timoshenko-Mindlin plate theory). First, a generalised expression for the total sound power due to a moving load on a ship is formulated for various beam types by taking a Fourier transform of the governing equation and then non-dimensionalising to get the total sound power. The procedure employed is similar to that demonstrated by Keltie and Peng (1988) for a Timoshenko beam subjected to a moving harmonic force. This understanding is then extended to model a floating airport by assuming that the runway behaves as a simple, infinitely long beam floating on water and supported by buoyancy. To make the calculation procedure user friendly, generic and to speed up the user's work, a* ***Graphical User Interface*** *has been developed for undertaking the analysis. Herein the effect of structural damping on sound power is analysed for a ship while the effect of*

mean flow and inplane loading on sound power is considered for a floating airport.

For an elastic structure such as a floating airport subjected to a landing / taking off load of an airplane ***dynamic analysis*** *has its importance because a floating runway is flexible and receives buoyant support from the water. This makes the runway to deflect due to it's weight and hence will form a dish-like "dent" around the aircraft when the aircraft is static. However this dent moves and progresses like a wave down the runway when the airplane takes off. This moving dent in return causes an increased drag on the aircraft resulting into increased time, distance of take-off and fuel thus leading to increased operating cost. The designer is thus required to address the transient dynamics problem due to the impulsive and moving loads excited by the landing / taking off of an airplane on these structures which has been additionally studied. In developing an expression for this study, a Fourier transformation in space for the whole structure in wavenumber domain is utilised rather than using the wave propagation method to reduce the analysis to a substructure. The procedure employed is similar to that demonstrated by Cray (1994) for stiffened plates and Cheng (1999) and Cheng* et al. *(2000, 2001) for calculating the transverse response and acoustic radiation of a periodically supported beam. The advantage of expressing the response in terms of a wavenumber arises from the fact that the periodic boundary conditions and the phase relation between two adjacent substructures will not be required to be used.*

Other areas where the ***sound radiation from structure*** *has relevance are that of floating ladder tracks, airplane landing on ice, sound radiation from tyres and transportation structures to name a few.*

Contents

List of Figures

List of Tables

Chapter 1

General Introduction

1.1 Preamble

Sound is present all around us in different forms. We experience some form of sound right from the moment we get up to the time we go off to sleep. We continue to experience sound even when asleep. What is remarkable of this form of energy is that we cannot protect ourselves from it naturally. If we do not wish to see a thing, we can close our eyes as we do so while sleeping, but we cannot do the same with sound as we continue to hear it even without being aware of it. Nature has given our visual capabilities limitations, wherein we cannot see something behind us but we can surely hear it. Sound *happens* because of quickly varying pressure wave within a medium due to a vibrating structure or an unsteady aerodynamic flow. The sound so produced may or may not be audible. Noise, on the other hand is the unwanted and undesirable product of this radiated sound.

A ship at sea or an aircraft in flight responds to the surface forces applied by the relative motion of the fluid they are traveling in. This response is in the form of vibration which can get converted to sound if the structure can impart kinetic energy to the surrounding fluid as pressure waves. These propagating pressure waves are audible as sound if their speed is greater than the speed of sound. Similarly, structures such as a floating airport,

a bridge, guideway, overhead crane, cableways, rails or roadways; are static while being subject to a moving load unlike a ship or an aircraft, where the structure is moving and the surface force is at rest. Advances in speed and weight of vehicles in all branches of transport in the last few decades have resulted into increased vibrations and hence increased noise levels. It has thus become essential to study effect of moving load on such transportation structures modeled as continuously supported beams and plates. May it be (a) a moving structure in static fluid; (b) a moving force over a static structure; or (c) both the force and the structure moving; the resultant effect is vibration, hence sound. Keeping in mind this thought process, the effect of *moving load on the sound power* is studied. Some areas where this nature of study has relevance are that of ships moving in water, floating ladder tracks, floating airports, tyres and transportation structures to name a few.

1.2 Prelude

The ocean is a noisy place. There are many sources of sound, and sound travels efficiently in water. Natural ocean sounds are produced by wind, waves, precipitation, cracking ice, seismic events, and marine organisms. The hearing ability of marine mammals has evolved to deal with these natural sounds of the ocean. Since the advent of the industrial age, sounds made by human beings have combined with natural ocean sounds, resulting in elevated noise levels, primarily in the frequency region below $1kHz$ and is assumed to affect the ability of marine mammals to communicate and to receive information about their environment. Such noise may interfere with or mask the sounds used and produced by these animals and thereby interfere with their natural behavior. Higher levels of human-made sounds can cause obvious disruptions; they may frighten, annoy, or distract the animals and lead to physiological and behavioral disturbances. They can cause reactions that might include disruption of marine mammals' normal activities and, in some cases, short- or long-term displacement from areas important for feeding or reproduction. They may also disturb the species such as fishes, squids, and crustaceans upon which the marine mammals prey. At still higher levels, human-made

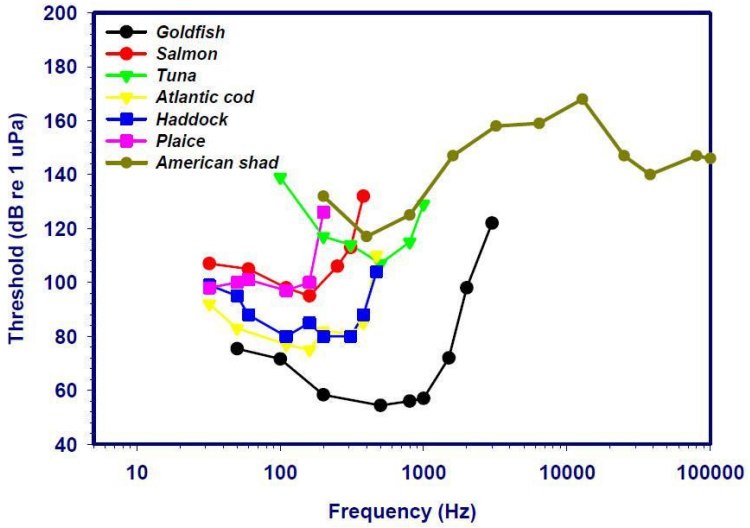

Fig. 1.1 Hearing curves for select teleost fishes (Popper (2008))

noise may cause temporary or permanent hearing impairment in marine mammals. Such impairment would have the potential to diminish the individual's chances for survival. At greater range the underwater sound wave may not directly injure animals, but has the potential to cause behavioural disturbance or even physical or physiological disturbance. Hearing thresholds have been determined for perhaps 100 of the more than 29,000 living fish species (Figure 1.1). These studies show that, with few exceptions, fish are sensitive to low frequency sound below $1kHz$, and that marine mammals are very sensitive to sound of frequencies above $1kHz$.

1.3 Motivation

Warships, Figure 1.2, might look like all-powerful vessels but they are also highly vulnerable to being spotted by the enemy. The radiated noise signature of a warship is composed of a variety of noises; those generated by running machinery, sensor systems, crew activity, by the hull moving through the water (pressure signature) and by the propeller (such as cavitation and blade rate). The output of these noise sources defines the global level of the radiated signature and of any discrete components within it. The level of the radiated acoustic signature is therefore a critical parameter in the operational success of any warship. It is this signature that will affect the means by which, and the

Fig. 1.2 Ship at Sea (flickr.com)

range at which, the vessel may be detected, classified, tracked and engaged. Since the acoustic waves can propagate in the sea 4-5 times faster than in air and without substantial loss, any source of sound from a vessel gets detected in the sea more conveniently. One component of this noise signature is due to the ship's movement; the relative motion of the ship and the sea water being the source. This relative motion between the ship and the sea water may be conceptualised as a *moving load on a static structure*.

Very Large Floating Structures (VLFS in short), Figure 1.3, with typical di-

Fig. 1.3 A Very Large Floating Platform (Kobe Airport, Tokyo Bay, Japan)

mensions of 5 km long, 1 km wide, and only a few meters deep can be used to create

floating airports, bridges, breakwaters, piers and docks, storage facilities, wind and solar power plants, military stations, industrial space, emergency bases, entertainment facilities, recreation parks, mobile offshore structures and even for habitation and may be located near the coastline or in the open sea. Because of their relatively simple construction and ease of maintenance, *pontoon-type VLFS* (which just floats on the sea surface) are used as a floating airport or runway. They are constructed particularly in calm waters, often inside a cove or a lagoon and near the shoreline, to minimize ocean effects on them, where marine life is abundant in variety and quantity. This marine life is effected undesirably by noise pollution as confirmed by recent studies. Having a floating airport, increases the noise pollution in these sheltered areas due to activities such as movement of equipment, people, cargo (dry and liquid), variable ballast (dry and liquid), aircraft landing, crane handling, berthing and docking, connection and disconnection, running machinery onboard etc. Most of these sounds can be reduced or controlled, and have been studied independent of the VLFS. However, sound radiation due to an airplane taking off / landing has not been been reported in the literatures available.

A modern ladder rail track design, Figures 1.4 and 1.5, where steel rails are fixed onto

Fig. 1.4 Train on a floating ladder track (Wikipedia)

successive ladder-like sections of two parallel longitudinal reinforced concrete sleepers up to 15 m long, when mounted upon discrete resilient supports on a concrete bed are called

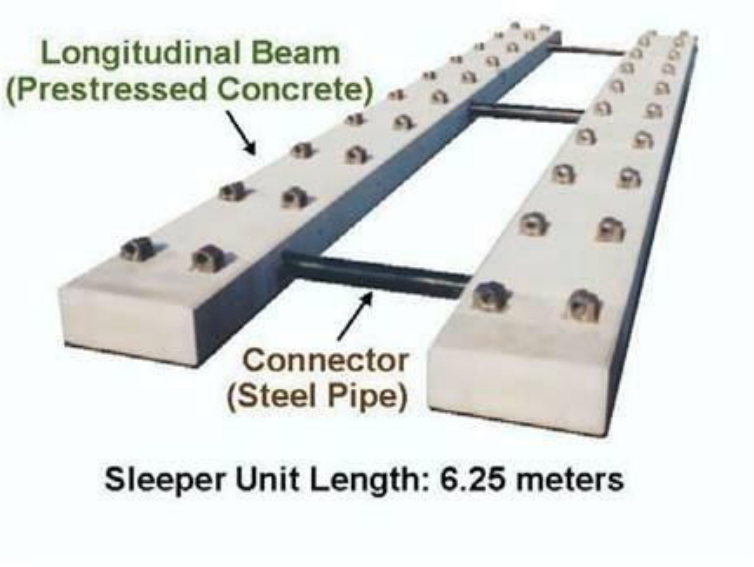

Fig. 1.5 Floating ladder track (Railway Technology Avalanche (2004))

as **floating ladders**. These have significant advantages which include robust structure, reduced settlement and much less vibration and noise. Floating ladder tracks are in use in Japan and with trains touching speeds of an upward of 500 km/h, the study of the effect of moving loads (in the form of fast moving trains) on floating ladders takes importance.

The subject of moving load problem becomes increasingly important owing to its broad applications in the **transportation industry** as seen in Figures 1.6 and 1.7. For instance, in recent years high-speed trains and automobiles are actively promoted for future surface transportation. At low speed, the dynamic effect of moving load to structures such as railways, highways, and airfields is insignificant. However, when vehicle speed increases, moving load effect can no longer be ignored and more sophisticated models of vehicle-structure interaction need to be considered. The study of the beam response to moving load also provides basis for vehicle detection, classification and weight-in-motion, structural health monitoring, and non-destructive evaluation.

Apart from these areas as discussed above, the relevance of moving load on structures has it's importance in various other fields such as guideway, overhead crane or cableways. In

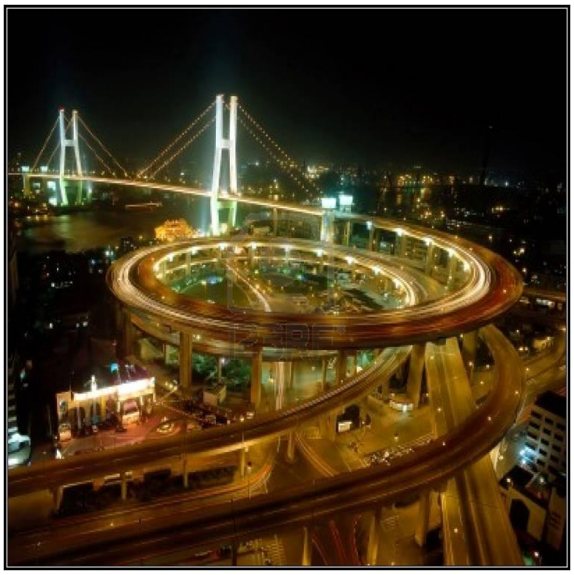

Fig. 1.6 The fast moving transportation
(*http* : *//www.*123*rf.com/photo* − 4884460 − *transportation* − *centre* − *wth* − *cross* − *sea* − *bridge.html*)

Fig. 1.7 Modern transports on bridges (flickr.com)

some of these fields; the structure is static while being subject to a moving load; while in others such as a ship, the structure is moving and the surface force is at rest. May it be a moving structure in static fluid; a moving force over a static structure or both the force and the structure moving; the resultant effect is vibrations that result into *sound*. Such requirements have resulted in numerous investigations of moving load on continuously supported beams and plates but limited to vibrations. It is this lack of work in the study

of sound due to a moving load that the present study is motivated.

1.4 Literature Survey

Governments up until the 1970s viewed noise as a "nuisance" rather than an environmental problem. With an increasing awareness of "noise health effects" the science of sound (called acoustics) has developed increasingly in importance. Acoustics is an interdisciplinary science that deals with the study of all mechanical waves (in gases, liquids or solids) including vibration, sound, ultrasound and infrasound. The study of acoustics revolves around the *cause, generation, propagation, reception and effect* of mechanical waves and vibrations. These steps are the same for all problems may it be an earthquake, a rock band or a submarine using a sonar. The *cause* or the initiating force may be natural and/or man made while the *generation process* of acoustic energy, can be of various types. There is one fundamental equation that describes acoustic wave *propagation* which transfers energy through the propagating medium and is *received* by the receiver. The final *effect* may be purely physical or it may reach far into the biological or volitional domains.

Traditionally, noise problems have been identified and solved in a *trial and error* manner. The numerical analysis has invariably been relegated to a supporting role, and numerical results have often been greeted with skepticism. For large structures such as a ship or a floating airport, the trail and error methodology may not be a suitable means of study, owing to their size. Hence the numerical method for analysing sound from such large structures is considered as an acceptable norm. Since the sound produced by structures has been studied from the time of Rayleigh (1896), the available literature is vast and varied. We shall review in brief the work undertaken for beams and plates causing forced vibrations, the Very Large Floating structures, acoustics due to moving loads, mean flow, inplane loading and effect of noise on marine life.

1.4.1 Structural Geometry

Simple geometrical structures idealized as a membrane, a thin elastic plate or a thick elastic plate (with Timoshenko-Mindlin equation of motion) which are of infinite extent and are homogeneous have been studied extensively. This is done not only due to the frequent occurrences of these structures in several engineering disciplines, but also to simplify the mathematical structure of the governing equations compared with a full three-dimensional equation. The structure is assumed to have the same static inviscid fluid on both sides, or a vacuum on one side. The exciting fields such as a point source, a concentrated mechanical line force and moment or point-force have been studied. Owing to the available efficient analytical techniques, the results have been limited to very distant structural and fluid wave fields which are quantities of physical interest. Results for a membrane covering various distances from the excitation and frequencies have been given by Crighton (1983).

1.4.2 Forced Vibration

A "moving load", which is the *cause* in the present study, makes structural analysis very difficult since the interacting force varies in time and space. Not withstanding the associated difficulties, the study of such moving load on structures has been of interest to researchers both theoretically and experimentally since the first railway bridge was built in the early 19^{th} century. The investigations have hence resulted in a large number of publications. We shall break up our survey so as to limit it to **beams** and **plates**.

1.4.2.1 Beam

Theoretically, the problem of moving load was first tackled for a case in which the beam mass was considered small against the mass of a single, constant load. The original approximate solution is due to Willis *et al.* (1851), one of the early experimenters in the field. Since then these problems has become more dynamic in character mainly due to the increased vehicle speed and structural flexibility. Frýba (1999), while documenting a large number of related cases used the Fourier sine (finite) integral transformation and the

Laplace-Carson integral transformation and obtained the dynamic response in the form of a series solutions. Ting *et al.* (1974) solved the problem using static Green function, distributed inertial effects as applied external forces and numerical integration at each position of the mass over the length of the beam. Hamada (1981) using the double Laplace transformation with respect to both time and length transform solved the response for a simply supported and damped Euler-Bernoulli uniform beam of finite length traversed by a constant force moving at a uniform speed. Yoshimura *et al.* (1986) used the Galerkin method to study the effect of geometric non-linearity while Lee (1996) used the Runge-Kutta method to study a clamped-clamped beam and Esmailzadeh and Ghorashi (1994) studied the forced vibration of a Timoshenko beam. Gbadeyan and Oni (1994) gave a technique based on modified generalized finite integral transforms and the modified Struble's method to study finite Rayleigh beams and plates having arbitrary end supports and under an arbitrary number of moving masses. Foda and Abduljabbar (1994) used a Green function approach to study an undamped simply supported Euler-Bernoulli beam of finite length subject to a moving mass traversing its span at constant speed. Henchi and Fafard (1997) using a variational finite element approach solved a continuous Euler-Bernoulli beam, with several loads but ignored inertia. Wang (1998) considered random vibrations of a Timoshenko beam under a random moving load. Zibdeh and Juma (1999) considered a rotating beam subjected to a random moving load for the Euler-Bernoulli, Rayleigh and Timoshenko beam models. Visweswara Rao (2000) studied a Euler-Bernoulli beam under moving loads by mode superposition. Ichikawa *et al.* (2000) gave an analytical solution based on eigenfunction expansion for a general continuous Euler-Bernoulli beam subjected to a moving mass. Wu *et al.* (2001) used a combined finite element and analytical method for determining the dynamic responses of a clamped-clamped beam subjected to a single mass moving along the beam. Sun (2001) obtained the Green's function of the beam on an elastic foundation by means of Fourier transform. Abu-Hilal (2003) used a Green's function method for single and multi-span Euler-Bernoulli beam subjected to distributed and concentrated loads. Michaltsos (2002) gave analytical solutions for a vehicle modeled as two moving loads on a bridge approximated as a beam ignoring the dynamics of the vehicle itself while Esmailzadeh and Jalili (2003) accounted for the dynamics

of the vehicle. Both Kargarnovin and Younesian (2004) and Lee (1998) considered the Timoshenko beam on an elastic foundation subject to moving loads, by analytical approaches. Kim (2004) studied axially loaded beams on elastic foundations subject to harmonic moving loads. The linear finite element analysis was applied to analyze a simply supported Euler-Bernoulli beam under the act of moving loads by Ju *et al.* (2006) and Kidarsa *et al.* (2008). In Kargarnovin *et al.* (2005) and Younesian *et al.* (2006), nonlinear dynamical behavior of Timoshenko beams with infinite length under the act of traveling harmonic loads resting on viscoelastic foundations are studied. Dynamic response of an inclined Euler-Bernoulli beam subjected to a moving mass has been investigated in Wu (2005) using the linear finite element method considering transversal and longitudinal displacements for the beam. In Yanmeni Wayou *et al.* (2004), the nonlinear vibration of a horizontal pinned-pinned thin beam under the act of a moving mass considering the influence of the load inertia and the nonlinearity caused by stretching effect of mid-plane of the beam due to the immovable supports was studied. Recently, the nonlinear dynamic analysis of an eccentrically prestressed beam under the act of a concentrated moving harmonic load including damping effect has been studied in Simsek and Kocaturk (2009). In that paper, the nonlinear deflections behavior of the beam is approximated by some polynomial functions and material of the beam was assumed to follow the Kelvin-Voigt model. Furthermore, the effects of large deflections, the internal damping of the beam, the velocity of the moving harmonic load, the prestress load, and the excitation frequency were discussed. Mehri *et al.* (2009) using a dynamic green function, presented the linear dynamic response of uniform beams with different boundary conditions excited by a moving load, based on the Euler-Bernoulli beam theory. An exact and direct modeling technique is presented with various boundary conditions, subjected to a load moving at a constant speed. Influence of variation in speed on the dynamic response was studied and the results given in graphical and tabular form. Dehestani *et al.* (2009) Presented an analytical-numerical method which can be used to determine the dynamic response of beams carrying a moving mass, with various boundary conditions. Results illustrated that the speed of a moving mass has direct influence on the entire structural dynamic response, depending on its boundary conditions.

As can be seen, over the years many investigators have used different methods for solving the forced vibration problem. The most used method for determining these vibrations is the eigenfunctions method wherein the applied loads and the dynamic responses are expanded in terms of the undamped beams. This method gives the solution as an infinite series, which is truncated after a number of terms and an approximate solution obtained.

1.4.2.2 Plate

The dynamic response of rectangular plates to uniformly moving loads has been subjected to many investigations. Solutions have been presented by Holl (1950) and Piszczek (1959), Nowacki (1963) showing that a critical velocity existed for each vibrational mode. Steady state solutions of an infinite plate carrying a uniformly moving load were given by Livesley (1953), Reismann (1959) and Morley (1962). Gbadeyan and Oni (1994) and Frýba (1999) investigated the dynamic behaviour of beams and plates subjected to moving forces and moving masses. Manoach (1993) studied elastoplastic thick circular plates subjected to different types of pulses by using the Mindlin plate theory. Bert *et al.* (1994) used the differential quadrature method. Rossi *et al.* (2001) studied the forced vibration responses of a rectangular plate subjected to a stationary distributed harmonic loading. Zhu and Law (2000) and Marchesiello *et al.* (1999) studied the dynamic behaviour of bridges by considering the structure to be composed of rectangular plates. Shadnam *et al.* (2001*a*) considered a single force (or mass) moving along an arbitrary trajectory; however, they studied a straight path problem by means of analytical and numerical approach. The nonlinear plate version of the same problem was considered by Takabatake (1998), using a Galerkin approach, but with discontinuously changing plate thickness and later by Shadnam *et al.* (2001*b*). Wu *et al.* (2001) used the FEM and the Newmark direct integration method. Composite plates were considered by Lee and Yhim (2004) using finite elements and third-order plate theory and later by Au and Wang (2005) computed sound radiated from a composite plate due to moving loads. Kim *et al.* (2005) used a finite element model for a bridge while Li *et al.* (2005) extended the work by taking into account the wind loads on the vehicle. The bridge-vehicle interaction using a Lagrangian

approach was studied by Yagiz and Sakman (2006). The literature cited above are some of the main contributors who have undertaken the study of moving loads on plates and cannot be considered as complete.

1.4.3 Very Large Floating Structure

Many developed countries with long coastlines for want of land space have successfully reclaimed land from sea. Such activities have a negative ecological impact on the coastline surrounding the reclamation. In response to this requirement researchers and engineers proposed the construction of **Very Large Floating Structures** (VLFS in short) with typical dimensions of 5 km long, 1 km wide, and only a few meters deep. These structures can be constructed to create floating airports, bridges, breakwaters, piers and docks, storage facilities, wind and solar power plants, military stations, industrial space, emergency bases, entertainment facilities, recreation parks, mobile offshore structures and even for habitation and may be located near the coastline or in the open sea. Because of their relatively simple construction and ease of maintenance, *pontoon-type VLFS* (which just floats on the sea surface) are used for a floating airport or runway. They are constructed particularly in calm waters, often inside a cove or a lagoon and near the shoreline, to minimize ocean effects on them, wherein marine life is abundant in variety and quantity. Recent studies by marine biologists have confirmed undesirable effects of noise pollution on marine life. Having a floating airport, compounds the noise pollution in these sheltered areas due to activities such as movement of equipment, people, cargo (dry and liquid), variable ballast (dry and liquid), aircraft landing, crane handling, berthing and docking, connection and disconnection, running machinery onboard etc. Most of these sounds can be reduced or controlled, and have been studied independent of the VLFS over the years. However, the sound radiation by the VLFS when subjected to an airplane landing / taking off and efforts of reduction to protect the marine life from noise pollution, **has not been studied**.

The difficulties in solving this *transient dynamic problem* has resulted in only a few simplified studies to have been reported to date. Using a finite element (FE) program, Watanabe and Utsunomiya (1996) presented the numerical results for elastic responses

due to prescribed impulsive loading on a circular very large floating structure excited by impulsive loading. Kim and Webster (1998) and Yeung and Kim (1998) studied transient phenomena of an infinite elastic runway using a double Fourier transform approach. The former studied the added drag caused by the flexibility of the runway while the latter focused on the resonance phenomenon caused by the accumulation of energy near the moving load. Ohmatsu (1998) developed another kind of time-domain analysis method in which the structural response is obtained from the convolution integral of the frequency response function and impulse response function. Endo and Yago (1999) adopted a FE scheme and Wilson-θ method to investigate the transient behavior of an airplane taking off from and landing on a VLFS in rough sea conditions using a triangle time impulse load applied at the nodes of the structure to represent the loads introduced by the weight of the airplane. Endo (2000) calculated the behaviour of a VLFS and airplane during takeoff / landing run in wave condition allowing for the effects of hydroelasticity. Lee and Choi (2003) developed a FE-BE hybrid method to analyze transient hydroelastic response of VLFS. Kashiwagi (2004) presented the transient elastic deformation of a pontoon-type VLFS caused by the landing and takeoff of an airplane based on the mode superposition method using realistic numerical data from a Boeing 747-400 jumbo jet. Fleischer and Park (2004) used the modal analysis with Fourier series to solve the plane hydroelastics of a beam due to uniformly moving one-axle vehicle. Kyoung *et al.* (2006) developed a finite element method for the time-domain analysis of the hydroelastic deformation of a pontoon-type very large floating structure with fully nonlinear free-surface conditions. Jin and Xing (2007) proposed a mixed mode function-boundary element method to solve the dynamic responses of a floating beam excited by landing loads. Liu-chao and Liu (2007) proposed a time-domain finite element procedure to analyze the transient hydroelastic responses of VLFS subjected to dynamic loads. Liu-chao (2009) proposed a time-domain finite element model to analyze the fluid-structure interactive dynamical system. He validated the proposed approach by comparing the existing experimental and numerical results with the results obtained.

The present study concentrates largely on the sound generated by such floating

structures. So far no study of this nature has been reported in the literatures available.

1.4.4 Acoustics

The literature on analytical methods in acoustic radiation is vast and chronologically ranges from the late 19^{th} century with the work of Rayleigh (1896), essentially defining the science of acoustics. Inherently the problem of acoustic radiation includes the problem of vibrations of the structures under consideration. The most important theories and analytical methods can be found in the classical acoustic textbooks Junger and Feit (1986), Fahy and Gardonio (2007), Pierce (1989), Cremer *et al.* (1988). Techniques for dealing with fully coupled motions of elastic plates and shells immersed in air or water were simply not available in Rayleigh's time, but have become available in the past three decades or so.

1.4.4.1 Static load

Early investigations of sound radiation from a force excited, elastic, fluid-loaded plate by Gutin (1965), Maidanik and Kerwin (1966) and Feit (1967) were primarily concerned with the far field pressure and power radiated in to the acoustic medium. Ranganath Nayak (1970), using the Fourier integral representation of the solution was able to numerically evaluate the integral representation for the velocity response to determine the drive line admittance for a line-driven plate. Crighton in a series of papers Crighton (1972, 1977, 1979, 1983) had analysed both the near-and far field response of locally excited plates. Crighton's results although probably the most complete to date in this field, are somewhat difficult to visualize due to the complexity of the problem and that they have not been displayed in a graphical form.

1.4.4.2 Moving Load

Sound radiation by beams due to moving loads is however a relatively newer area of interest. Keltie and Peng (1988) investigated the sound radiation from a fluid-loaded beam subject to a moving harmonic line force. Their study was the first of it's kind

and showed some important characteristics of structures subject to a moving load. The results showed that for beams under light fluid loading, the coincidence sound radiation peak for a stationary force is split into two coincidence peaks due to the effects of the Doppler shift, while for beams under heavy fluid loading there are no pronounced sound radiation peaks. Following the study of Keltie and Peng (1988), Cheng (1999) formulated the vibration response of periodically simply supported beam on the whole structure in wavenumber domain through Fourier transform. This problem was an advance on traditional substructure methods. For an air-loaded beam subjected to a stationary line force, they showed that the radiated sound power exhibited peaks at certain wavenumber ratios. The wavenumber ratios at which radiation peaks occur nearly coincide with the lower bounding wavenumber ratios of the odd number of propagation zones. However, Cheng's formulation did not include the presence of numerous wavenumber components induced from the elastic supports and is subject to the restriction that the external force is located on one of the elastic supports. Cheng *et al.* (2000, 2001) introduced a "wavenumber harmonic series" to discuss the vibro-acoustic response when a fluid-loaded beam on periodic elastic supports is subjected to a moving load. Results show that the response of a beam on an elastic foundation can be approximated using a periodically, elastically supported beam when the support spacing is small compared with the flexural wavelength. For such beams when the force is stationary a single radiation peak occurs which splits into two peaks due to Doppler shift when the force becomes traveling. Au and Wang (2005) studied the vibrations of a rectangular orthotropic thin plate with general boundary conditions traversed by moving loads. The effects of light and heavy moving loads were separately studied. Based on the Rayleigh integral and the analytical dynamic response of the plate, the acoustic pressure distributions around the plate were obtained in the time domain. It was concluded that the boundary conditions affect the acoustic pressure generated by moving loads. It was observed that the stiffer the plate, the higher the structural frequencies, and the larger the sound pressure caused by moving loads.

To solve the forced response of rectangular plates with elastic support, Yufeng and Qibai

(2009) adopted approximate solutions in conjunction with numerical methods. They investigated the effect of the moving force on the radiated sound from the rectangular plate with elastic support and concluded that the speed of the moving force can change the sound radiated from the plate with elastic support to become flat in special frequency range.

1.4.5 Mean Flow

The literature on fluid-structure interaction in the presence of fluid flow is relatively scarce. This is not because fluid flow is unimportant, but because problems often get too complicated when relative motion between an elastic structure and a surrounding fluid medium is involved. This is especially true when the dimension of a structure is finite, and the compressibility and viscosity of the fluid medium must be considered. One way of obtaining an understanding of the physics behind this type of fluid-structure interaction is to examine a simplified version of the problem in which the dimension of a structure extends to infinity, the fluid moves at a constant (mean) speed, and the effects of fluid compressibility and viscosity are neglected. Brazier-Smith and Scott (1984) present a numerical study of such a problem. Specifically, they study the dynamic response and instability of an infinite elastic plate in the presence of mean flow based on a causality analysis. Brazier-Smith and Scott's numerical analysis is supported by Crighton and Oswell (1991) analytical work based on an asymptotic expansion analysis. In particular, Crighton and Oswell (1991) shed some light on the mechanism of the onset of convective instability. The mechanism of the onset of absolute instability was uncovered by Wu and Maestrello (1995). Further, Wu and Zhu (1995) show that the amplitude of the plate response is always bounded by the structural nonlinearities and instabilities depicted by Brazier-Smith and Scott (1984) never really occur.

1.4.6 Inplane loading

The first theoretical examination of plate under uniform compression was by Bryan (1891), who obtained a solution to the problem in 1891. Since then numerous researchers

have investigated local instability in plates under a wide variety of loading and boundary conditions using many different methods of analysis. There has been a number of excellent textbooks such as Timoshenko and Gere (2010) and Bulson (1970) that have described the main results of these investigations. An area analogus to floating airports is the study of ice packs wherein existence of compressive stresses has been long recognized in ship design for the Arctic. A well known example of a research vessel designed to withstand ice pack compression is the polar research ship *Fram* that was designed by Colin Archer for Fritjof Nansen in the 19^{th} century. The effects of mean compression on wave propagation in the ice pack were recognized by Mollo-Christensen (1983*b*), Mollo-Christensen (1983*a*). He found that edge waves can have very low group velocity, and suggested it as an explanation of ice ride-up on shore. Schulkes *et al.* (1987) investigated the flexural gravity wave pattern excited on a floating ice plate by including the effect of compressive stress in the plane of the plate, uniform flow and stratification of the underlying water. Their work was followed by Liu and Mollo-Christensen (1988), who showed that wave energy can be concentrated because of pack compression through two very different mechanisms, namely a very small group velocity caused by high compressive stress and the increased instability of nonlinear modulations also caused by pack compression.

1.4.7 Effect of noise on Marine Life

Hearing in fishes was first demonstrated in cyprinids as early as 1903. Quantitative work on the range of frequencies over which fish hear and on representatives of several different families was later carried out by von Frisch and his colleagues in 1936. Since then most investigations on sound detection in fishes, have been performed under quiet laboratory conditions. Hearing thresholds have been determined for perhaps 100 of the more than 29,0009 living fish species. (see Fay (1988); Popper (2003); Ladich and Popper (2004); Nedwell *et al.* (2004) for data on hearing thresholds). These studies show that, with few exceptions, fish cannot hear sounds above about 3-4 kHz, and that the majority of species are only able to detect sounds to 1 kHz or even below. The following are the major effects of increased ambient noise on marine life:

1.4.7.1 Masking

Increased ambient noise causes masking of biologically significant sounds resulting into interference with clear reception of signals of interest. This disrupts activities such as breeding, navigation and communication.

1.4.7.2 Behavioural effect

Increased noise affects the behavior of marine mammals ranging from subtle to severe such that reactions to noise may range from a shift in orientation toward a sound source, to an escape or flight response.

1.4.7.3 Physiological effect

Noise can result in a range of physiological effects on marine mammals. Long-term noise exposure may cause stress responses in a manner similar to humans who live near busy highways or airports.

1.4.8 Parallel studies

A major motivation for the study of a moving load on a flexible beam or plate has been its application to transport systems (rail tracks, roads or runways), originally in temperate lands and subsequently in cold regions, where, in particular, floating ice sheets may be exploited. Acoustic pressure field radiated from a vibrating structures subjected to a moving load have been studied in various fields such as:

- **Road-bridge noise problems**: In recent years high-speed trains and automobiles are actively promoted for future surface transportation. At low speed, the dynamic effect of moving load to structures such as railways, highways, and airfields is insignificant. However, when vehicle speed increases, moving load effect can no longer be ignored and more sophisticated models of vehicle-structure interaction need to be considered. Studies devoted to vehicle-structure interaction include those by Frýba (1999); Sun (1996); Cebon (1999); Sun and Greenberg (2000); Deng and Sun (2000).

- **Vibration of railway bridges traversed by high speed trains**: A modern ladder rail track design, produces much less vibration and noise if it is mounted upon discrete resilient supports on a concrete bed, when it is called a floating ladder track. Several studies have been undertaken to reduce the sound generated by the fast moving trains on these tracks. (see Wilson (2004); Hosking and Milinazzo (2007); Yuan *et al.* (2009); Asanuma and Wakui (2012), Hosking and Milinazzo (2012))

- **Floating Ice** : Ice sheets are used for ice roads, ice bridges, construction platforms, airstrips and recreational activities. It hence becomes very important to know when the ice is safe to use. Several major theoretical and experimental studies have been undertaken to understand the effect of aircraft and vehicle operation on floating ice (see Davys *et al.* (1985); Schulkes and Sneyd (1988); Milinazzo *et al.* (1995); Yeung and Kim (2000); Wang *et al.* (2004); Squire (2007)).

- **Sound Radiation from Tyres**: In modern times, ride improvement and quietness of vehicle are demanded due to growing concerns over environment. This has forced detailed study in tire performance. In this regards experimental work was initiated in 1966 followed by theoretical work (see Keltie (1982); Heckl (1985); Kim *et al.* (2006); Kropp (2011); Kropp *et al.* (2012)).

1.4.9 Conclusion

From the literature review undertaken above, one realizes that the structures can be idealized as Membrane, a thin elastic plate, a thick elastic plate or as a cylinder. Similarly the force can be applied as a point force, line force or a moment. The structure may have simple inhomogeneities such as ribs, supports or abrupt thickness change. The fluid present may be the same on both sides or may have vacuum on one side.

Keeping the range of possibilities and those already studied by others, we shall look at

- An idealized beam or plate as the floating structure.

- A line or distributed harmonic moving load.
- Consider no inhomogeneities.
- One side fluid (water) and other as vacuum.

1.5 Objectives

The main objectives of the present study are:

- For a **ship** (modeled as a floating beam) defined by a Timoshenko beam model, a Rayleigh beam model, a Shear beam model and an Euler-Bernoulli beam model, develop an analytical formulation for *total sound power* due to a moving harmonic load.
- Perform numerical analysis for the ship model for
  - Various beam models and compare the total sound power generated.
  - Timoshenko beam model to analyze effect of loss factor on total sound power.
- For a **floating airport** (modeled as a Timoshenko-Mindlin plate) subjected to the landing / takeoff of an airplane (modeled as a moving harmonic load)
  - Develop an analytical formulation for *total sound power* and *structural response*
  - Extend the analytical formulation to include effect of current.
  - Extend the analytical formulation to include effect of inplane loading.
- Perform numerical analysis for the floating airport model to
  - Study the total sound power generated.
  - Study effect of current on total sound power.
  - Study effect of inplane loading on total sound power.
  - Study the structural response due to harmonic and point moving load.

- Develop a **Graphical User Interface** as a tool for the user to obtain total sound power for a *ship* and a *floating airport* with different combinations of variables.

Sound power level is related to the amount of acoustical energy produced by a sound source and does not take into account its surroundings (unlike sound power level which takes into account the surroundings). If an object is rated at some sound power level, it means that that is the amount of power it is capable of radiating. When attempting to measure sound power level, an engineer will find that he cannot measure sound power emitted by the source. Instead, **sound power level** is calculated from several sound pressure measurements created by a source in a particular test environment using one of four common methods: **free-field, reverberation room, progressive wave (in-duct), and sound intensity**. Once the sound pressure level is measured, the sound power level can then be determined mathematically.

Since the only accurate sound data an engineer / designer can provide is expressed as sound power, *the same would be calculated in this study* (by measuring sound intensity and then calculating sound power mathematically) to provide a common reference measurement that is independent of distance and acoustical conditions of the environment.

Since this type of study has been undertaken earlier in a limited form, the results obtained based on the application of the derived expression shall be analyzed based on the studies undertaken by various researchers and logic. The developed model has been validated with published results and discussed in section 5.2. The numerical results using the above formulation for different conditions shall be discussed. Application of the developed expression shall provide a first hand approximation of the sound power expected from a moving load on a structure floating on water.

1.6 Brief Outline of the Work Pursued in the Thesis

The content of the thesis is divided into *six* chapters for ease of explanation and the problems investigated.

Chapter 1, gives a **basic introduction and the motivation** behind the present study. The available literature relevant to the present study is reviewed thoroughly followed by a brief introduction of the research work pursued in this thesis. The basic physical equations, boundary conditions associated with acoustic problems associated with fluids and moving loads and the preliminary mathematical tools relevant to the thesis are discussed.

In *Chapter 2*, the generalized expression for the total sound power due to a **moving load on a ship** (modeled as a beam) as given by Keltie and Peng (1988) is formulated in detail for the various beam types, viz. *Rayleigh beam*, *Shear beam* and the *Euler-Bernoulli beam*.

Studies of sound generated from **floating airfields** due to the traveling load of starting, landing or taxiing planes is a natural extension of the ship (modeled as a floating beam) studied in the previous chapter. A dynamic analysis of a three-dimensional runway with time varying loading during landing / take-off however would be exceeding difficult. In *Chapter 3*, this analysis is made simpler by assuming that the runway behaves as a simple, infinitely long beam floating on water and supported by buoyancy. The model is assumed to be a one dimensional plate, described by the Timoshenko-Mindlin plate equation. The understanding of radiated sound power as established in chapter 2 has been extended to model a **floating airport**. The sound generated and platform response in frequency domain by the landing / taking-off of an airplane from such an airport, which would be akin to a moving load, has been analysed in section 3.2 of the chapter. Acoustic analysis in the presence of a **mean flow or current** complicates the analysis of a floating airport by modifying the effect of the moving load. The effect of mean flow on the response of a fluid-loaded structure has been studied in section 3.3. Even though a VLFS is structurally very long, the longitudinal strength does not play an important role in their design. The most severe type of loading for the bottom plate occurs when the structure is subjected to the combined action of uniformly distributed hydrostatic lateral loading and compression due to hogging. Similarly for the deck plate, maximum loading

occurs when the structure is subjected to compression and tension due to sagging and hogging respectively. The inplane loading plays an important role for such structures during berthing, plate connections at ends, initial deformation and corrosion to name a few and hence needs to be accounted for. This effect of **inplane loading** has been studied in section 3.4 by extending the formulation developed in section 3.2.

Having developed the general expressions for the ship (in chapter 2) and floating airport (in chapter 3), one needs to validate the model. This is done by using the published results for a Timoshenko beam by Keltie and Peng (1988). Once the model has been validated, a **Graphical User Interface** for undertaking numerical calculations using these mathematical formulations is developed and discussed in *Chapter 4*. The GUI has been generated to make the calculation procedure user friendly and speed up the user's work especially for non-technical people.

The GUI developed in chapter 4 has been used to undertake **numerical analysis** to understand the total sound power radiated due to a moving load on a ship (modeled as a beam) and a floating airport (modeled as a plate) in *Chapter 5*. Using the **beam model** to represent the ship, we first analyse the total sound power produced by a Timoshenko beam, a Rayleigh beam, a Shear beam and an Euler-Bernoulli beam. We then compare them to understand which beam type produces the maximum sound power and the reasons associated with it in section 5.5. This is followed by the calculation and analysis of the total sound power from a Timoshenko beam due to varying loss factor in section 5.6. Having analysed the beam model, the **plate model** is used to undertake the numerical analysis of the total sound power from a floating airport due to a landing / taking off of an airplane. The analysis is carried out for aluminium and steel and the **effect of the material** on the total sound power is studied in section 5.7. The same plate model is then extended by modifying the governing equation Equation (3.3) to Equation (3.21) to incorporate the **effect of mean flow** and the numerical results of the total sound power are obtained and analysed in section 5.8. Another extension is obtained by incorporating the **inplane loading** to the plate model to get Equation (3.35). This is analysed nu-

merically next in section 5.9 to understand the effect of compressive and tensile inplane loads on the floating airport. The numerical analysis terminates with the **structural response** of the floating airport due to airplane landing / taking off modeled as a point and a harmonic moving load in section 5.10.

Finally, *Chapter 6*, **summarizes** the work done in the thesis followed by the future scope of research. Major contributions made in the thesis are also highlighted in this chapter.

Additional information used and derived is enumerated in the Appendices for clarity of the methods described in the chapters and as a starting point for future researchers working in this area.

- Appendix A : Time Averages of Products.
- Appendix B : Detailed derivation for the non-dimensionalized sound power.

1.7 Papers and Publications

The following papers have been written during the preparation of the present thesis and the details of their publication status are as given below.

1.7.1 Published

1. **Agarwala, Nitin.** 2009 Study of Acoustic Stealth. *Shiptechnic* **XXV**, 169-174.
2. **Agarwala, Nitin.** 2009 Acoustic Cloaking - The new mantra of acoustic stealth. *Commodore Garg Memorial Lecture, Published by INA, Delhi Chapter*, 55-59.
3. **Agarwala, Nitin.** 2010 On the Structural-Acoustic Solution of a Flat Plate. *Shiptechnic* **XXVI**, 86-98.

4. **Agarwala, Nitin. and Nair, E. M. S.** 2012 Acoustic-Structure Interaction for a Floating Airport subject to a Moving Load. *International Journal of Innovative Research and Development, ISSN 2278-0211 (online)*, **1(10) (Special Issue)**, 330-344.

5. **Agarwala, Nitin. and Nair, E. M. S.** Fluid Loading in Structural-Acoustic Problems. *Communicated and accepted for publication by Commodore Garg Memorial Lecture, Published by INA, Delhi Chapter.*

6. **Agarwala, Nitin. and Nair, E. M. S.** On Horizontal Beams and Sound Radiation due to a Moving Load. *The Online Journal of Science and Technology (TOJSAT), ISSN 2146-7390*, 3(3), 120 - 133

7. **Agarwala, Nitin. and Nair, E. M. S.** Effect of inplane loading on sound radiation of a floating runway when an airplane is taking off. *Journal of Naval Architecture and Marine Engineering, ISSN 1813-8535 (Print), 2070-8998 (Online), 10(1), 41- 48*

1.7.2 Under review

1. **Agarwala, Nitin. and Nair, E. M. S.** Sound Radiation from a Floating Runway due to an Airplane Taking Off Affected by Mean Flow. *Submitted to Journal of Computational and Applied Research in Mechanical Engineering (JCARME) on 01 Nov 13.*

2. **Agarwala, Nitin. and Nair, E. M. S.** Structural Response of a Floating Runway excited by the taking off of an Airplane. *Submitted to Journal of Mechanical Engineering and Technology (JMET) (ISSN 2180-1053)on 29 Oct 13.*

3. **Agarwala, Nitin. and Nair, E. M. S.** Sound Radiation of a floating runway due to Inplane loading when an Airplane is taking off. *Submitted to Journal of Engineering Science and Technology Review (JESTR) on 13 Feb 13.*

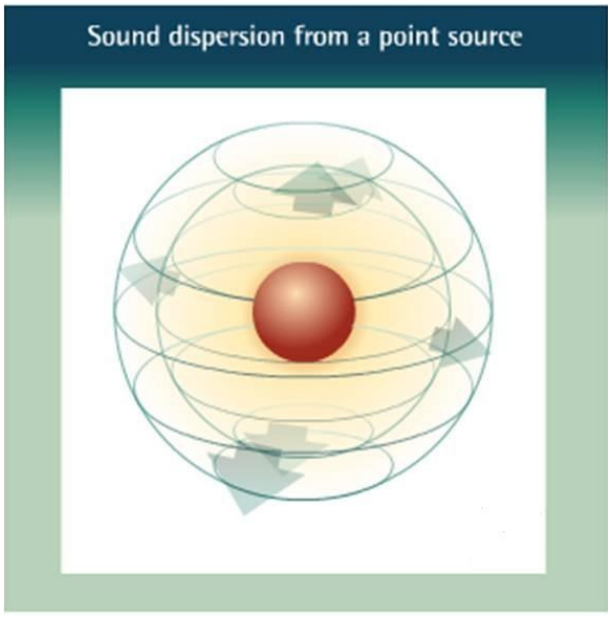

Fig. 1.8 Sound dispersion from a point source
($http://www.epd.gov.hk/epd/noise-education/web/ENG-EPD-HTML/m1/intro-6.html$)

1.8 Understanding Sound

1.8.1 Basic Elements

In general, every noise problem involves a system of three basic elements: noise source, transmission path and a receiver.

1.8.1.1 Noise Source

A source is an excitation that results in noise, either at the point of excitation or elsewhere. Most sounds or noises we encountered in our daily life are from sources which can be characterized as *point* or *line* sources.

Point Source In a free field condition, any source with its characteristic dimension being small compared to the wavelength of the sound generated, is considered as a point source. Alternatively a source is considered a point source if the receiver is at a large distance away from the source. If a sound source produces spherical spreading of sound in all directions, as seen in Figure 1.8, it is a point source. For a point source, the noise level decreases by 6 dB per doubling of distance from it.

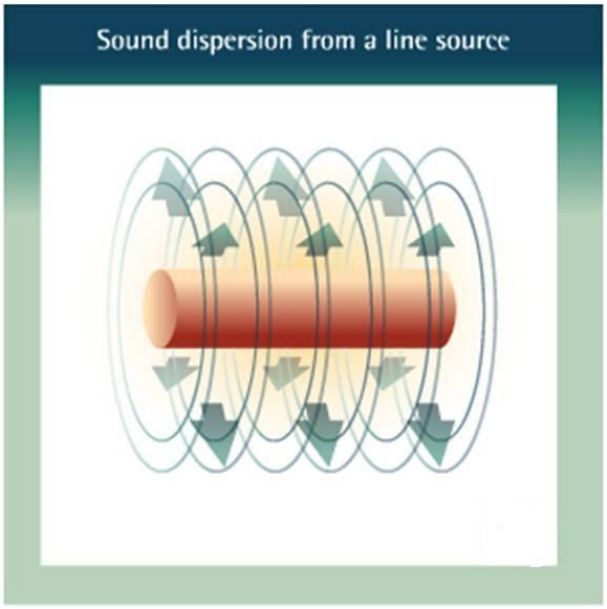

Fig. 1.9 Sound dispersion from a line source
($http://www.epd.gov.hk/epd/noise-education/web/ENG-EPD-HTML/m1/intro-6.html$)

Line Source A line source is a source of air, noise, water contamination or electromagnetic radiation that emanates from a linear (one-dimensional) geometry as seen in Figure 1.9. If the sound source produces cylindrical spreading, such as stream of motor vehicles on a busy road at a distance, it may be considered as a line source. For a line source, the noise level decreases by 3 dB per doubling of distance from it.

1.8.1.2 Transmission Path

The path is the route(s) that energy takes in traveling from a source to the radiator.

1.8.1.3 Receiver

The receiver is a person or an object where the sound is perceived and accessed.

1.8.2 Sound Fields

Sound fields are typically "-near" , "-far", "-free" and "-reverberant" field.

1.8.2.1 Near Field

In the near field, close to the sound source, there can be a large amount of pressure variations, from one position to another position. Sound pressure level measurements in the near field are therefore forbidden in many applications. In the near field the sound field is very complex and complicated, and hence the sound pressure distribution and the sound intensity distribution may look completely different.

1.8.2.2 Far Field

In the far field, there is a more consistency in the sound field and sound pressure levels will not vary too much when the measurement position is moved slightly. The far field is also experienced if there is a free field situation.

1.8.2.3 Free Field or Direct Field

When a point source (or any source that radiates equally in all directions) radiates into free space, the intensity of the sound varies as I/r^2 where r is the distance from the source, the intensity is given by $I = W/(4\pi r^2)$ and W is the power of the source.This may be understood as a given amount of sound power being distributed over the surface of an expanding sphere with area $4\pi r^2$. An environment in which there are no reflections is called as a free field.

1.8.2.4 Reverberant Field or Diffuse Field

If the measurement position is close to some boundary like floors, walls and ceilings, there might be reflections of sound as well as direct sound. In such a sound field, a change in position further away or closer to the sound source may not give a significant change in the sound pressure level, because a lot of the sound pressure is caused by reflection. This is called a reverberant field or a diffuse sound field.

1.9 Sound Parameters

The three different quantities describing sound are *sound pressure*, *sound intensity* and *sound power*.

1.9.1 Sound Pressure

Sound pressure is a scalar, describing the pressure fluctuation at a given position and is measured in Pascal (Pa). Sound pressure is typically measured at the receiver's position for evaluation of the harmfulness and the annoyance of a noise source.

1.9.2 Sound Intensity

Sound intensity is a vector quantity, that describes the amount and the direction of flow of acoustic energy at a given position. The unit for sound intensity is Watt per square meter (W/m^2). It is used for noise source location, rating of noise sources and noise measurement in the medium at a listener's location. For plane progressive waves with a harmonic source, the sound intensity over all time as given in Fahy and Gardonio (2007) is

$$I(R, \phi, \theta) = \frac{|P(R, \phi, \theta)|^2}{2\rho c}$$

where $|P(R, \phi, \theta)|$ is the amplitude of $P(R, \phi, \theta, t)$ without the time dependent term $e^{-i\omega t}$.

1.9.3 Sound Power

Sound power radiation can be defined as the rate of acoustic energy delivered by a source which can be obtained by integrating the sound intensity over a surface of convenience. It can only be calculated or determined either based upon sound intensity measurement or based upon sound pressure measurement. The main use of sound power is for noise rating so as to compare how noisy sources are. The unit for sound power is Watt (W). Sound power is an important index in acoustic radiation analysis because it is a single global quantity which can be used to characterize the strength of the sound generated by a source. Estimation of sound power is a common practice of identifying dominant sources

prior to a noise control project. Many standard methods are available for sound power estimation. They may be based on pressure measurement or intensity measurement. Some of them require free-field environment while others require diffuse field (where there is preponderance of reflected or reverberant sound signal in relation to the direct sound signal) environment.

1.10 Sound Terminologies

1.10.1 Decibel

The scale often used for describing a measurement of sound is the decibel unit (dB). The decibel is a comparison of intensities or energy densities. It is not an absolute unit, but a ratio. Without a reference level, it means nothing. The decibel represents a measure of the sound power relative to a reference sound power, normally 1 pW (picoWatt). By definition, sound power level (PWL) is expressed as

$$PWL = 10\ log\frac{W}{W_{ref}}$$

where W is the radiated sound power in Watts and W_{ref} is the reference power 10^{-12} watts. Since the decibel scale is logarithmic, it is convenient for dealing with large differences in the measured quantities. Multiplication and division of decibel units becomes simple because they are reduced to an addition and a subtraction operation respectively.

1.10.2 The sound impedance (Z)

Sound impedance is a frequency dependent parameter and is very useful for describing the behaviour of sound producing object. The acoustic impedance at a particular frequency indicates how much sound pressure is generated by a given air vibration at that frequency. It hence varies strongly with the change of frequency. Mathematically, it is the ratio of the sound pressure P and the product of the particle velocity v and the surface area S, through which an acoustic wave propagates. Acoustic impedance can be expressed in

either its constituent units (pressure per velocity per area) or in rayls per square meter. Hence

$$Z = \frac{P}{vS}$$

1.10.3 Subsonic Flows

The defining property of subsonic flow is that the flow speed is lesser than the local speed of sound. The condition for a flow to be subsonic in terms of the Mach number is $M < 1$ where $M(= \frac{V}{C_0})$ is the Mach number and C_0 is the local speed of sound. In subsonic flow at low Mach number the viscosity and heat conduction are normally important effects as the timescale is relatively long, $M << 1$ and density effectively remains constant, this is not so in supersonic flows.

1.11 Understanding Load

1.11.1 Concentrated Load

Force applied at a single point is called as a concentrated load. Concentrated loads are useful mathematical idealizations, but do not exist in the real world. A concentrated load can be applied at more than one location on a structure, and multiple loading points may exist on the same structure.

1.11.2 Distributed Load

Concentrated / point forces are models. These forces do not exist in the exact sense. Every external force applied to a body is distributed over a finite contact area. The following distinctions are made, depending on the dimension of the area of application:

1.11.2.1 Line Load

Load distributed along a line is called as a line load. The intensity of this force is expressed as force per unit length of line (N/m).

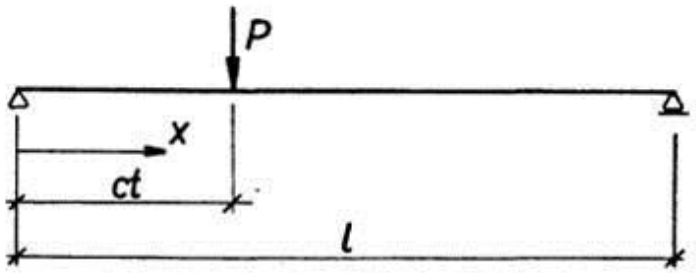

Fig. 1.10 Concentrated Force (Frýba (1999))

1.11.2.2 Surface Load

Load applied over an area. The intensity of these forces (called pressure) is expressed as force per unit area. The units for the surface force are N/m^2

1.11.2.3 Volume Load

Forces distributed over the volume of the body. Also called as body forces. The units for the intensity of body forces are N/m^3

1.12 Understanding Moving Load

1.12.1 Moving Load Types

The moving load itself is modeled in various forms. Of the many the most commonly used are

1.12.1.1 Concentrated force

For a single point force the Dirac (impulse, also delta) function that expresses the concentrated load as $p(x,t) = \delta(x)P$, where P is the vehicle weight as seen in Figure 1.10.

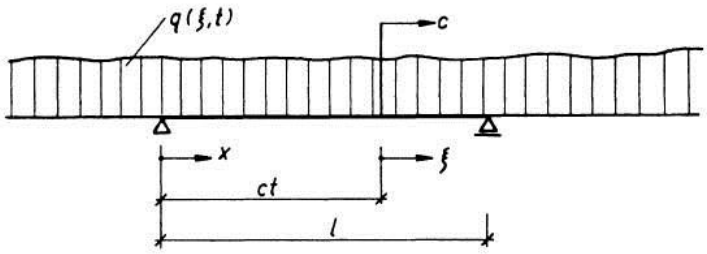

Fig. 1.11 Moving Continuous Force (Frýba (1999))

1.12.1.2 Moving Harmonic force

The time variable concentrated force is given as $p(t) = Q\ sin\ \omega t$ where Q is the amplitude and ω the circular frequency of the harmonic force.

1.12.1.3 Moving Continuous force

This is frequently used in the calculation of dynamic stresses in pipelines carrying moving fluids, large-span railway bridges, resulting from the traverse of a train of cars hauled by a locomotive. The moving continuous force as seen in Figure 1.11 is represented as $p(x,t) = q(\xi,t) - \mu_q(\xi)\frac{d^2v(x,t)}{dt^2}$ where $\xi = x - ct$ and by neglecting the second order terms we get $p(x,t) = q[1 - H(x - ct)]$

1.12.1.4 Moving force arbitrarily varying in time

Forces in this form are used in calculations of structures exposed to the effects of explosion, pressure waves, impacts of flat wheels on large-span railway bridges etc. as seen in Figures 1.12 and 1.13.

1.12.1.5 Platoon Load

This is a mix of both the constant load and the harmonic load. Hence the type of moving dynamic loads considered are moving constant loads and moving harmonic loads.

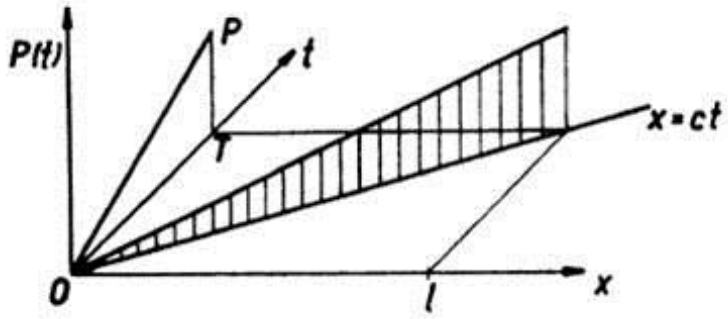

Fig. 1.12 Moving force linearly increasing in time (Frýba (1999))

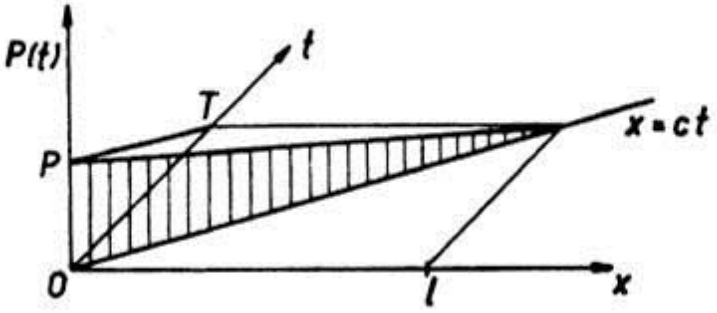

Fig. 1.13 Moving force linearly decreasing in time (Frýba (1999))

1.12.2 Moving Load Models

Moving loads have a great effect on dynamic stresses in structures, and cause them to vibrate intensively, resulting into sound, especially at high velocities. Their peculiar feature is that they are variable in both time and space. If we think of a moving load as of a mass body moving in a generally curved path over the structure being examined, we see that according to d'Alembert's principle its effects are twofold: the *weight effects* (or gravitational) of the moving load, and the *inertial effects* of the load mass on the deformed structure. If only the weight effect is considered, and the mass of the moving load neglected against the mass of the structure, the computation of strains in the solid is not easy. It becomes more complicated when the structure mass is assumed to be negligible against the load mass. The most difficult of all is the problem involving both the gravitational and the inertial action of moving loads having masses commensurable

with the mass of the structure. Mathematically these models are expressed as

1.12.2.1 Moving force model

In the moving force model, the force is assumed to be constant and equal to the vehicle weight, hence $f_c(x,t) = P\delta(x - vt)$; where P is the vehicle weight. This is the simplest vehicle model, since we have only two parameters: vehicle weight and speed.

1.12.2.2 Moving mass model

The moving mass model accounts for the inertial effect of the moving load. We apply this method by modeling the moving mass as an oscillator with large spring stiffness. The force is given by $f_c(x,t) = [(P - m\frac{d^2w(vt,t)}{dt^2}\delta(x - vt)]$. The difference between solutions of the moving force and moving mass models grows with increasing speed.

1.12.2.3 Moving oscillator model

In the moving oscillator model, the mass m_0 is attached to the continuum through a spring and dashpot, $f_c(x,t) = [P + k(z(t) - w(vt,t)) + c(\dot{z}(t) - \dot{w}(vt,t))]\delta(x - vt)$ where k and c are spring and dashpot coefficients and $z(t)$ is the vertical displacement of the mass. In this case, we have an additional degree of freedom and, thus, need an additional equation of motion, $m\ddot{z} = -k[z(t) - w(vt,t)) - c(\dot{z}(t) - \dot{w}(vt,t)]$

1.12.2.4 Moving Multiple Degrees of Freedom model

The moving MDOF model accounts for the facts that (i) the vehicle is not a lumped mass but rather consists of several elastically interacting components and (ii) it interacts with the structure carrying it at several contact points.

1.13 Understanding Material

1.13.1 Beams

A beam is a rod-like structural member that can resist transverse loading applied between its supports. By "rod-like" it is meant that one of the dimensions is considerably larger than the other two. This dimension is called the longitudinal dimension and defines the longitudinal direction or axial direction. Directions normal to the longitudinal directions are called transverse. The longitudinal axis of a beam is directed along the longitudinal direction and passes through the centroid of the cross sections. A beam is straight if the longitudinal direction is a straight line. A beam is prismatic if the cross section is uniform.

1.13.2 Plates

Plates are defined as plane structural elements with a small thickness compared to the planar dimensions. The typical thickness to width ratio of a plate structure is less than 0.1. A plate theory takes advantage of this disparity in length scale to reduce the full three-dimensional solid mechanics problem to a two-dimensional problem. The aim of plate theory is to calculate the deformation and stresses in a plate subjected to loads. Of the numerous plate theories that have been developed since the late 19^{th} century, two are widely accepted and used in engineering. These are

- The Kirchhoff-Love theory of plates (classical plate theory)
- The Mindlin-Reissner theory of plates (first-order shear plate theory)

1.13.2.1 Kirchhoff-Love theory

Kirchhoff-Love theory is an extension of Euler-Bernoulli beam theory to thin plates. The theory was developed in 1888 by Love. using assumptions proposed by Kirchhoff. It is assumed that a mid-surface plane can be used to represent the three-dimensional plate in two dimensional form. The following kinematic assumptions are made in this theory:

- straight lines normal to the mid-surface remain straight after deformation

- straight lines normal to the mid-surface remain normal to the mid-surface after deformation

- the thickness of the plate does not change during a deformation.

1.13.2.2 Mindlin-Reissner Plate Theory

Mindlin's theory assumes that there is a linear variation of displacement across the plate thickness but that the plate thickness does not change during deformation. This implies that the normal stress through the thickness is ignored; an assumption which is also called the "plane stress" condition. On the other hand, Reissner's theory assumes that the bending stress is linear while the shear stress is quadratic through the thickness of the plate. This leads to a situation where the displacement through-the-thickness is not necessarily linear and where the plate thickness may change during deformation. Therefore, Reissner's theory does not invoke the plane stress condition.

The Mindlin-Reissner theory is often called the first-order shear deformation theory of plates. Since a first-order shear deformation theory implies a linear displacement variation through the thickness, it is incompatible with Reissner's plate theory.

The vibration equation for the elastic plate, including rotational inertia and transverse shear effects, as given by the Mindlin plate equation is

$$\left(\nabla^2 - \frac{\rho_v}{\kappa^2 G}\frac{\partial^2}{\partial t^2}\right)\left(D_s\nabla^2 - \frac{\rho_v h^3}{12}\frac{\partial^2}{\partial t^2}\right)u + \rho_v h\frac{\partial^2 u}{\partial t^2}$$
$$= \left(1 - \frac{D_s}{\kappa^2 G h}\nabla^2 + \frac{\rho_v h^2}{12\kappa^2 G}\frac{\partial^2}{\partial t^2}\right)[f(x,t) - p(x, y=0, t)] \tag{1.1}$$

1.13.3 Need for inclusion of Rotational inertia and Transverse shear effect

For short, sturdy beams the shear effect cannot be neglected as in conventional analysis using the Bernoulli-Euler's beam theory. The situation occurs when the cross section of the beam is relatively large in comparison with the beam span. Although the correction for the shear effect may yield results only a few percent more accurate in frequency prediction than those from classical beam theory for a moderately thick beam, the accuracy improvement may be quite profound when performing dynamic response analysis. It is with this reasoning that a Timoshenko-Mindlin plate is utilized for the present study.

1.13.4 Finite Vs Infinite beams

1.13.4.1 Finite beam

For finite beams the problem is one-dimensional wherein the beam boundaries generate standing waves. Because of this, sound can be radiated at frequencies both below and above the critical frequency. However the radiation ratio (γ) of finite beam is not zero below the critical frequency. These plates demonstrate boundary effect.

1.13.4.2 Infinite beam

A beam is considered infinite if the excitation occurs far enough from the ends such that the reflected energy is negligible. Derivation of the input impedance for such cases is simpler than that for semi-infinite / finite beams. At the point of application of the force, the beam moves straight up and down without rotation.

At low frequencies, the input impedance is four times as large as that for a semi-infinite beam. As frequency increases, the reactive term increases more rapidly than the resistive term. The magnitude of the impedance therefore continues to increase with frequency rather than approaching a constant value, as does that for a semi-infinite beam. In an infinite beam sound radiation only occurs above the critical frequency. At frequencies

above the critical frequency finite beams behave in a similar manner to infinite beams, but this is not the case at lower frequencies. Above the critical frequency, the radiation ratio (γ), is the same in both cases.

1.14 Basic Mathematical Tools Relevant to the Thesis

1.14.1 Analysis Methods

The problem at hand of a structure subjected to a load (moving or static) is to determine the deflections and stress resultants of the structure under the action of load. In order to solve such problems the analysis may be undertaken in either of the two domains, namely the *time domain* or the *frequency domain*.

1.14.1.1 Frequency Domain Analysis

When the motion of a structure and the surrounding water are time harmonic, they can be analyzed in the frequency domain. The relevant analysis methods are known as frequency domain methods. In this case it is the *amplitudes of the motions* that are to be determined. The commonly-used approaches for the analysis of VLFS in the frequency domain are the modal expansion method and the direct method.

Modal Expansion method This method consists of separating the hydrodynamic analysis and the dynamic response analysis of the structure. The deflection of the structure with free edges is decomposed into vibration modes that can be arbitrarily chosen. These modes may be that of the *dry type* or the *wet type*. Most analysts use the dry-mode approach because of its simplicity and numerical efficiency. Next, the hydrodynamic radiation forces are evaluated for unit amplitude motions of each mode. The Galerkin's method, by which the governing equation of the structure is approximately satisfied, is then used to calculate the modal amplitudes, and the modal responses are summed up to obtain the total response.

Direct method This method is straightforward, but must solve a large scale matrix equation and this means that a large amount of memory space and CPU time is required. In this method, the deflection of the structure is determined by directly solving the motion of equation without any help of eigenmodes. In this solution procedure, the potentials of diffraction and radiation problems are established, and the deflection of structure is determined by solving the combined hydroelastic equation via the finite difference scheme.

In sum, the principal difference between the modal superposition method and the direct method lies in the treatment of the radiation motion for determining the radiation pressure.

1.14.1.2 Time Domain Analysis

When the motion of a structure and the surrounding fluid are time dependent or transient, they must be analyzed in the time domain. The corresponding methods are known as time domain methods. In this case it is the *time histories of the structural motions* that are determined. The commonly-used approaches for the time-domain analysis are the *direct time integration method* and the *Fourier transform method*. Time-domain analysis for hydroelasticity of VLFS is necessary for design purposes since some of the design cases, such as the airplane landing and take-off, is a transient phenomenon and can not be solved in the frequency-domain. Only a few studies of transient problems have been reported to date, and most of them are still too computationally intensive for practical use in VLFS design.

Direct Time integration method In the direct time integration method, the equations of motion are discretized for both the structure and the fluid domain.

Fourier transform method In the Fourier transform method, we first obtain the frequency domain solutions for the fluid domain and then Fourier transform the results for substitution into the differential equations for elastic motions. The equations are then solved directly in the time domain analysis by using the finite element method or other

suitable computational methods.

As seen above, the analysis may be carried out in the frequency domain or in the time domain. However most hydroelastic analysis are carried out in the frequency-domain, being the simpler of the two. For transient responses and for nonlinear equations of motion (due to effects of a mooring system or nonlinear wave as in a severe wave condition), it is necessary to perform the analysis in the time-domain. It is well-known that the time-domain and frequency domain analysis are reversible through Fourier transformation. Although the solutions in the time and frequency domains can be conveniently linked through the Fourier and inverse Fourier transforms, it is time consuming and difficult to perform these transforms in some cases. One of the difficulties in undertaking an inverse Fourier transform from the frequency domain to time domain is the evaluation of the integrals over an infinite frequency range. Thus it is necessary to truncate the integral at a finite frequency and to assess the accuracy of the truncated interval.

1.14.2 Solution Methodologies

Differential equation solution for beams and plates is a vast topic with many variations. These can be broken down into two solution groups the first being **exact** (i.e analytical) solutions and the second being **approximate** (i.e numerical) solutions. The advantages of *analytical methods* are that they can predict results without many computations, in a shorter time and usually without frequency limitations. They can shed light on physical mechanisms involved in certain phenomena and can be used to quickly compare different design alternatives without the need for considerable analysis effort, by roughly seeing how different parameters influence quantities such as radiated sound pressure or sound power. This can be very useful in the conceptual stage. The main disadvantage of analytical methods is that they can be used only for simple problems (e.g. simple structures). On the other hand *numerical methods* are very powerful in accurately modeling real life situations including complex structures. The most widely used numerical methods are the Finite Element Method (FEM) and the Boundary Element Method (BEM). Both of them can be used for structural and acoustic analysis but due to certain advantages

and disadvantages FEM is mainly used for structural problems whereas BEM is used for acoustical problems. In contrast with analytical methods, numerical methods require a great number of computations and usually take a long time to be performed. Moreover, they need considerable manual effort to design detailed models. They are also only applicable for low-frequency analysis. Numerical methods are used extensively in the detailed design stage. For the purpose of minimisation of sound radiation by structures, numerical methods have been used in conjunction with numerical optimisation algorithms to achieve optimum designs.

1.14.3 Approaches available

Three approaches are used to obtain the total acoustic power radiated from planar sources;

- Far-field approach
- Surface integration approach
- Fourier transform approach

1.14.3.1 Far-field Approach

This approach was developed by Rayleigh for a plate vibrating in an infinite baffle. It uses the Rayleigh surface integral to calculate the acoustic pressure, acoustic intensity and hence the acoustic power radiation. Each elemental area on the plate surface is assumed to be a point source of sound wave and their individual contributions are summed to yield the total acoustic power radiation. The radial component of the acoustic intensity is integrated over an imaginary far-field hemisphere enclosing the source (Junger and Feit (1986)), and this explains the use of spherical coordinates for writing the far-field pressure expressions.

1.14.3.2 Surface Integration Approach

This approach is suitable for baffled and unbaffled plates. The real acoustic intensity is integrated over the surface of the vibrating structure. The acoustic pressure is determined in terms of surface velocity, using the Rayleigh integral.

1.14.3.3 Fourier Transform Approach

In this approach, the velocity and its complex conjugate are employed for approximating the sound power radiated from the vibrating surface. Thus

$$\Pi = \frac{1}{2} Re\left(\int_s p_s v^* dS \right)$$

where p_s is the surface pressure, v^* is the complex conjugate of surface velocity and S is the area of the radiating surface.

1.14.4 Fourier Transformation

Time is fundamental in our everyday life in the 4-dimensional world. We see things move as a function of time. On the other hand, although sound waves are composed of moving atoms, their movement is too small and the frequency of the vibration is too fast for us to observe directly. It is thus easier to describe sounds in frequency space rather than time space. We can transform sound, or other things in physics for that matter, from time space to frequency space by the technique of Fourier transform. The Fourier transform (FT) is one type of mathematical transformation which changes one axis variable to another variable. The exponential Fourier transforms, are defined as

$$\begin{aligned} \tilde{w}(\xi) &= \textstyle\int_{-\infty}^{\infty} w(x) e^{-i\xi x} dx \\ w(x) &= \tfrac{1}{2\pi} \textstyle\int_{-\infty}^{\infty} \tilde{w}(\xi) e^{i\xi x} d\xi \end{aligned} \tag{1.2}$$

The spatial transform variable, ξ, has physical significance as the wave number, and the wave number response or spectrum, $w(\xi)$, is simply the structure's response in the

wave number domain. When using Fourier transforms, it is assumed that both transforms exist over their entire domain of definition, where the $\sim$ denotes the transformed expressions.

Chapter 2

Beam Model

2.1 General Introduction

In chapter 1 we discussed the need for studying the effect of a moving load on total sound radiation and the tools required to make the handling of such problems simpler. Using these tools, Keltie and Peng (1988) gave the basic formulation for a Timoshenko beam subjected to moving load. Using the general equation of the beam, as given in Junger and Feit (1986), the generalised expression for the sound power as obtained by Keltie and Peng (1988) is derived in explicit form. Taking Fourier transform of the governing equation and then non-dimensionalising, the total sound radiation is obtained. The formulation takes into account the complex shear and complex elastic modulus; thus accounting for structural damping. The derived formulation is then extended to the *Rayleigh beam*, *Shear beam* and *Euler- Bernoulli beam*. The variation of total sound power due to the moving load on various beam types is analyzed to understand the contributions of loss factor, rotatory inertia and shear effect on sound radiation.

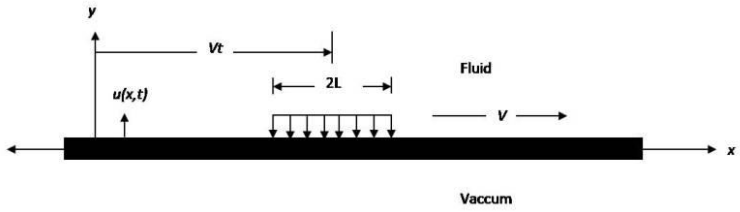

Fig. 2.1 Schematic representation of a beam subject to a moving load

2.2 Formulation

2.2.1 Structure Definition

The motion of an infinite beam excited by a force of length 2L moving at a subsonic speed V is formulated. The problem is considered in two-dimensional Cartesian co-ordinate system with x-axis being in the horizontal direction and y-axis in the vertically upward positive direction, as seen in Figure 2.1. The beam occupies the plane $y = 0$. The space $y > 0$ is filled with an acoustic medium (water, air etc). The moving force may be assumed to be:
A uniform distributed line force given by

$$f(x,t) = \frac{f_0}{2L}[H(x - Vt + L) - H(x - Vt - L)]e^{j\omega t} \tag{2.1a}$$

and a point force given by

$$f(x,t) = f_0 e^{j\omega t}\delta(x - Vt) \tag{2.1b}$$

where f_0 is the strength of external force per unit width, $H(x)$ is the Heavyside step function and $\delta(x - Vt)$ is a Delta function.

2.2.2 Governing Equation

The vibration equation for the elastic beam, including rotational inertia and transverse shear effects, as given by Junger and Feit (1986) is given as:

$$\bar{E}I\frac{\partial^4 u(x,t)}{\partial x^4} + \rho_v h\frac{\partial^2 u(x,t)}{\partial t^2} - \rho_v I\left(1 + \frac{\bar{E}}{\kappa^2\bar{G}}\right)\frac{\partial^4 u(x,t)}{\partial x^2\partial t^2} + \rho_v I\frac{\rho_v}{\kappa^2\bar{G}}\frac{\partial^4 u(x,t)}{\partial t^4}$$

$$= \left(1 - \frac{\bar{E}I}{\kappa^2\bar{G}h}\frac{\partial^2}{\partial x^2} + \frac{\rho_v h^2}{12\kappa^2\bar{G}}\frac{\partial^2}{\partial t^2}\right)[f(x,t) - p(x,y=0,t)] \tag{2.2a}$$

where

$u(x,t)$	is the transverse displacement of the beam
$\bar{E} = E(1+\eta j)$	is the complex elastic modulus
E	is the elastic modulus
η	is the loss factor
$\bar{G} = \bar{E}/2(1+\nu)$	is the complex shear modulus
$I = h^3/12$	is the cross sectional moment of inertia per unit width
h	is height of the beam
ν	the Poisson's ratio
ρ_v	is the mass density of the material
$\kappa^2 = \pi^2/12$	is the cross sectional shape factor or the shear correction factor
$p(x,y=0,t)$	is the acoustic pressure acting on the beam's surface

From this equation follow three special cases:

(a) *Rayleigh beam*: If the effect of rotary inertia is considered and the effect of shear is neglected, the Rayleigh beam model results which partially corrects the overestimation of natural frequencies in the Euler-Bernoulli model. Thus Equation (2.2a) reduces to

$$\bar{E}I\frac{\partial^4 u(x,t)}{\partial x^4} + \rho_v h\frac{\partial^2 u(x,t)}{\partial t^2} - \rho_v I\frac{\partial^4 u(x,t)}{\partial x^2\partial t^2} = [f(x,t) - p(x,y=0,t)] \tag{2.2b}$$

(b) *Shear Beam*: If the effect of rotatory inertia is neglected and effect of shear on the dynamic deflection of beam is considered, Equation (2.2a) reduces to

$$\bar{E}I\frac{\partial^4 u(x,t)}{\partial x^4} + \rho_v h\frac{\partial^2 u(x,t)}{\partial t^2} - \frac{\bar{E}I\rho_v}{\kappa^2\bar{G}}\frac{\partial^4 u(x,t)}{\partial x^2\partial t^2} = (1 - \frac{\bar{E}I}{\kappa^2\bar{G}h}\frac{\partial^2}{\partial x^2})[f(x,t) - p(x,y=0,t)] \tag{2.2c}$$

(c)*Euler-Bernoulli beam*: If we neglect the effect of both shear and rotatory inertia we obtain the classical Euler-Bernoulli beam model.

$$\bar{E}I\frac{\partial^4 u(x,t)}{\partial x^4} + \rho_v h\frac{\partial^2 u(x,t)}{\partial t^2} = [f(x,t) - p(x,y=0,t)] \tag{2.2d}$$

2.2.3 Boundary Conditions

The pressure distribution induced by the vibrating beam in the acoustic medium is denoted by $p(x,y,t)$ and satisfies the wave equation in two-dimensional space, given by

$$(\frac{\partial^2}{\partial x^2} + \frac{\partial^2}{\partial y^2} - \frac{1}{C_0^2}\frac{\partial^2}{\partial t^2})p(x,y,t) = 0 \tag{2.3}$$

where C_0 is the sound speed in the acoustic medium.
If ρ_0 is the mass density of the acoustic medium, the boundary condition at $y = 0$ is given by

$$\rho_0\frac{\partial^2 u}{\partial t^2} = -\frac{\partial p}{\partial y}\bigg|_{y=0} \tag{2.4}$$

2.2.4 Transformation

By applying the spatial Fourier transformation as discussed in Equation (1.2)

$$FT() = \int_{-\infty}^{\infty}()e^{i\xi x}dx$$

with ξ as the wave number variable, the force function in wave number domain may be written as

$$\begin{aligned}\tilde{f}(\xi,t) &= f_0\tfrac{sin(\xi L)}{\xi L}e^{j(\omega+\xi V)t} = F(\xi)e^{j(\omega+\xi V)t} && \text{for harmonic line force}\\ \tilde{f}(\xi,t) &= f_0 e^{j(\omega+\xi V)t} = F(\xi)e^{j(\omega+\xi V)t} && \text{for a point force}\end{aligned} \tag{2.5a}$$

while the transformed displacement is written as

$$\tilde{U}_s(\xi,t) = U_s(\xi)e^{j(\omega+\xi V)t} \tag{2.5b}$$

and the transformed pressure as

$$\tilde{P}(\xi,y,t) = P(\xi,y)e^{j(\omega+\xi V)t} \tag{2.5c}$$

Taking Fourier transformation of Equation(2.3) and using Equation (2.5c) we get

$$(\frac{\partial^2}{\partial y^2} - \xi^2 - \frac{j^2(\omega+\xi V)^2}{C_0^2})P(\xi,y)e^{j(\omega+\xi V)t} = 0$$

$$(\frac{\partial^2}{\partial y^2} - \xi^2 + \left[\frac{\omega+\xi V}{C_0}\right]^2)P(\xi,y)e^{j(\omega+\xi V)t} = 0 \tag{2.6}$$

Defining $M(= V/C_0)$ as the Mach number and $K_0(= \omega/C_0)$ as the acoustic wave number, Equation (2.6) can be rewritten as

$$(\frac{\partial^2}{\partial y^2} - \underbrace{\{\xi^2 - [K_0+\xi M]^2\}}_{K_y^2})P(\xi,y)e^{j(\omega+\xi V)t} = 0$$

where K_y is defined as

$$K_y = \begin{cases} -j\sqrt{\xi^2 - (K_0+M\xi)^2} & for \quad \xi^2 > (K_0+M\xi)^2 \\ \\ \sqrt{(K_0+M\xi)^2 - \xi^2} & for \quad \xi^2 < (K_0+M\xi)^2 \end{cases} \tag{2.7}$$

Similarly taking Fourier transformation of Equation (2.4) and using Equation (2.5b) and Equation (2.5c) we get

$$-\rho_0(\omega+\xi V)^2 U_s(\xi)e^{j(\omega+\xi V)t} = -\frac{P(\xi,y)}{\partial y}e^{j(\omega+\xi V)t}\Big|_{y=0} \tag{2.8}$$

For sound pressure on the surface ($y = 0$) from Equation (2.4) we get

$$P(\xi, y) = P(\xi, y = 0)e^{-jK_y y}$$

Hence Equation (2.8) gets modified as

$$\begin{aligned}
-\rho_0(\omega + \xi V)^2 U_s(\xi)e^{j(\omega+\xi V)t} &= -\frac{P(\xi, y = 0)e^{-jK_y y}}{\partial y}e^{j(\omega+\xi V)t}\bigg|_{y=0} \\
&= -P(\xi, y = 0)(-jK_y)e^{-jK_y y}e^{j(\omega+\xi V)t}\bigg|_{y=0} \\
&= -P(\xi, y = 0)(-jK_y)e^{j(\omega+\xi V)t}
\end{aligned}$$

Simplifying

$$\begin{aligned}
P(\xi, y = 0) &= -\rho_0\frac{(\omega + \xi V)^2}{jK_y}U_s(\xi) \\
&= j\rho_0\frac{(\omega + \xi V)^2}{K_y}U_s(\xi)
\end{aligned} \tag{2.9}$$

2.2.5 Combined Governing Equation

Taking a Fourier transformation of the relevant beam equation, say Equation (2.2a), we get

$$\begin{aligned}
&\bar{E}I\xi^4 U_s(\xi)e^{j(\omega+\xi V)t} - \rho_v h(\omega + \xi V)^2 U_s(\xi)e^{j(\omega+\xi V)t} - \rho_v I\left(1 + \frac{\bar{E}}{\kappa^2\bar{G}}\right)\xi^2 U_s(\xi)e^{j(\omega+\xi V)t}(\omega + \xi V)^2 \\
&\quad + \rho_v I\frac{\rho_v}{\kappa^2\bar{G}}U_s(\xi)e^{j(\omega+\xi V)t}(\omega + \xi V)^4 \\
&= \left(1 + \frac{\bar{E}I}{\kappa^2\bar{G}h}\xi^2 - \frac{\rho_v h^2}{12\kappa^2\bar{G}}(\omega + \xi V)^2\right)[F(\xi)e^{j(\omega+\xi V)t} - P(\xi, y = 0)e^{j(\omega+\xi V)t}]
\end{aligned}$$

$$\begin{aligned}
&\left[\bar{E}I\xi^4 - \rho_v h(\omega + \xi V)^2 - \rho_v I\left(1 + \frac{\bar{E}}{\kappa^2\bar{G}}\right)\xi^2(\omega + \xi V)^2 + \rho_v I\frac{\rho_v}{\kappa^2\bar{G}}(\omega + \xi V)^4\right]U_s(\xi) \\
&= \left(1 + \frac{\bar{E}I}{\kappa^2\bar{G}h}\xi^2 - \frac{\rho_v h^2}{12\kappa^2\bar{G}}(\omega + \xi V)^2\right)[F(\xi) - P(\xi, y = 0)]
\end{aligned} \tag{2.10}$$

Finally using the transformed and combined acoustic boundary condition as defined by Equation (2.9) in the transformed equation, Equation (2.10) reduces the equation as

$$\underbrace{\left[\bar{E}I\xi^4 - \rho_v h(\omega+\xi V)^2 - \rho_v I\left(1+\frac{\bar{E}}{\kappa^2\bar{G}}\right)\xi^2(\omega+\xi V)^2 + \rho_v I\frac{\rho_v}{\kappa^2\bar{G}}(\omega+\xi V)^4\right]}_{\text{Plate Impedance Operator} = Z_m} U_s(\xi)$$

$$= \underbrace{\left(1+\frac{\bar{E}I}{\kappa^2\bar{G}h}\xi^2 - \frac{\rho_v h^2}{12\kappa^2\bar{G}}(\omega+\xi V)^2\right)}_{Z_F}[F(\xi) - \underbrace{j\rho_0\frac{(\omega+\xi V)^2}{K_y}}_{\text{Acoustic Impedance Operator} = Z_a} U_s(\xi)] \quad (2.11)$$

On rearranging the terms we get

$$\mathbf{U_s}(\xi) = \frac{\mathbf{Z_F F}(\xi)}{\mathbf{Z_m} + \mathbf{Z_F Z_a}} \quad (2.12)$$

where

- **The Acoustic Impedance Operator** (Z_a) for the *Timoshenko beam*, *Rayleigh beam*, *Shear beam* and *Euler-Bernoulli beam* is given by

$$Z_a = \frac{j\rho_0(\omega+\xi V)^2}{K_y} \quad (2.13)$$

- **The Plate Impedance Operator** (Z_m) as

$$Z_m = \bar{E}I\xi^4 - \rho_v h(\omega+\xi V)^2 - \xi^2\rho_v I\left(1+\frac{\bar{E}}{\kappa^2\bar{G}}\right)(\omega+\xi V)^2 + \rho_v I\frac{\rho_v}{\kappa^2\bar{G}}(\omega+\xi V)^4$$

$$\ldots \quad Timoshenko\,beam \quad (2.14a)$$

$$Z_m = \bar{E}I\xi^4 - \rho_v h(\omega+\xi V)^2 - \xi^2\rho_v I(\omega+\xi V)^2 \qquad \ldots \quad Rayleigh\,beam \quad (2.14b)$$

$$Z_m = \bar{E}I\xi^4 - \rho_v h(\omega+\xi V)^2 - \xi^2\frac{\bar{E}I\rho_v}{\kappa^2\bar{G}}(\omega+\xi V)^2 \qquad \ldots \quad Shear\,beam \quad (2.14c)$$

$$Z_m = \bar{E}I\xi^4 - \rho_v h(\omega + \xi V)^2 \quad \ldots \quad Euler - Bernoulli\,beam \quad (2.14d)$$

- **The** (Z_F) by

$$Z_F = 1 + \frac{\bar{E}I}{\kappa^2 \bar{G}h}\xi^2 - \frac{\rho_v h^2}{12\kappa^2 \bar{G}}(\omega + \xi V)^2 \quad \ldots \quad Timoshenko\,beam \quad (2.15a)$$

$$Z_F = 1 \quad \ldots \quad Rayleigh\,beam \quad (2.15b)$$

$$Z_F = 1 + \frac{\bar{E}I}{\kappa^2 \bar{G}h}\xi^2 \quad \ldots \quad Shear\,beam \quad (2.15c)$$

$$Z_F = 1 \quad \ldots \quad Euler - Bernoulli\,beam \quad (2.15d)$$

Equation (2.12) is the expression that gives the structural response in the frequency domain. With the structural response known the acoustic power can be calculated. We shall now discuss the methodology of finding the total acoustic power.

2.2.6 Total Acoustic Power

The time averaged sound intensity is given by Morse and Ingard (1968) as

$$\bar{I} = \frac{1}{T}\int_0^T \overline{PV}dt \quad or \quad \bar{I} = \frac{1}{2}Re[P\dot{U}_s^*]$$

where

$\bar{I}$	is the time averaged sound intensity
P	is the sound pressure on the beam surface
$\dot{U}_s^*(\xi, t)$	is the beam surface velocity of conjugation

and

$$\dot{U}_s(\xi) = \frac{dU_s(\xi)}{dt} = j(\omega + \xi V)U_s(\xi) \tag{2.16}$$

In order to find the total acoustic power (Π), the surface acoustic intensity distribution needs to be integrated over the infinite length of the beam as

$$\Pi = \int_{-\infty}^{\infty} \frac{1}{2} Re[P(\xi, y = 0, t)\dot{U}_s^*(\xi, t)]d\xi$$

Upon substituting the sound pressure Equation (2.9) and calculating the surface velocity using Equation (2.16), the sound power radiated per unit width of the beam can be simplified as discussed in Appendix - A to yield

$$\Pi = \frac{\rho_0}{4\pi} Re\left[\int_{-\infty}^{\infty} \frac{(\omega + \xi V)^3}{K_y} |U_s(\xi)|^2 d\xi\right] \tag{2.17}$$

Limiting the study to subsonic motion of the moving load, the limits within which K_y is real is given by

$$\xi_1 = \frac{-K_0}{1+M} \leq \xi \leq \xi_2 = \frac{K_0}{1-M}$$

This allows us to rewrite the expression for the sound power as Equation (A.16) (see Appendix - A for detailed derivation) reproduced below as

$$\Pi = \frac{\rho_0}{4\pi} Re\left[\int_{\xi_1}^{\xi_2} \frac{(\omega + \xi V)^3}{K_y} |U_s(\xi)|^2 d\xi\right] \tag{2.18}$$

This completes the formulation of an expression for the total acoustic power for various beam types subjected to a moving load.

2.2.7 Nondimensionalization

To be able to solve Equation (2.18) numerically, the concept of non-dimensional parameters as discussed in Appendix - B is used. Using Equation (2.12) in Equation (2.18) and

using the non-dimensional parameters we get Equation (B.20) as

$$W = \int_{\zeta_1}^{\zeta_2} \alpha^3 \beta \left| Z_F F(\xi) \right|^2 |D|^{-2} d\zeta$$

Using the requisite non-dimensional force (in the present case a moving harmonic force) acting on the beam the above expression simplifies to

$$W = \int_{\zeta_1}^{\zeta_2} \alpha^3 \beta \left| Z_F \frac{sin(\zeta K_0 L)}{\zeta K_0 L} \right|^2 |D|^{-2} d\zeta \tag{2.19}$$

where

$$\zeta_1 = \frac{-1}{1+M} \leq \zeta \leq \zeta_2 = \frac{1}{1-M}$$

$$\alpha = 1 + M\zeta$$

$$\beta = \sqrt{\alpha^2 - \zeta^2}$$

$$D = \beta(D_1 - D_2 + D_3) + jD_4$$

The expression for D_1, D_2, D_3, D_4 and Z_F vary based on the type of the beam as under

(a) *Timoshenko beam*:

$$Z_F = 1 + \frac{2(1+\nu)\gamma^4}{\kappa^2} \left(\frac{C_0}{C_L} \right)^2 \left[\zeta^2 - \frac{1}{1+\eta j} \left(\frac{C_0}{C_L} \right)^2 \alpha^2 \right]$$

$$D_1 = \gamma^4 \zeta^4 (1 + \eta j)$$

$$D_2 = \alpha^2 \left[1 + [1 + \frac{2(1+\nu)}{\kappa^2}] \gamma^4 \zeta^2 \left(\frac{C_0}{C_L} \right)^2 \right]$$

$$D_3 = \frac{2(1+\nu)}{\kappa^2(1+\eta j)} \alpha^4 \gamma^4 \left(\frac{C_0}{C_L} \right)^4$$

$$D_4 = Z_F \frac{\alpha_0 \alpha^2}{\gamma^2}$$

(b) *Rayleigh beam*:

$$
\begin{aligned}
Z_F &= 1 \\
D_1 &= \gamma^4\zeta^4(1+\eta j) \\
D_2 &= \alpha^2\left[1+\gamma^4\zeta^2\left(\frac{C_0}{C_L}\right)^2\right] \\
D_3 &= 0 \\
D_4 &= Z_F\frac{\alpha_0\alpha^2}{\gamma^2}
\end{aligned}
$$

(c) *Shear beam*:

$$
\begin{aligned}
Z_F &= 1+\frac{2(1+\nu)\gamma^4}{\kappa^2}\left(\frac{C_0}{C_L}\right)^2\zeta^2 \\
D_1 &= \gamma^4\zeta^4(1+\eta j) \\
D_2 &= \alpha^2\left[1+\frac{2(1+\nu)}{\kappa^2}\gamma^4\zeta^2\left(\frac{C_0}{C_L}\right)^2\right] \\
D_3 &= 0 \\
D_4 &= Z_F\frac{\alpha_0\alpha^2}{\gamma^2}
\end{aligned}
$$

(d) *Euler-Bernoulli beam*:

$$
\begin{aligned}
Z_F &= 1 \\
D_1 &= \gamma^4\zeta^4(1+\eta j) \\
D_2 &= \alpha^2 \\
D_3 &= 0 \\
D_4 &= Z_F\frac{\alpha_0\alpha^2}{\gamma^2}
\end{aligned}
$$

Equation (2.19) is used for undertaking a numerical analysis for the beam model. This numerical analysis is discussed in chapter 5 sections 5.5 and 5.6.

Chapter 3

Floating Airport

3.1 General Introduction

In Chapter 2 we formulated an expression for calculating the sound power radiated from a **ship** modeled as a beam subjected to a moving load. A natural extention to a beam problem is a plate problem and hence this chapter looks at the formulation of an expression of sound power from a floating airport modeled as a plate. Sound radiation caused by taking off of an airplane from a floating airport is an unexplored area which has a serious but unstudied impact on marine life.

In this chapter, we develop an expression for sound radiation using a Timoshenko-Mindlin plate model in section 3.2. Presence of mean flow and inplane loading on total sound power generated are further formulated in section 3.3 and section 3.4 respectively.

3.2 Floating Airport

3.2.1 Introduction

Because of their relatively simple construction and ease of maintenance, pontoon-type Very Large Floating Structures (VLFS) are considered to be one of the most promis-

ing designs for a floating airport or runway, particularly in sheltered areas. The typical dimensions are 5 km long, 1 km wide, and only a few meters deep. Due to their dimensions, even when no incoming waves exist, the structure still responds flexurally to moving loads like those from an airplane during landing or take-off. Thus the study of transient responses of a VLFS to impulsive and moving loads are a must. Only a few studies of transient problems for VLFS have been reported to date.

Like flexural deflections, the *sound generated* by moving loads on such structures is another important area of concern as it causes acoustic pollution for the marine life and has not been addressed to date. To study acoustic effects, a dynamic analysis of a three-dimensional runway with time varying loading during take-off would be exceeding difficult. This analysis can be made simpler by assuming that the runway behaves as a simple, infinitely long beam floating in water and supported by buoyancy. The model can be assumed to be a simple beam, described by a one dimensional Timoshenko-Mindlin plate equation.

To the best of the knowledge, no study of acoustic radiation from a floating airport (VLFS) due to moving loads has been reported in the literature. The aim of this study is to propose a simple methodology for calculating the sound radiation from such structures due to moving loads such as airplanes. An expression for the sound radiation for a floating platform is hence developed for a wavenumber ratio of 0.1 to 2.2. In developing the expression, Fourier transform methodology for a Timoshenko-Mindlin plate is utilised as suggested in Keltie and Peng (1988). Structural damping is ignored since there is no apparent resonant mechanism for such problems.

3.2.2 Formulation

3.2.2.1 Structure Definition

To eliminate the boundary effect of the finite length of the plate, they are assumed to extend to infinity. We assume that the runway behaves as a simple, infinitely long beam

floating in water and supported by buoyancy. The geometry and material properties are assumed to be linearly elastic. The structural damping is ignored since there is no apparent resonant mechanism in this problem. The water is assumed to be inviscid, and the flow resulting from the airplane take-off is irrotational. The x-axis is aligned with the length of the runway and the y-axis is directed vertically upwards, as seen in Figure 3.1. Because the floating runway is very narrow compared with its length, as a simplification, we assume:

- The deformation and loading do not vary across the runway.
- The structure behaves like a beam, described by the Timoshenko-Midlin plate equation.
- An excitation force of length $2L$ moving at a subsonic speed V is acting on the runway.
- The space $y > 0$ is filled with an acoustic medium such as water. The other side of the plate is assumed to be vacuum.

The moving force considered is given as a uniform distributed line force, given by

$$f(x,t) = \frac{f_0}{2L}[H(x - Vt + L) - H(x - Vt - L)]e^{j\omega t} \tag{3.1a}$$

or a point force given by

$$f(x,t) = f_0 e^{j\omega t}\delta(x - Vt) \tag{3.1b}$$

where f_0 is the strength of external force per unit width, $H(x)$ is the Heavyside step function, and $\delta(x - Vt)$ is a Delta function.

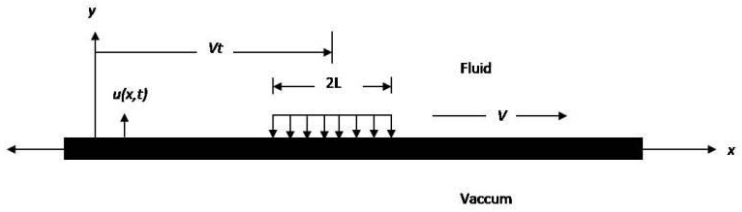

Fig. 3.1 Schematic representation of a floating airport problem

3.2.2.2 Governing Equation

The vibration equation for the elastic plate, including rotational inertia and transverse shear effects, is given by the Mindlin plate equation as

$$\left(\nabla^2 - \frac{\rho_v}{\kappa^2 G}\frac{\partial^2}{\partial t^2}\right)\left(D_s\nabla^2 - \frac{\rho_v h^3}{12}\frac{\partial^2}{\partial t^2}\right)u + \rho_v h\frac{\partial^2 u}{\partial t^2}$$
$$= \left(1 - \frac{D_s}{\kappa^2 G h}\nabla^2 + \frac{\rho_v h^2}{12\kappa^2 G}\frac{\partial^2}{\partial t^2}\right)[f(x,t) - p(x, y = 0, t)] \tag{3.2}$$

For a one dimensional plate, $\nabla = \frac{\partial}{\partial x}$, and the Timoshenko-Mindlin plate equation is obtained as

$$D_s\frac{\partial^4 u(x,t)}{\partial x^4} + \rho_v h\frac{\partial^2 u(x,t)}{\partial t^2} - \rho_v\left(I + \frac{D_s}{\kappa^2 G}\right)\frac{\partial^4 u(x,t)}{\partial x^2 \partial t^2} + \rho_v I\frac{\rho_v}{\kappa^2 G}\frac{\partial^4 u(x,t)}{\partial t^4}$$

$$= \left(1 - \frac{D_s}{\kappa^2 G h}\frac{\partial^2}{\partial x^2} + \frac{\rho_v h^2}{12\kappa^2 G}\frac{\partial^2}{\partial t^2}\right)[f(x,t) - p(x, y = 0, t)] \tag{3.3}$$

where

$u(x,t)$	is the transverse displacement of the plate
$D_s = \frac{Eh^3}{12(1-\nu^2)}$	is the flexural rigidity of the plate
E	the elastic modulus
$G = \frac{E}{2(1+\nu)}$	is the shear modulus
$I = \frac{h^3}{12}$	is the cross sectional moment of inertia per unit width
h	is height of the plate
ν	the Poisson's ratio
ρ_v	is the mass density of the material

$\kappa^2 = \frac{\pi^2}{12}$ is the cross sectional shape factor or the shear correction factor

$p(x, y = 0, t)$ is the acoustic pressure acting on the plate's surface.

3.2.2.3 Boundary Conditions

The pressure distribution induced by the vibrating beam in the acoustic medium is denoted by $p(x, y, t)$ and satisfies the wave equation in two-dimensional space, given by

$$(\frac{\partial^2}{\partial x^2} + \frac{\partial^2}{\partial y^2} - \frac{1}{C_0^2}\frac{\partial^2}{\partial t^2})p(x, y, t) = 0 \tag{3.4}$$

where C_0 is the sound speed in the acoustic medium.
If ρ_0 is the mass density of the acoustic medium, the boundary condition at $y = 0$ is given by

$$\rho_0 \frac{\partial^2 u}{\partial t^2} = -\frac{\partial p}{\partial y}\bigg|_{y=0} \tag{3.5}$$

3.2.2.4 Transforming Applicable Equations

The transformation of the response equation and the pressure equation has been discussed in section 2.2.4, however for completeness, the relevant expressions are reproduced. Applying the spatial Fourier transformation using Equation (1.2)

$$FT() = \int_{-\infty}^{\infty} () e^{i\xi x} dx$$

with ξ as the wave number variable, the force function in wave number domain may be written as

$$\begin{aligned} &\tilde{f}(\xi, t) = f_0 \tfrac{sin(\xi L)}{\xi L} e^{j(\omega + \xi V)t} = F(\xi) e^{j(\omega+\xi V)t} && \text{for harmonic line force} \\ &\tilde{f}(\xi, t) = f_0 e^{j(\omega+\xi V)t} = F(\xi) e^{j(\omega+\xi V)t} && \text{for a point force} \end{aligned} \tag{3.6a}$$

the transformed displacement may be written as

$$\tilde{U}_s(\xi,t) = U_s(\xi)e^{j(\omega+\xi V)t} \tag{3.6b}$$

and the transformed pressure may be written as

$$\tilde{P}(\xi,y,t) = P(\xi,y)e^{j(\omega+\xi V)t} \tag{3.6c}$$

Taking Fourier transformation of Equation (3.4) and using Equation (3.6c) we get

$$(\frac{\partial^2}{\partial y^2} - \xi^2 - \frac{j^2(\omega+\xi V)^2}{C_0^2})P(\xi,y)e^{j(\omega+\xi V)t} = 0$$

$$(\frac{\partial^2}{\partial y^2} - \xi^2 + \left[\frac{\omega+\xi V}{C_0}\right]^2)P(\xi,y)e^{j(\omega+\xi V)t} = 0 \tag{3.7}$$

Defining $M(= V/C_0)$ as the Mach number and $K_0(= \omega/C_0)$ as the acoustic wave number, Equation (3.7) can be rewritten as

$$(\frac{\partial^2}{\partial y^2} - \underbrace{\{\xi^2 - [K_0+\xi M]^2\}}_{K_y})P(\xi,y)e^{j(\omega+\xi V)t} = 0$$

where K_y is defined as

$$K_y = \begin{cases} -j\sqrt{\xi^2 - (K_0+M\xi)^2} & for \quad \xi^2 > (K_0+M\xi)^2 \\ \\ \sqrt{(K_0+M\xi)^2 - \xi^2} & for \quad \xi^2 < (K_0+M\xi)^2 \end{cases} \tag{3.8}$$

Similarly taking Fourier transformation of Equation (3.5) and using Equation (3.6b) and Equation (3.6c) we get

$$-\rho_0(\omega+\xi V)^2 U_s(\xi)e^{j(\omega+\xi V)t} = -\frac{P(\xi,y)}{\partial y}e^{j(\omega+\xi V)t}\Big|_{y=0} \tag{3.9}$$

For sound pressure on the surface ($y = 0$), from Equation (3.5) we get

$$P(\xi, y) = P(\xi, y = 0)e^{-jK_y y}$$

Hence Equation (3.9) gets modified as

$$\begin{aligned}
-\rho_0(\omega + \xi V)^2 U_s(\xi)e^{j(\omega+\xi V)t} &= -\frac{P(\xi, y = 0)e^{-jK_y y}}{\partial y}e^{j(\omega+\xi V)t}\bigg|_{y=0} \\
&= -P(\xi, y = 0)(-jK_y)e^{-jK_y y}e^{j(\omega+\xi V)t}\bigg|_{y=0} \\
&= -P(\xi, y = 0)(-jK_y)e^{j(\omega+\xi V)t}
\end{aligned}$$

Thus

$$\begin{aligned}
P(\xi, y = 0) &= -\rho_0\frac{(\omega + \xi V)^2}{jK_y}U_s(\xi) \\
&= j\rho_0\frac{(\omega + \xi V)^2}{K_y}U_s(\xi)
\end{aligned} \tag{3.10}$$

3.2.2.5 Combined Governing Equation

Taking Fourier transformation of the plate equation, Equation (3.3), we get

$$\begin{aligned}
&D_s\xi^4 U_s(\xi)e^{j(\omega+\xi V)t} - \rho_v h(\omega + \xi V)^2 U_s(\xi)e^{j(\omega+\xi V)t} - \rho_v\left(I + \frac{D_s}{\kappa^2 G}\right)\xi^2(\omega + \xi V)^2 U_s(\xi)e^{j(\omega+\xi V)t} \\
&\quad + \rho_v I\frac{\rho_v}{\kappa^2 G}U_s(\xi)e^{j(\omega+\xi V)t}(\omega + \xi V)^4 \\
&= \left(1 + \frac{D_s}{\kappa^2 G h}\xi^2 - \frac{\rho_v h^2}{12\kappa^2 G}(\omega + \xi V)^2\right)[F(\xi)e^{j(\omega+\xi V)t} - P(\xi, y = 0)e^{j(\omega+\xi V)t}]
\end{aligned}$$

$$\begin{aligned}
&\left[D_s\xi^4 - \rho_v h(\omega + \xi V)^2 - \rho_v\left(I + \frac{D_s}{\kappa^2 G}\right)\xi^2(\omega + \xi V)^2 + \rho_v I\frac{\rho_v}{\kappa^2 G}(\omega + \xi V)^4\right]U_s(\xi) \\
&= \left(1 + \frac{D_s}{\kappa^2 G h}\xi^2 - \frac{\rho_v h^2}{12\kappa^2 G}(\omega + \xi V)^2\right)[F(\xi) - P(\xi, y = 0)]
\end{aligned} \tag{3.11}$$

Finally using the transformed and combined acoustic boundary condition as defined by Equation (3.10) in the transformed equation, Equation (3.11) reduces to

$$\underbrace{\left[D_s\xi^4 - \rho_v h(\omega+\xi V)^2 - \rho_v\left(I + \frac{D_s}{\kappa^2 G}\right)\xi^2(\omega+\xi V)^2 + \rho_v I\frac{\rho_v}{\kappa^2 G}(\omega+\xi V)^4\right]}_{\text{Plate Impedance Operator} = Z_m} U_s(\xi)$$

$$= \underbrace{\left(1 + \frac{D_s}{\kappa^2 G h}\xi^2 - \frac{\rho_v h^2}{12\kappa^2 G}(\omega+\xi V)^2\right)}_{Z_F}[F(\xi) - \underbrace{j\rho_0\frac{(\omega+\xi V)^2}{K_y}}_{\text{Acoustic Impedance Operator} = Z_a} U_s(\xi)] \quad (3.12)$$

On rearranging terms we get

$$\mathbf{U_s}(\xi) = \frac{\mathbf{Z_F F}(\xi)}{\mathbf{Z_m} + \mathbf{Z_F Z_a}} \quad (3.13)$$

where

- **The Acoustic Impedance Operator** (Z_a) is given by

$$Z_a = j\rho_0\frac{(\omega+\xi V)^2}{K_y} \quad (3.14)$$

- **The Plate Impedance Operator** (Z_m) as

$$Z_m = D_s\xi^4 - \rho_v h(\omega+\xi V)^2 - \xi^2\rho_v\left(I + \frac{D_s}{\kappa^2 G}\right)(\omega+\xi V)^2 + \rho_v I\frac{\rho_v}{\kappa^2\bar{G}}(\omega+\xi V)^4 \quad (3.15)$$

- **The** (Z_F) by

$$Z_F = 1 + \frac{D_s}{\kappa^2 G h}\xi^2 - \frac{\rho_v h^2}{12\kappa^2 G}(\omega+\xi V)^2 \quad (3.16)$$

Equation (3.13) gives the structural response in the frequency domain. From this the acoustic power can be calculated. We shall now discuss the methodology of finding the total acoustic power.

3.2.2.6 Total Acoustic Power

The time averaged sound intensity is given by Morse and Ingard (1968) as

$$\bar{I} = \frac{1}{T}\int_0^T \overline{PV}dt \quad or \quad \bar{I} = \frac{1}{2}Re[P\dot{U}_s^*(\xi,t)]$$

where

$\bar{I}$	is the time averaged sound intensity
P	is the sound pressure on the plate surface
$\dot{U}_s^*(\xi,t)$	is the plate surface velocity of conjugation

and

$$\dot{U}_s(\xi) = \frac{dU_s(\xi)}{dt} = j(\omega + \xi V)U_s(\xi) \tag{3.17}$$

In order to find the total acoustic power (Π), the surface acoustic intensity distribution needs to be integrated over the infinite length of the plate as

$$\Pi = \int_{-\infty}^{\infty} \frac{1}{2}Re[P(\xi, y=0, t)\dot{U}_s^*(\xi,t)]d\xi$$

Upon substituting the sound pressure using Equation (3.10) and calculating the surface velocity using Equation (3.17), the sound power radiated per unit width of the plate can be simplified as discussed in Appendix - A to yield

$$\Pi = \frac{\rho_0}{4\pi}Re\left[\int_{-\infty}^{\infty}\frac{(\omega+\xi V)^3}{K_y}|U_s(\xi)|^2 d\xi\right] \tag{3.18}$$

Limiting the study to subsonic motion of the moving load, the limits within which K_y is real is given by

$$\xi_1 = \frac{-K_0}{1+M} \leq \xi \leq \xi_2 = \frac{K_0}{1-M}$$

This allows us to rewrite the expression for the sound power as Equation (A.16) (see

Appendix - A for detailed derivation) reproduced below as

$$\Pi = \frac{\rho_0}{4\pi} Re\left[\int_{\xi_1}^{\xi_2} \frac{(\omega + \xi V)^3}{K_y} |U_s(\xi)|^2 d\xi\right] \tag{3.19}$$

This completes the formulation of an expression for the total acoustic power for a floating airport subjected to the landing / taking off of an airplane.

3.2.2.7 Nondimensionalization

In order to present the numerical results, the concept of non-dimensional parameters as discussed in Appendix - B is used. Assuming that the moving load applied is a uniformly distributed line force, defined by Equation (3.1) we get the non-dimensional sound power as:

$$W = \int_{\zeta_1}^{\zeta_2} \alpha^3 \beta \left| Z_F \frac{sin(\zeta K_0 L)}{\zeta K_0 L} \right|^2 |D|^{-2} d\zeta \tag{3.20}$$

where

$$\zeta_1 = \frac{-1}{1+M} \leq \zeta \leq \zeta_2 = \frac{1}{1-M}$$

$$\alpha = 1 + M\zeta$$

$$\beta = \sqrt{\alpha^2 - \zeta^2}$$

$$D = \beta(D_1 - D_2 + D_3) + jD_4$$

where the expression for D_1, D_2, D_3, D_4 and Z_F for a Timoshenko-Mindlin plate are as under

$$Z_F = 1 + \frac{2(1+\nu)\gamma^4}{\kappa^2}\left(\frac{C_0}{C_L}\right)^2\left[\zeta^2 - \left(\frac{C_0}{C_L}\right)^2\alpha^2\right]$$

$$D_1 = \gamma^4\zeta^4$$

$$D_2 = \alpha^2\left[1 + [1 + \frac{2(1+\nu)}{\kappa^2}]\gamma^4\zeta^2\left(\frac{C_0}{C_L}\right)^2\right]$$

$$D_3 = \frac{2(1+\nu)}{\kappa^2}\alpha^4\gamma^4\left(\frac{C_0}{C_L}\right)^4$$

$$D_4 = Z_F \frac{\alpha_0 \alpha^2}{\gamma^2}$$

Solving Equation (3.20) numerically, the total sound power radiated by a floating airport subjected to a moving uniformly distributed line force can be obtained. The numerical analysis for this formulation is discussed in section 5.7.

3.3 Floating Airport subjected to a Mean Flow

3.3.1 General Introduction

The literature on fluid-structure interaction in the presence of fluid flow is relatively scarce. This is not because fluid flow is unimportant, but because problems often get too complicated when relative motion between an elastic structure and a surrounding fluid medium is involved. This is especially true when the dimension of a structure is finite, and the compressibility and viscosity of the fluid medium must be considered. One way of obtaining an understanding of the physics behind this type of fluid-structure interaction is to examine a simplified version of the problem in which the dimension of a structure extends to infinity, the fluid moves at a constant (mean) speed, and the effects of fluid compressibility and viscosity are neglected.

3.3.2 Introduction

Acoustic analysis in the presence of a *mean flow* or *current* complicates the problem further by modifying the effect of the moving load. The available literature on study of acoustics in mean flow is however very small. The main reason for this is that the mean flow speed is often too low to have any real impact on acoustics that are of practical engineering relevance. Another reason is that the fluid-structure interaction problem usually becomes too complicated to be solved analytically when mean flow is considered. Consequently problems are often treated in the same way as those in a stationary fluid medium. The effect of mean flow on the response of a fluid-loaded structure thus remains mostly unexplored. In this section, we shall formulate an expression to obtain the total sound power radiated by a floating airport subject to a moving load in the presence of a mean flow.

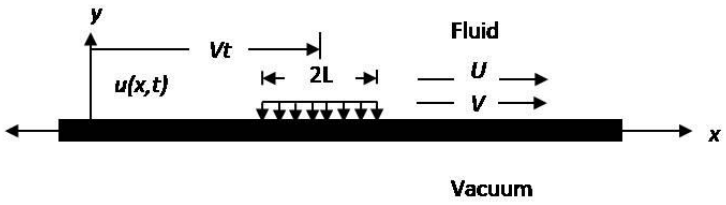

Fig. 3.2 Floating airport subjected to a moving load and mean flow

3.3.3 Formulation

3.3.3.1 Structure Definition

The structural definition of the floating airport as discussed in section 3.2.2.1 is utilised. To model a mean flow, a subsonic mean flow of speed U, moving in the positive x direction is considered to be present in the water as seen in Figure 3.2.

3.3.3.2 Governing Equation

Since the structural definition of the problem has not been altered from that defined in section 3.2.2.1 the general equation used herein is the same as Equation (3.3) i.e

$$D_s\frac{\partial^4 u(x,t)}{\partial x^4}+\rho_v h\frac{\partial^2 u(x,t)}{\partial t^2}-\rho_v\left(I+\frac{D_s}{\kappa^2 G}\right)\frac{\partial^4 u(x,t)}{\partial x^2\partial t^2}+\rho_v I\frac{\rho_v}{\kappa^2 G}\frac{\partial^4 u(x,t)}{\partial t^4}$$

$$=\left(1-\frac{D_s}{\kappa^2 G h}\frac{\partial^2}{\partial x^2}+\frac{\rho_v h^2}{12\kappa^2 G}\frac{\partial^2}{\partial t^2}\right)[f(x,t)-p(x,y=0,t)] \tag{3.21}$$

where

$u(x,t)$	is the transverse displacement of the plate
$D_s=\frac{Eh^3}{12(1-\nu^2)}$	is the flexural rigidity of the plate
E	the elastic modulus
$G=\frac{E}{2(1+\nu)}$	is the shear modulus
$I=\frac{h^3}{12}$	is the cross sectional moment of inertia per unit width
h	is height of the plate
ν	is the Poisson's ratio
ρ_v	is the mass density of the material

$\kappa^2 = \frac{\pi^2}{12}$ is the cross sectional shape factor or the shear correction factor

$p(x, y = 0, t)$ is the acoustic pressure acting on the plate's surface.

3.3.3.3 Boundary Condition

To account for the presence of current the operator $\frac{\partial}{\partial t}$ is replaced by the operator $\frac{\partial}{\partial t}+U\frac{\partial}{\partial x}$ in the expressions of pressure distribution and the boundary condition at $y = 0$. The pressure distribution induced by the vibrating plate in the acoustic medium denoted by $p(x, y, t)$ thus satisfies the wave equation in two-dimensional space, given by

$$\left[\frac{\partial^2}{\partial x^2} + \frac{\partial^2}{\partial y^2} - \frac{1}{C_0^2}\left(\frac{\partial}{\partial t} + U\frac{\partial}{\partial x}\right)^2\right] p(x, y, t) = 0 \tag{3.22}$$

where C_0 is the speed of sound in the acoustic medium and U is the speed of mean flow of the fluid. If ρ_0 is the mass density of the acoustic medium, the boundary condition at $y = 0$ is modified as

$$\rho_0\left(\frac{\partial}{\partial t} + U\frac{\partial}{\partial x}\right)^2 u = -\frac{\partial p}{\partial y}\bigg|_{y=0} \tag{3.23}$$

3.3.3.4 Transformation and Combined Governing Equation

By applying the spatial Fourier transformation $FT() = \int_{-\infty}^{\infty}()e^{i\xi x}dx$, with ξ as the wave number variable and proceeding in the same manner as explained in sections 3.2.2.4 and 3.2.2.5 we get the combined governing equation as

$$\mathbf{U_s}(\xi) = \frac{\mathbf{Z_F F}(\xi)}{\mathbf{Z_m} + \mathbf{Z_F Z_a}} \tag{3.24}$$

and

$$P(\xi, y = 0) = \frac{j\rho_0(\omega + \xi[V - U])^2}{K_y} U_s(\xi) \tag{3.25}$$

where the acoustic impedance operator (Z_a) is given by

$$Z_a = j\rho_0 \frac{(\omega + \xi[V-U])^2}{K_y} \tag{3.26}$$

the plate impedance operator (Z_m) as

$$Z_m = D_s\xi^4 - \rho_v h(\omega+\xi[V-U])^2 - \xi^2\rho_v\left(I+\frac{D_s}{\kappa^2 G}\right)(\omega+\xi[V-U])^2 + \rho_v I\frac{\rho_v}{\kappa^2 G}(\omega+\xi[V-U])^4 \tag{3.27}$$

the Z_F by

$$Z_F = 1 + \frac{D_s}{\kappa^2 G h}\xi^2 - \frac{\rho_v h^2}{12\kappa^2 G}(\omega + \xi[V-U])^2 \tag{3.28}$$

and K_y is given by

$$K_y = \begin{cases} -j\sqrt{\xi^2 - (K_0 + \bar{M}\xi)^2} & for \quad \xi^2 > (K_0 + \bar{M}\xi)^2 \\ \\ \sqrt{(K_0 + \bar{M}\xi)^2 - \xi^2} & for \quad \xi^2 < (K_0 + \bar{M}\xi)^2 \end{cases} \tag{3.29}$$

where $M(= V/C_0)$ is the Mach number, $\bar{M}(= [V-U]/C_0)$ the modified Mach number and $K_0(= \omega/C_0)$ the acoustic wave number.

We shall now discuss the methodology of finding the total acoustic power.

3.3.3.5 Total Acoustic Power

The time averaged sound intensity is given by Morse and Ingard (1968) as

$$\bar{I} = \frac{1}{T}\int_0^T \overline{PV}dt \quad or \quad \bar{I} = \frac{1}{2}Re[P\dot{U}_s^*(\xi,t)] \tag{3.30}$$

where

$\bar{I}$	is the time averaged sound intensity
P	is the sound pressure on the plate surface

$\dot{U}_s^*(\xi, t)$ is the plate surface velocity of conjugation

$$\dot{U}_s(\xi) = \frac{dU_s(\xi)}{dt} = j(\omega + \xi[V - U])U_s(\xi) \tag{3.31}$$

In order to find the total acoustic power (Π), the surface acoustic intensity distribution may be integrated over the infinite length of the plate as

$$\Pi = \int_{-\infty}^{\infty} \frac{1}{2} Re[P(\xi, y = 0, t)\dot{U}_s^*(\xi, t)]d\xi$$

Upon substituting the sound pressure given by Equation (3.25) and the surface velocity of the plate given by Equation (3.31), the sound power radiated per unit width of the plate can be simplified as

$$\Pi = \frac{\rho_0}{4\pi} Re\left[\int_{-\infty}^{\infty} \frac{(\omega + \xi[V - U])^3}{K_y} |U_s(\xi)|^2 d\xi\right] \tag{3.32}$$

Limiting the study to subsonic motion of the moving load, the limits within which K_y is real is given by

$$\xi_1 = \frac{-K_0}{1 + \bar{M}} \leq \xi \leq \xi_2 = \frac{K_0}{1 - \bar{M}}$$

This allows us to rewrite the expression for the sound power as

$$\Pi = \frac{\rho_0}{4\pi} Re\left[\int_{\xi_1}^{\xi_2} \frac{(\omega + \xi[V - U])^3}{K_y} |U_s(\xi)|^2 d\xi\right] \tag{3.33}$$

This completes the formulation of an expression for the total acoustic power for a Timoshenko-Mindlin plate subjected to a moving load in the presence of a mean flow in the fluid.

3.3.3.6 Nondimensionalization

In order to present the numerical results, the concept of non-dimensional parameters as discussed in Appendix - B is used to get the dimensionless radiated sound power per

unit width. Assuming that the moving load applied is a uniformly distributed line force, defined by Equation (3.1) we get the non-dimensional sound power as:

$$W = \int_{\zeta_1}^{\zeta_2} \alpha^3 \beta \left| Z_F \frac{sin(\zeta K_0 L)}{\zeta K_0 L} \right|^2 |D|^{-2} d\zeta \tag{3.34}$$

where

$$\zeta_1 = \frac{-1}{1+\bar{M}} \leq \zeta \leq \zeta_2 = \frac{1}{1-\bar{M}}$$

$$\alpha = 1 + \bar{M}\zeta$$

$$\beta = \sqrt{\alpha^2 - \zeta^2}$$

$$D = \beta(D_1 - D_2 + D_3) + jD_4$$

$$Z_F = 1 + \frac{2(1+\nu)\gamma^4}{\kappa^2}\left(\frac{C_0}{C_L}\right)^2 \left[\zeta^2 - \left(\frac{C_0}{C_L}\right)^2 \alpha^2(1-\nu^2)\right]$$

$$D_1 = \gamma^4 \zeta^4$$

$$D_2 = \alpha^2 \left[1 + [1 + \frac{2(1+\nu)}{\kappa^2(1-\nu^2)}]\gamma^4\zeta^2 \left(\frac{C_0}{C_L}\right)^2 (1-\nu^2)\right]$$

$$D_3 = \frac{2(1+\nu)}{\kappa^2}\alpha^4\gamma^4 \left(\frac{C_0}{C_L}\right)^4 (1-\nu^2)$$

$$D_4 = Z_F \frac{\alpha_0 \alpha^2}{\gamma^2}$$

Numerical solution to Equation (3.34) provides the total sound power generated from a floating airport subjected to a moving load in the presence of a mean flow. The numerical analysis using this formulation has been discussed in section 5.8.

3.4 Floating Airport subjected to Inplane Loading

3.4.1 General Introduction

In section 3.2 we developed the generalised equation for calculating the total sound power for a floating airport subjected to the landing / taking off of an airplane. This expression was then extended in section 3.3 with the floating airport being subjected to a mean flow. In the present section we shall look at the same floating airport as discussed in section 3.2 but subjected to an inplane loading in place of a mean flow. The physical presence of such loads is seen when the structure is subjected to loads such as berthing, plate connections, dynamic loading and initial structural imperfections.

3.4.2 Introduction

Berthing, plate connections, initial plate deformation, corrosion, hogging, sagging are some forms of inducing additional loads in the form of compression / tension to the plating of a VLFS. The effect of such loads cannot be neglected. Sound radiation caused by taking off of an airplane from a floating VLFS is a design use of such structures which is bound to get effected by these added loads. Even though a VLFS is structurally very long, the longitudinal strength does not play an important role in their design. However the most severe type of loading for the bottom plate occurs when the structure is subjected to the combined action of uniformly distributed hydrostatic lateral loading and compression due to hogging. Similarly for the deck plate, maximum loading occurs when the structure is subjected to compression / tension due to sagging / hogging respectively. The inplane loading plays an important role for such structures during berthing, plate connections at ends, initial deformation and corrosion to name a few and hence needs to be accounted for in the studies. A compressive inplane load of magnitude Q per unit width is considered to be present. If the load is tensile then it attains a magnitude $-Q$.

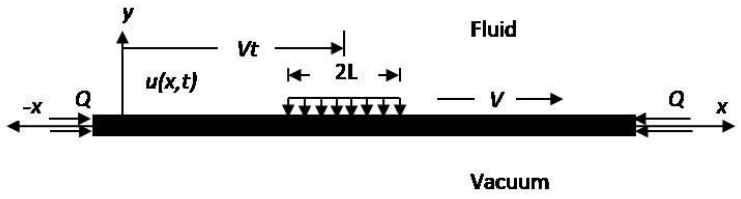

Fig. 3.3 Floating airport subjected to a moving load and inplane load

3.4.3 Formulation

3.4.3.1 Structural Definition

The structural definition of the floating airport as discussed in section 3.2.2.1 is utilised in this section too. To model the inplane loading a compressive inplane load of magnitude Q per unit width is considered to be present as seen in Figure 3.3. If the load is tensile then it attains a magnitude $-Q$.

3.4.3.2 Governing Equation

The vibration equation for a dimensional elastic plate, including rotational inertia, transverse shear effects and inplane loading, is given by the Timoshenko-Mindlin plate equation as

$$D_s\frac{\partial^4 u(x,t)}{\partial x^4}+Q\frac{\partial^2 u(x,t)}{\partial x^2}+\rho_v h\frac{\partial^2 u(x,t)}{\partial t^2}-\rho_v\left(I+\frac{D_s}{\kappa^2 G}\right)\frac{\partial^4 u(x,t)}{\partial x^2\partial t^2}+\rho_v I\frac{\rho_v}{\kappa^2 G}\frac{\partial^4 u(x,t)}{\partial t^4}$$

$$=\left(1-\frac{D_s}{\kappa^2 G h}\frac{\partial^2}{\partial x^2}+\frac{\rho_v h^2}{12\kappa^2 G}\frac{\partial^2}{\partial t^2}\right)[f(x,t)-p(x,y=0,t)] \tag{3.35}$$

where

$u(x,t)$	is the transverse displacement of the plate
$D_s=\frac{Eh^3}{12(1-\nu^2)}$	is the flexural rigidity of the plate
E	the elastic modulus
$G=\frac{E}{2(1+\nu)}$	is the shear modulus
$I=\frac{h^3}{12}$	is the cross sectional moment of inertia per unit width
h	is height of the plate

ν	the Poisson's ratio
ρ_v	is the mass density of the material
$\kappa^2 = \frac{\pi^2}{12}$	is the cross sectional shape factor or the shear correction factor
$p(x, y = 0, t)$	is the acoustic pressure acting on the plate's surface.
Q	Compressive inplane load

3.4.3.3 Boundary Conditions

The boundary conditions valid for this formulations are the same as discussed in section 3.2.2.3. However for continuity, we repeat them, wherein the pressure distribution induced by the vibrating plate in the acoustic medium is denoted by $p(x, y, t)$ and satisfies the wave equation in two-dimensional space, given by

$$(\frac{\partial^2}{\partial x^2} + \frac{\partial^2}{\partial y^2} - \frac{1}{C_0^2}\frac{\partial^2}{\partial t^2})p(x, y, t) = 0 \tag{3.36}$$

where C_0 is the sound speed in the acoustic medium.
If ρ_0 is the mass density of the acoustic medium, the boundary condition at $y = 0$ is given by

$$\rho_0 \frac{\partial^2 u}{\partial t^2} = -\frac{\partial p}{\partial y}\bigg|_{y=0} \tag{3.37}$$

3.4.3.4 Transforming Applicable Equations

The transformation of the response equation and the pressure equation has been discussed in section 2.2.4, however for completeness, the relevant expression are reproduced here. Applying the spatial Fourier transformation using Equation (1.2)

$$FT() = \int_{-\infty}^{\infty} () e^{i\xi x} dx$$

with ξ as the wave number variable, the force function in wave number domain may be written as

$$\begin{aligned} \tilde{f}(\xi,t) &= f_0 \tfrac{sin(\xi L)}{\xi L} e^{j(\omega+\xi V)t} = F(\xi) e^{j(\omega+\xi V)t} \quad \text{for harmonic line force} \\ \tilde{f}(\xi,t) &= f_0 e^{j(\omega+\xi V)t} = F(\xi) e^{j(\omega+\xi V)t} \qquad \text{for a point force} \end{aligned} \tag{3.38a}$$

the transformed displacement as

$$\tilde{U}(\xi,t) = U(\xi) e^{j(\omega+\xi V)t} \tag{3.38b}$$

and the transformed pressure as

$$\tilde{P}(\xi,y,t) = P(\xi,y) e^{j(\omega+\xi V)t} \tag{3.38c}$$

Taking Fourier transformation of Equation (3.36) and using Equation (3.38c) we get

$$(\frac{\partial^2}{\partial y^2} - \xi^2 - \frac{j^2(\omega+\xi V)^2}{C_0^2}) P(\xi,y) e^{j(\omega+\xi V)t} = 0$$

$$(\frac{\partial^2}{\partial y^2} - \xi^2 + \left[\frac{\omega+\xi V}{C_0}\right]^2) P(\xi,y) e^{j(\omega+\xi V)t} = 0 \tag{3.39}$$

Defining $M(= V/C_0)$ as the Mach number and $K_0(= \omega/C_0)$ as the acoustic wave number, Equation (3.39) can be rewritten as

$$(\frac{\partial^2}{\partial y^2} - \underbrace{\{\xi^2 - [K_0 + \xi M]^2\}}_{K_y}) P(\xi,y) e^{j(\omega+\xi V)t} = 0$$

where K_y is defined as

$$K_y = \begin{cases} -j\sqrt{\xi^2 - (K_0 + M\xi)^2} & for \quad \xi^2 > (K_0 + M\xi)^2 \\ \\ \sqrt{(K_0 + M\xi)^2 - \xi^2} & for \quad \xi^2 < (K_0 + M\xi)^2 \end{cases} \tag{3.40}$$

Similarly taking Fourier transformation of Equation (3.37) and using Equation (3.38b) and Equation (3.38c) we get

$$-\rho_0(\omega+\xi V)^2 U_s(\xi)e^{j(\omega+\xi V)t} = -\frac{P(\xi,y)}{\partial y}e^{j(\omega+\xi V)t}\bigg|_{y=0} \tag{3.41}$$

For sound pressure on the surface ($y=0$), from Equation (3.37) we get

$$P(\xi,y) = P(\xi,y=0)e^{-jK_y y}$$

Hence Equation (3.41) gets modified as

$$\begin{aligned}
-\rho_0(\omega+\xi V)^2 U_s(\xi)e^{j(\omega+\xi V)t} &= -\frac{P(\xi,y=0)e^{-jK_y y}}{\partial y}e^{j(\omega+\xi V)t}\bigg|_{y=0} \\
&= -P(\xi,y=0)(-jK_y)e^{-jK_y y}e^{j(\omega+\xi V)t}\bigg|_{y=0} \\
&= -P(\xi,y=0)(-jK_y)e^{j(\omega+\xi V)t}
\end{aligned}$$

Thus

$$\begin{aligned}
P(\xi,y=0) &= -\rho_0\frac{(\omega+\xi V)^2}{jK_y}U_s(\xi) \\
&= j\rho_0\frac{(\omega+\xi V)^2}{K_y}U_s(\xi)
\end{aligned} \tag{3.42}$$

3.4.3.5 Combined Governing Equation

Taking Fourier transformation of the plate equation, Equation (3.35), we get

$$\begin{aligned}
&D_s\xi^4 U_s(\xi)e^{j(\omega+\xi V)t} - Q\xi^2 U_s(\xi)e^{j(\omega+\xi V)t} - \rho_v h(\omega+\xi V)^2 U_s(\xi)e^{j(\omega+\xi V)t} \\
&\quad - \rho_v\left(I + \frac{D_s}{\kappa^2 G}\right)\xi^2(\omega+\xi V)^2 U_s(\xi)e^{j(\omega+\xi V)t} + \rho_v I\frac{\rho_v}{\kappa^2 G}(\omega+\xi V)^4 U_s(\xi)e^{j(\omega+\xi V)t} \\
&= \left(1 + \frac{D_s}{\kappa^2 Gh}\xi^2 - \frac{\rho_v h^2}{12\kappa^2 G}(\omega+\xi V)^2\right)[F(\xi)e^{j(\omega+\xi V)t} - P(\xi,y=0)e^{j(\omega+\xi V)t}]
\end{aligned}$$

$$\left[D_s\xi^4 - Q\xi^2 - \rho_v h(\omega+\xi V)^2 - \rho_v\left(I + \frac{D_s}{\kappa^2 G}\right)\xi^2(\omega+\xi V)^2 + \rho_v I\frac{\rho_v}{\kappa^2 G}(\omega+\xi V)^4\right]U_s(\xi)$$
$$= \left(1 + \frac{D_s}{\kappa^2 G h}\xi^2 - \frac{\rho_v h^2}{12\kappa^2 G}(\omega+\xi V)^2\right)[F(\xi) - P(\xi, y=0)] \tag{3.43}$$

Finally using the transformed and combined acoustic boundary condition as defined by Equation (3.42) in the transformed equation, Equation (3.43) reduces to

$$\underbrace{\left[D_s\xi^4 - Q\xi^2 - \rho_v h(\omega+\xi V)^2 - \rho_v\left(I + \frac{D_s}{\kappa^2 G}\right)\xi^2(\omega+\xi V)^2 + \rho_v I\frac{\rho_v}{\kappa^2 G}(\omega+\xi V)^4\right]}_{\text{Plate Impedance Operator} = Z_m} U_s(\xi)$$

$$= \underbrace{\left(1 + \frac{D_s}{\kappa^2 G h}\xi^2 - \frac{\rho_v h^2}{12\kappa^2 G}(\omega+\xi V)^2\right)}_{Z_F}[F(\xi) - \underbrace{j\rho_0\frac{(\omega+\xi V)^2}{K_y}}_{\text{Acoustic Impedance Operator} = Z_a} U_s(\xi)] \tag{3.44}$$

On rearranging terms we get

$$\mathbf{U_s}(\xi) = \frac{\mathbf{Z_F F}(\xi)}{\mathbf{Z_m} + \mathbf{Z_F Z_a}} \tag{3.45}$$

where

- **The Acoustic Impedance Operator** (Z_a) is given by

$$Z_a = j\rho_0\frac{(\omega+\xi V)^2}{K_y} \tag{3.46}$$

- **The Plate Impedance Operator** (Z_m) as

$$Z_m = D_s\xi^4 - Q\xi^2 - \rho_v h(\omega+\xi V)^2 - \xi^2\rho_v\left(I + \frac{D_s}{\kappa^2 G}\right)(\omega+\xi V)^2 + \rho_v I\frac{\rho_v}{\kappa^2 G}(\omega+\xi V)^4 \tag{3.47}$$

- **The** (Z_F) by

$$Z_F = 1 + \frac{D_s}{\kappa^2 G h}\xi^2 - \frac{\rho_v h^2}{12\kappa^2 G}(\omega+\xi V)^2 \tag{3.48}$$

Equation (3.45) is the expression that gives the structural response in the frequency domain. With the structural response known the acoustic power can be calculated. We shall now discuss the methodology of finding the total acoustic power.

3.4.3.6 Total Acoustic Power

The time averaged sound intensity is given by Morse and Ingard (1968) as

$$\bar{I} = \frac{1}{T}\int_0^T \overline{PV}\,dt \quad or \quad \bar{I} = \frac{1}{2}Re[P\dot{U}_s^*(\xi,t)]$$

where

$\bar{I}$	is the time averaged sound intensity
P	is the sound pressure on the plate surface
$\dot{U}_s^*(\xi,t)$	is the plate surface velocity of conjugation

and

$$\dot{U}_s = \frac{dU_s(\xi)}{dt} = j(\omega + \xi V)U_s(\xi) \tag{3.49}$$

In order to find the total acoustic power (Π), the surface acoustic intensity distribution needs to be integrated over the infinite length of the plate as

$$\Pi = \int_{-\infty}^{\infty} \frac{1}{2}Re[P(\xi, y=0, t)\dot{U}_s^*(\xi,t)]d\xi$$

Upon substituting the sound pressure Equation (3.42) and calculating the surface velocity using Equation (3.49), the sound power radiated per unit width of the plate can be simplified as discussed in Appendix - A to yield

$$\Pi = \frac{\rho_0}{4\pi}Re\left[\int_{-\infty}^{\infty} \frac{(\omega+\xi V)^3}{K_y}|U_s(\xi)|^2 d\xi\right] \tag{3.50}$$

Limiting the study to subsonic motion of the moving load, the limits within which K_y is

real is given by

$$\xi_1 = \frac{-K_0}{1+M} \leq \xi \leq \xi_2 = \frac{K_0}{1-M}$$

This allows us to rewrite the expression for the sound power as Equation (A.16) (see Appendix - A for detailed derivation) reproduced below as

$$\Pi = \frac{\rho_0}{4\pi} Re\left[\int_{\xi_1}^{\xi_2} \frac{(\omega+\xi V)^3}{K_y} |U(\xi)|^2 d\xi\right] \tag{3.51}$$

This completes the formulation of an expression for the total acoustic power for a floating airport subjected to the landing / taking off of an airplane in the presence of inplane loading.

3.4.3.7 Nondimensionalization

In order to present the numerical results, the concept of non-dimensional parameters as discussed in Appendix - B is used. Assuming that the moving load applied is a uniformly distributed line force, defined by Equation (3.1) we get the non-dimensional sound power as:

$$W = \int_{\zeta_1}^{\zeta_2} \alpha^3 \beta \left| Z_F \frac{sin(\zeta K_0 L)}{\zeta K_0 L} \right|^2 |D|^{-2} d\zeta \tag{3.52}$$

where

$$\zeta_1 = \frac{-1}{1+M} \leq \zeta \leq \zeta_2 = \frac{1}{1-M}$$

$$\alpha = 1 + M\zeta$$

$$\beta = \sqrt{\alpha^2 - \zeta^2}$$

$$D = \beta(D_1 - D_2 + D_3 - D_5) + jD_4$$

and the expression for D_1, D_2, D_3, D_4, D_5 and Z_F for a Timoshenko-Mindlin plate are

$$Z_F = 1 + \frac{2(1+\nu)\gamma^4}{\kappa^2}\left(\frac{C_0}{C_L}\right)^2\left[\zeta^2 - \left(\frac{C_0}{C_L}\right)^2\alpha^2(1-\nu^2)\right]$$

$$D_1 = \gamma^4\zeta^4$$

$$D_2 = \alpha^2\left[1 + [1 + \frac{2(1+\nu)}{\kappa^2(1-\nu^2)}]\gamma^4\zeta^2\left(\frac{C_0}{C_L}\right)^2(1-\nu^2)\right]$$

$$D_3 = \frac{2(1+\nu)}{\kappa^2}\alpha^4\gamma^4\left(\frac{C_0}{C_L}\right)^4(1-\nu^2)$$

$$D_4 = Z_F\frac{\alpha_0\alpha^2}{\gamma^2}$$

$$D_5 = \frac{Q}{\rho_v h}(\frac{\zeta^2}{C_0^2})$$

Numerical solution to Equation (3.52) provides the total sound power from a floating airport subjected to a combination of inplane and moving load. The numerical results are discussed in section 5.9.

3.5 Structural Response of a Floating Airport

3.5.1 General Introduction

Many developed countries with long coastlines for want of space have successfully reclaimed land from sea, however due to negative ecological effects, researchers and engineers proposed the construction of *Very Large Floating Structures* (VLFS). The relatively simple construction and ease of maintenance of a VLFS thus makes it a promising design candidate for floating airports or runways. Unlike conventional floating structures, the VLFS is flexible because of its huge horizontal dimensions compared to its height. This implies that when the VLFS is subjected to a landing / take off load of an airplane it is likely to exhibit larger elastic deformation. It hence becomes essential that the dynamic analysis of a VLFS when subjected to such transient loads is done carefully.

Dynamic analysis of elastic structures has attracted much attention from researchers for many years. The problem arose from the observation that a structure subjected to moving loads can exhibit higher deflections and stresses than those for static loads. Today, the analysis of moving load problem is applicable for various engineering applications such as high speed drilling, turning, workpiece transportation, fluid flow induced vibrations to name a few. For an elastic structure such as a VLFS subjected to a landing / taking off load of an airplane this analysis has its importance because a floating runway is flexible and receives buoyant support from the water. This makes the runway to deflect due to it's weight and hence will form a dish-like "dent" around the aircraft when the aircraft is static. However this dent moves and progresses like a wave down the runway when the airplane takes off. This moving dent in return causes an increased drag on the aircraft resulting into increased time, distance of take-off and fuel thus leading to increased operating cost. The designer is thus required to address the transient dynamics problem due to the impulsive and moving loads excited by the landing / taking off of an airplane on these structures. An expression for the structural response of such a floating platform subjected to a moving load is studied in this section.

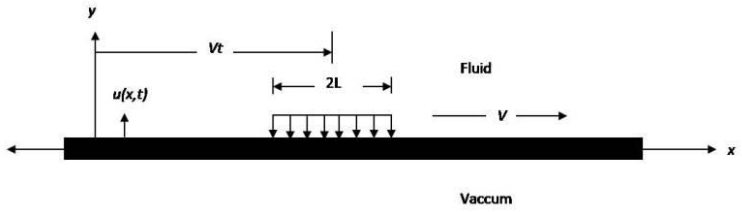

Fig. 3.4 Schematic representation of a floating airport

3.5.2 Introduction

The structural response of a floating airport subject to an airplane taking off / landing is considered essential towards the safety of the aircraft. In the present section, an expression for the structural response of a floating airport due to an airplane landing / taking off modeled as a moving load is proposed. In developing this expression, a Fourier transformation in space for the whole structure in wavenumber domain is utilised rather than using the wave propagation method to reduce the analysis to a substructure. The procedure employed is similar to that demonstrated by Cray (1994) for stiffened plates and Cheng (1999) and Cheng *et al.* (2000, 2001) for calculating the transverse response and acoustic radiation of a periodically supported beam. The advantage of expressing the response in terms of a wavenumber arises from the fact that the periodic boundary conditions and the phase relation between two adjacent substructures will not be required to be used. Accordingly the expression for the structural response as obtained in Equation (3.13) is used to analyse the structural response of a floating airport subject to a moving load.

3.5.3 Formulation

3.5.3.1 Structural Definition

The structural definition of the floating airport as discussed in section 3.2.2.1 is utilised. The schematic representation of problem the geometry is as seen in Figure 3.4.

3.5.3.2 Governing Equation

As discussed in section 3.2.2.5 the expression for structural response is given by Equation (3.13) which is expressed as

$$\mathbf{U_s}(\xi) = \frac{\mathbf{Z_F F}(\xi)}{\mathbf{Z_m} + \mathbf{Z_F Z_a}} \tag{3.53}$$

where

- **The Acoustic Impedance Operator** (Z_a) is given by

$$Z_a = \frac{j\rho_0(\omega + \xi V)^2}{K_y}$$

- **The Plate Impedance Operator** (Z_m) as

$$Z_m = D_s\xi^4 - \rho_v h(\omega + \xi V)^2 - \xi^2\rho_v I\left(1 + \frac{D_s\rho_v}{\kappa^2 G}\right)(\omega + \xi V)^2 + \rho_v I\frac{\rho_v}{\kappa^2\bar{G}}(\omega + \xi V)^2$$

- **The** (Z_F) by

$$Z_F = 1 + \frac{D_s}{\kappa^2 G h}\xi^2 - \frac{\rho_v h^2}{12\kappa^2 G}(\omega + \xi V)^2$$

3.5.3.3 Nondimensionalization

In order to present the numerical results, the concept of non-dimensional parameters is used. Using Equation (3.53) and non-dimensionalising we get an expression for

$$Displacement\ of\ plate\ [U_s(\zeta)] = \frac{E}{f_0 h}U(\xi)$$

$$Strength\ of\ external\ force\ [F(\zeta)] = \frac{F(\xi)}{f_0}$$

$$K_0 h = \left[\frac{K_0}{K_B}\right]^2\left[\frac{12\rho_v C_0^2}{E}\right]^{1/2}$$

Hence

$$U_s(\zeta) = \frac{E}{f_0 h} U_s(\xi) = \frac{E}{f_0 h} \frac{Z_F F(\xi)}{(Z_m + Z_F Z_a)}$$

$$= \frac{F(\zeta) A(\zeta)}{B(\zeta) + A(\zeta) C(\zeta)} \tag{3.54}$$

where

$$F(\zeta) = f_0 \frac{sin(K_0 \zeta L)}{K_0 \zeta L} = f_0 \frac{sin[(K_0 h)\zeta(L/h)]}{(K_0 h)\zeta(L/h)} \quad \text{for harmonic line force}$$

$$F(\zeta) = f_0 \qquad \text{for a point force}$$

$$A(\zeta) = 1 + \left(\frac{1+\nu}{6\kappa^2}\right)(K_0 h)^2 \zeta^2 - \left(\frac{1+\nu}{6\kappa^2}\right)\left(\frac{C_0}{C_L}\right)^2 (K_0 h)^2 H(\zeta)$$

$$B(\zeta) = \frac{Z_m}{E/h}$$

$$= \frac{1}{12}(K_0 h)^4 \zeta^4 - H(\zeta)\left(\frac{C_0}{C_L}\right)^2 (K_0 h)^2 \left[1 + \frac{(K_0 h)^2}{12}\left(1 + \frac{2(1+\nu)}{\kappa^2}\right)\zeta^2\right]$$
$$+ \frac{(1+\nu)}{6\kappa^2}\left(\frac{C_0}{C_L}\right)^4 (K_0 h)^4 H(\zeta)^2 - \frac{Q}{\rho_v h}\left(\frac{\zeta^2}{C_0^2}\right)(K_0 h)^2$$

$$C(\zeta) = \frac{Z_a}{E/h}$$

$$= j \frac{H(\zeta)}{\sqrt{H(\zeta) - \zeta^2}} \left(\frac{C_0}{C_L}\right)^2 \frac{\rho_0}{\rho_v}(K_0 h)$$

$$H(\zeta) = (\zeta M + 1)^2$$

The non dimensional Equation (3.54) gives the structural response of a fluid loaded Timoshenko-Mindlin plate subjected to a moving force which is numerically analysed in

section 5.10.

Chapter 4

Graphical User Interface

4.1 General Introduction

The mathematical formulation for the beam model and the plate model floating in water in the presence of a harmonic moving load have been discussed in chapters 2 and 3 respectively. In this chapter, we shall discuss the Graphical User Interface (GUI) for undertaking numerical calculations using these mathematical formulations. The GUI allows the user to vary the input parameters and hence obtain results for different combinations of parameters. All calculations have been undertaken using MATLAB.

4.2 Introduction

A graphical user interface (GUI) is a human-computer interface (i.e., a way for humans to interact with computers) that uses windows, icons and menus and which can be manipulated by a mouse (and often to a limited extent by a keyboard as well). A major advantage of GUIs is that they make computer operation more intuitive, and thus easier to learn and use. it can be user-friendly and speed up the user's work. A GUI can be more attractive for non-technical people. In general, it looks more professional, however this does not mean it is always the best solution.

When it is not properly built, it can be very difficult to work with. It generally requires more memory resources than a non-graphical one and might require the installation of additional software, e.g., the "runtime environment". Depending on the programmer, it might require more time to be implemented.

Not withstanding the above, the GUI has became much more than a mere convenience. It has also become the standard in human-computer interaction, and it has influenced the work of a generation of computer users.

4.3 Front page

The front page of the GUI is the start page that allows the user to select and vary the input parameters. The front page of the GUI opens up as is shown in Figure 4.1. Once the user clicks the **Process»** button, the programme checks for missing parameters based on the type of the analysis as selected by the user. Missing / incorrect data is prompted to the user to make the necessary corrections. The results of the analysis are plotted in the graph block on the front page itself.

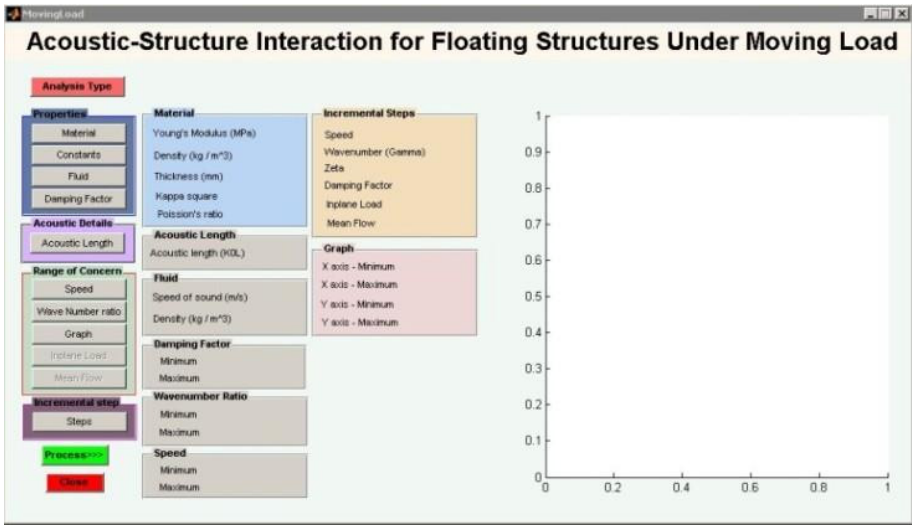

Fig. 4.1 Front page of the GUI

4.4 Entering parameters

The entry of the parameters is governed by the "pushbuttons" on the GUI. Using a pushbutton activates a pop-up window wherein the values relevant to the pushbutton can be entered. Once the values are entered and the **Save Settings!** button is activated, the pop-up window closes while updating the relevant values in the front page. We shall now discuss the available range of values for every pushbutton.

4.4.1 Analysis Type

The "analysis type" pushbutton allows the selection of the type of model as seen in Figure 4.2. The analysis included are a **Ship modeled as a Beam** and a **Floating Airport modeled as a 1D plate**.
Beams that can be analysed are

- A Timoshenko beam.
- A Rayleigh beam.
- A Shear beam.
- A Euler-Bernoulli beam.
- A Comparative analysis of 4 beam types
- Beams with varying loss factor

1D plates that can be analysed are

- A Timoshenko plate.
- A Timoshenko plate with Mean flow.
- A Timoshenko plate with Inplane Load.

This definition of the analysis type is essential to define the equation to be used for undertaking the numerical evaluation of the sound power generated by a moving load on such floating structures.

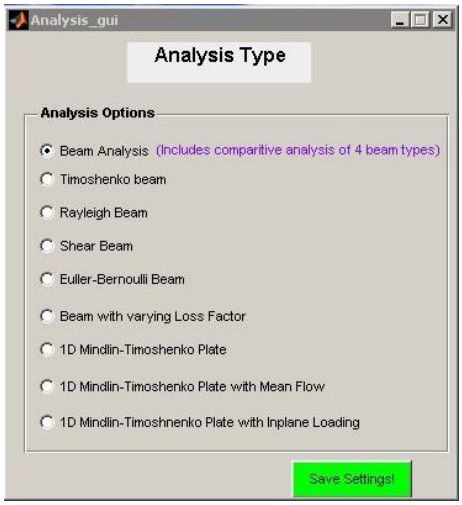

Fig. 4.2 Analysis Type

4.4.2 Material Properties

The properties that need to be entered in this are

- Young's Modulus
- Material density
- Material Thickness

The input pop-up menu is as seen in Figure 4.3. It may be noted that the unit of the values to be entered is explicitly mentioned in the pop-up menu. Values that may be used are given in Table 4.1

Table 4.1: Material Properties

Parameter	**Steel**	**Aluminium**	**Unit**
E $(Young's\ Modulus)$	200	71	MPa
ρ_v $(Material\ Density)$	7800	2700	kg/m^3
h $(Material\ Thickness)$	25.4	25.4	mm

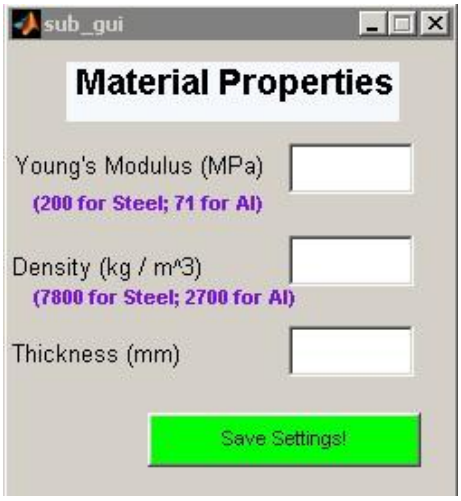

Fig. 4.3 Material Properties

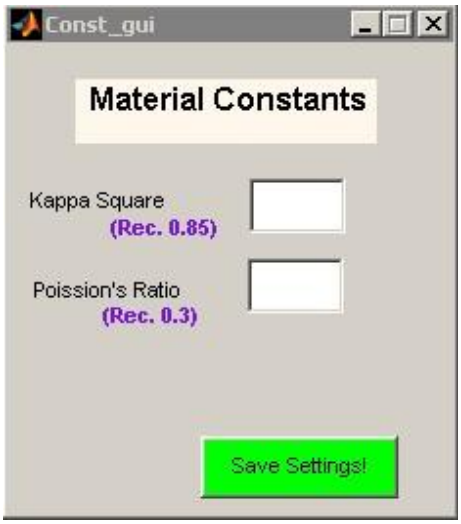

Fig. 4.4 Material Constant Properties

4.4.3 Material Constant Properties

The properties that need to be entered in this are

- Poission's Ratio (ν)
- Cross sectional shape factor(κ^2)

The input pop-up menu is as seen in Figure 4.4. It may be noted that the unit of the values to be entered is explicitly mentioned in the pop-up menu. Values that may be used are as given in Table 4.2

Table 4.2: Material Constants

Parameter	Value
ν	0.3
κ^2	0.85

4.4.4 Fluid Properties

Sound waves can travel through any substance, including gases (such as air), liquids (such as water), and solids (such as the seafloor). Even though sound waves in water and sound waves in air are basically similar, the way that sound levels in water and sound levels in air are reported is very different, and comparing sound levels in water and air must be done carefully. The properties hence need to be specified to specify the medium. Hence we need to specify

- Speed of Sound (C_0)
- Density of Medium (ρ_m)

The input pop-up menu is as seen in Figure 4.5. It may be noted that the unit of the values to be entered is explicitly mentioned in the pop-up menu. Values that may be used are as given in Table 4.3

Table 4.3: Fluid Properties

Parameter	Water	Air	Unit
$C_0(Speed\ of\ Sound)$	1000	341	m/s
$\rho_m(Density\ of\ Medium)$	7800	1.24	kg/m^3

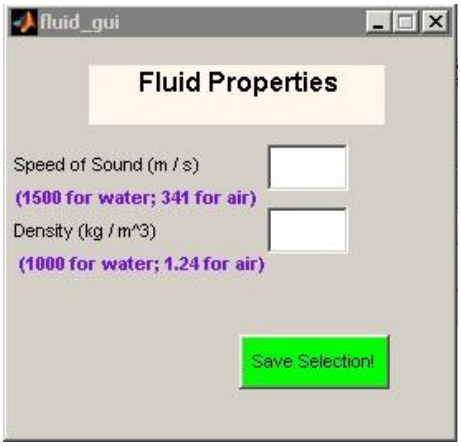

Fig. 4.5 Fluid Properties

4.4.5 Damping Factor Properties

Damping is the ability of a material to dissipate vibration energy into heat. Usually, damping is characterised by the loss factor, often denoted by η, and which is defined as the ratio of lost energy to the vibratory reversible energy during one cycle of vibration. Due to its importance in noise and vibration control, and in the prevention of fatigue in structural elements, the study of damping in materials has been given some attention. We use a "constant loss factor" model for the damping mechanism. The need to analyse the effect of loss factor separately arises because increased vibrational levels due to reduced damping (hence reduced loss factor) lead directly to increased sound radiation. Although the contribution of the damping factors may yield results only a few percentage more accurate and their effect is quite profound when dynamic response analysis is undertaken, it may be an overestimate for slender bodies. The value of η is taken as 0.01 where required as found in Ungar (1988). The range for the damping factor that may be entered is between 0 and 1. The input pop-up menu is as seen in Figure 4.6.

4.4.6 Acoustic Length Properties

The product of the acoustic wave number (K_0) and the half length of the moving force acting on the structure is defined as the acoustic length. A small value of acoustic length ($K_0 L << 1$) is indicative of a point force. The values for the acoustic length is usually

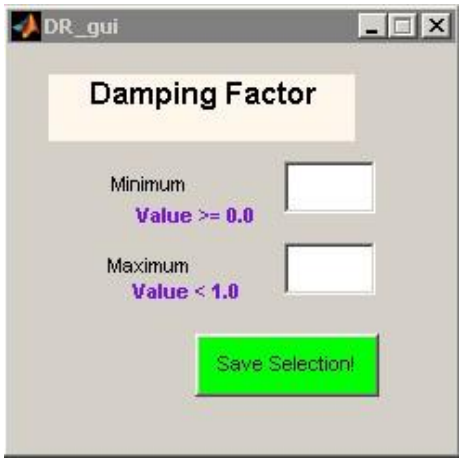

Fig. 4.6 Damping Factor Properties

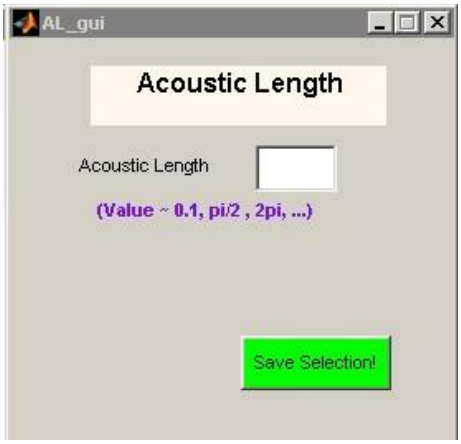

Fig. 4.7 Acoustic Length Properties

either a small value as 0.1 or a multiple of π. The input pop-up menu is as seen in Figure 4.7.

4.4.7 Speed

In the present formulation the moving load is considered to be moving with a speed which needs to be defined. This speed may be considered as fixed or be in a range. The speed is defined by Mach number ($M = V/C_0$) where, V is the speed of the moving load in m/s and C_0 is the speed of sound in the medium under consideration in m/s. Since the calculations have been defined for subsonic speeds, i.e speeds below the speed of sound, the range of the speed for these calculations is limited within 0 and 1. It is noted that the

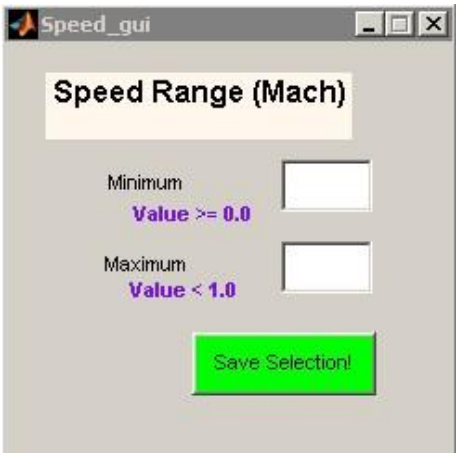

Fig. 4.8 Speed Properties

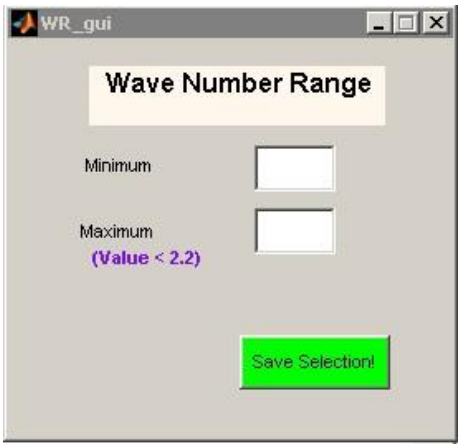

Fig. 4.9 Wavenumber ratio Properties

values to be entered are non dimensional. The input pop-up menu is as seen in Figure 4.8.

4.4.8 Wavenumber ratio (γ)

The non dimensional ratio of the acoustic wavenumber (K_0) and the free bending wave number (K_B), given by γ ($= K_0/K_B$) (or non dimensional frequency), is called as the wavenumber ratio. The input pop-up menu is as seen in Figure 4.9. The range for which these calculations are valid are $0 < \gamma < 2.2$

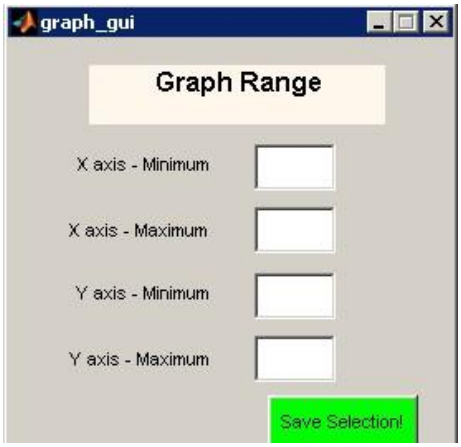

Fig. 4.10 Graph Range Properties

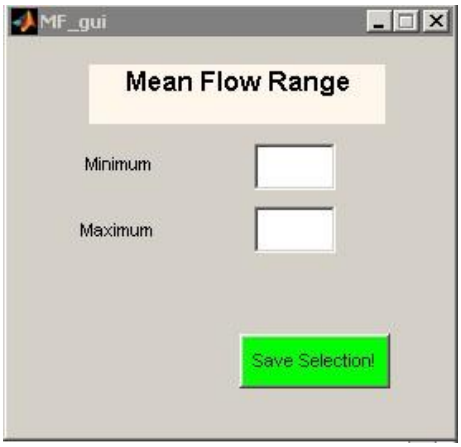

Fig. 4.11 Mean Flow Properties

4.4.9 Graph

To be able to plot the graphs, the range for the X axis and Y axis needs to be defined. The input pop-up menu is as seen in Figure 4.10.

4.4.10 Mean Flow

To model a current or mean flow, a subsonic mean flow of speed U, moving in the positive x direction is considered to be present in the water. In actual the maximum surface current in the ocean is that of Gulf stream at 2.5 m/s followed by the Agulhas current at 2 m/s. This mean flow velocity is taken to be varying. The input pop-up menu is as seen in Figure 4.11.

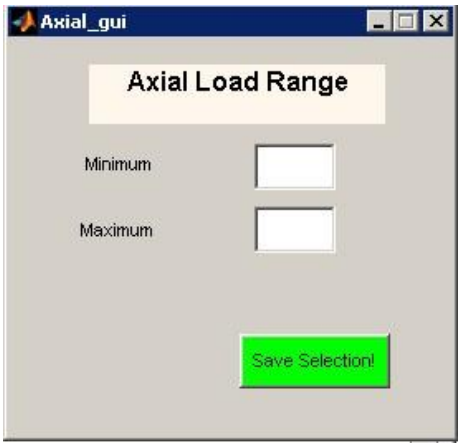

Fig. 4.12 Inplane load Properties

4.4.11 Inplane Load

Berthing, plate connections, initial plate deformation, corrosion, hogging, sagging are some forms of inducing additional loads in the form of inplane loads to the plating of a structure. The input pop-up menu is as seen in Figure 4.12.

4.4.12 Incremental Steps

The incremental steps are the computational step that need to be defined by the user. The value of these steps defines the accuracy of the result and are required for completion of the calculation. The input pop-up menu is as seen in Figure 4.13.

4.5 Calculating

Once all the values, as required, for undertaking the calculations have been entered by the user, the calculating process can commence. As a start point, the validity of the entered values is checked before actual calculations commence. Incase of a missing / incorrect value, an error message is flashed for the user to allow him to make corrections. One such error message is shown in Figure 4.14.

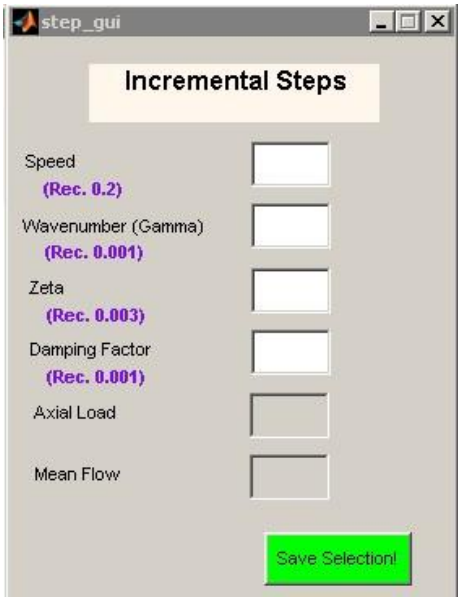

Fig. 4.13 Incremental Step Properties

Fig. 4.14 Error Message

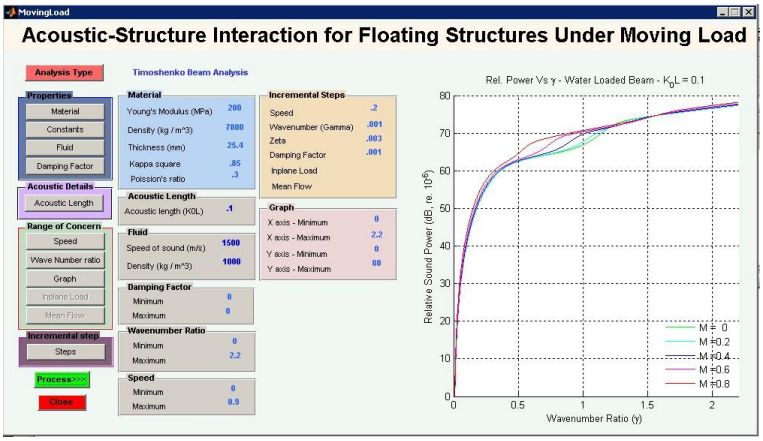

Fig. 4.15 Output Page

4.6 Graphical Output

The calculated result is plotted in the graph on the GUI on completion of the calculations. The resulting screen shot of the GUI on completion is as seen in Figure 4.15.

4.7 Save Graph

The graph that has been generated can be saved by using the **save graph** button. Prior to saving the graph, the file name and required extension for the graph needs to be provided. The path wherein the graph is assumed to be saved is the current directory.

4.8 Close

The **Close** button allows the user to exit the GUI while closing any linked window.

4.9 Conclusion

GUI as a tool has been generated for undertaking the calculations based on the formulation discussed in chapter 2 and 3. With this tool the user can study the sound radiation from floating structures under the influence of moving loads.

Chapter 5

Numerical Analysis

5.1 General Introduction

The mathematical formulation for the beam model and the plate model floating in water in the presence of a harmonic moving load have been discussed in chapters 2 and 3 respectively. However before the mathematical formulation can be fruitfully used, it needs to be validated. For any mathematical model to be validated, either experimental results or published results are required. In the present case, since experimental validation is difficult owing to the complexity of the structure and the speeds associated, previously published results are used to validate the formulation. This process of validation has been discussed in section 5.2. Once the existing model was validated, the formulation extended to the areas of this study. With the necessary formulations in place, a GUI was created which has been discussed in chapter 4. In the present chapter, we discuss the results obtained from the numerical analysis using the formulations obtained in the previous chapters and by using the GUI. All calculations have been undertaken using MATLAB. The flow chart used for the numerical analysis has been discussed in section 5.3.

Using a **beam model** we first analyse the total sound power produced by a Timo-

shenko beam, a Rayleigh beam, a Shear beam and an Euler-Bernoulli beam. We then compare them to understand which beam type produces the maximum sound power and the reasons for the increased sound power in section 5.5. This is followed by the calculation and analysis of the total sound power from a Timoshenko beam due to varying loss factor in section 5.6.

Using a **plate model**, numerical analysis of the total sound power from a floating airport due to a landing / taking off of an airplane is undertaken. The analysis is carried out for steel and aluminium and the effect of the material on the total sound power is studied in section 5.7. The same plate model is then extended by modifying the governing equation from Equation (3.3) to Equation (3.21) to incorporate the effect of mean flow and the numerical results of the total sound power are obtained and analysed in section 5.8. Another extension is obtained by incorporating the inplane loading to the plate model to get Equation (3.35). The effect of compressive and tensile inplane loads on the floating airport is hence studied in section 5.9.

Finally the **structural response** of the plate model to point and harmonic moving load is analysed in section 5.10.

5.2 Validation

No numerical model can be considered to be acceptable till the model is validated by either earlier published or experimental results. In the problem at hand, experimental validation is difficult since the speeds one is looking at varies from 0 to 0.9 Mach. Similarly since the structure under consideration is a VLFS, experimental (laboratory) modeling is considered difficult but not impossible. For such studies mathematical, numerical modeling and field testing are considered as an acceptable methodology for obtaining the desired results.

In order to validate this numerical model, the results as published by Keltie and Peng

(1988) in **"Sound radiation from beams under the action of moving line forces", ASME Transactions Series E Journal of Applied Mechanics, 1988, 55, pp 849-854**, have been used. In this section we reproduce the parameters and results as published in this paper along with the results obtained by the present mathematical model and compare them. However the comparison of the results is limited to the case of heavy fluids (water) which is the medium for this study.

5.2.1 Study by Keltie and Peng (1988)

The problem of sound radiation from a harmonic line force moving along an infinite beam at a constant subsonic speed has been investigated by Keltie and Peng (1988). By integrating the surface acoustic intensity over the entire beam, the non-dimensional sound power is formulated and then examined as a function of Mach number, acoustic length of the line force and the wave number ratio. The entire analysis has been undertaken for a *Timoshenko beam* filled with an acoustic medium (water, air etc) in the space y>0, such that the formulation is valid for beams under heavy fluid loading at high frequencies or for thick beams. Discussions however are largely for light fluid loading (air).

Before moving ahead, it is essential to mention a word on fluid loading. Fluid loading effects have been categorized as **light, significant or heavy** by Crighton and Innes (1984). They found that under light loading conditions the fluid plays no appreciable role; under heavy loading conditions simple asymptotic forms of the structural and fluid response may be obtained; but for significant loading conditions no simple solution is possible. They have further concluded that, for heavy fluid loading, the structure may safely be considered infinite if it is large compared to K_0^{-1} at the frequency of interest. The flexural wave number K_0 is never less than the in vacuo plate bending wave number K_B . Usually **air** is considered as a **light loading** condition while **water** is considered as a **heavy loading** condition.

The analysis undertaken by Keltie and Peng (1988) **is limited** to an elastic beam, including rotational inertia and transverse shear effects given by the Timoshenko beam

equation. Figures 5.1 and 5.3 are results obtained by Keltie and Peng (1988) for a range of M values for $K_0L = 0.1$ and 2π respectively.

5.2.2 Study by the present model

The present study may be considered as an extension of the work of Keltie and Peng (1988). The study is commenced by remodeling the Timoshenko beam as modeled by Keltie and Peng (1988) for validation of the model (which can be considered as the only similarity between the two studies).

The study is then extended by remodeling for the Euler-Bernoulli, Rayleigh and Shear beams and comparing the results obtained to discuss the performance of the beam model in section 5.5. The effect of the varying loss factor (structural damping) on sound radiation by floating beams has then been evaluated in section 5.6.

This model has then been extended to a floating airport modeled as a one dimensional plate described by the Timoshenko-Mindlin plate in section 5.7. The effect of presence of current and inplane loading on the one dimensional plate model has then been studied in sections 5.8 and 5.9 respectively.

Further structural deflections of the floating airport have been analyzed in section 5.10.

A GUI for undertaking the above studies for both a ship (beam model) and a floating airport (plate model) has then been developed for making the calculation procedure more user friendly and speed up the user's work in *Chapter 4*.

To validate the present formulation, the calculations for a Timoshenko beam condition have been undertaken for $K_0L = 0.1$ and 2π for a range of M. The relative sound power obtained by using the present model are presented in Figures 5.2 and 5.4 respectively. It is necessary that when reporting the relative intensity of a sound, one says not only "dB", which is a relative unit of measure and not an absolute one as is watts per square meter,

but to also add the reference level. This is often written as "dB re 1 μPa" for sounds in water that are measured relative (re) to 1 μPa and "dB re 20 μPa" for sounds in air that are measured relative (re) to 20 μPa. The present study being limited to sounds in water, the results have been presented as "dB re 1 μPa".

5.2.3 Comparison of the two results

By comparing results as published by Keltie and Peng (1988) as seen in Figure 5.1 for $K_0L = 0.1$, with those obtained by the present model in Figure 5.2, one notices that the trend and the magnitudes of the curves obtained are similar. Similarly by comparing Figures 5.3 and 5.4 (results by Keltie and Peng (1988) and present model respectively) for $K_0L = 2\pi$, one notices that the trend of the curves obtained are similar.

For better comparison, the results obtained by Keltie and Peng (1988) and the present model are plotted together in Figures 5.5 and 5.6 for $K_0L = 0.1$ and 2π and a range of M respectively.

It is observed that comparison of published results and those obtained from the present model are negligible over the major range of the wave number ratio and for the entire range of the Mach number. The **minor variation** observed is attributed to the computation methodology available in 1988 (Keltie and Peng (1988)) and 2010-11 (present study).

Hence we can conclude that the developed numerical model is acceptable and can be considered as **validated**.

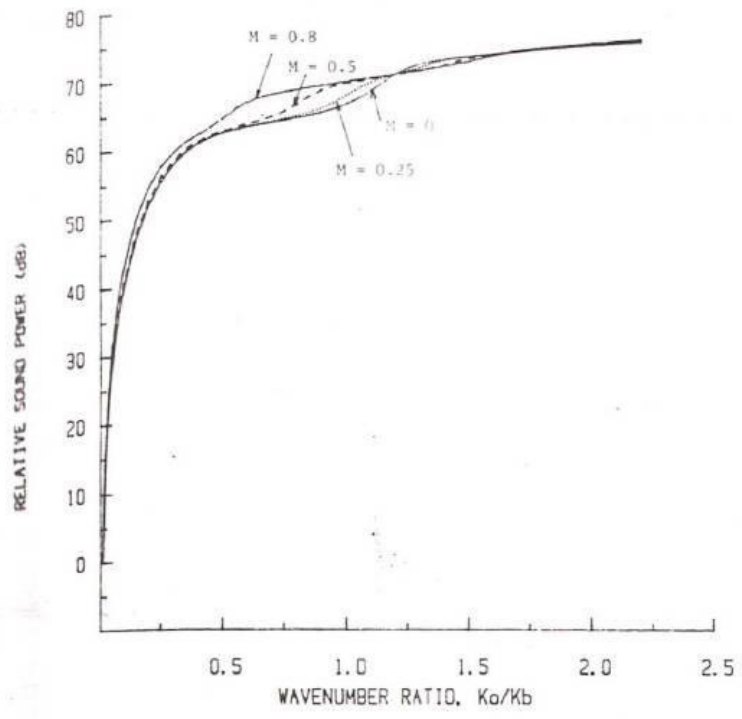

Fig. 5.1 Relative sound power v/s wavenumber ratio for a range of M values; $K_0L = 0.1$, in water (from Keltie and Peng (1988))

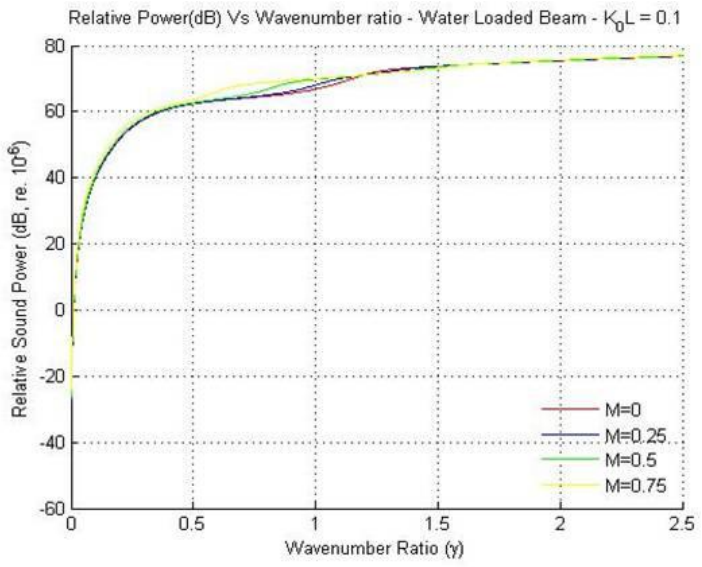

Fig. 5.2 Relative sound power v/s wavenumber ratio for varying M; $K_0L = 0.1$, (present model)

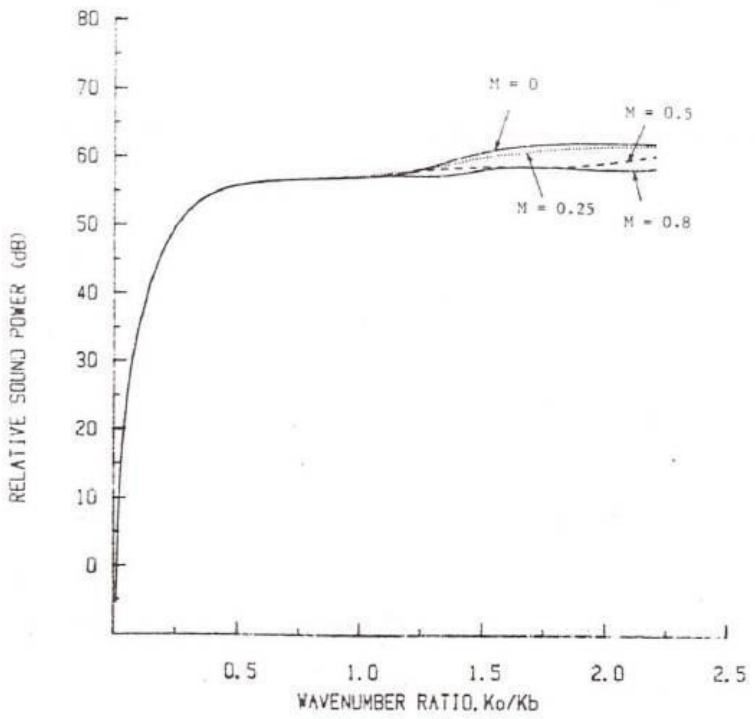

Fig. 5.3 Relative sound power v/s wavenumber ratio for a range of M values; $K_0L = 2\pi$, in water (from Keltie and Peng (1988))

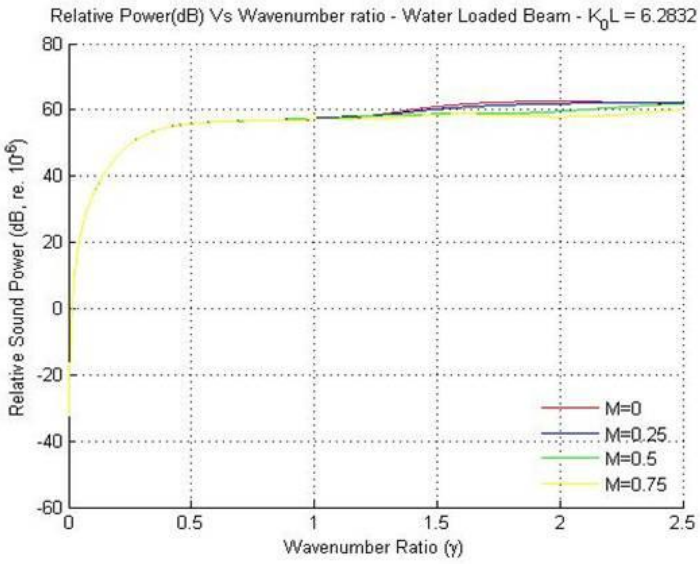

Fig. 5.4 Relative sound power v/s wavenumber ratio for varying M; $K_0L = 2\pi$, (present model)

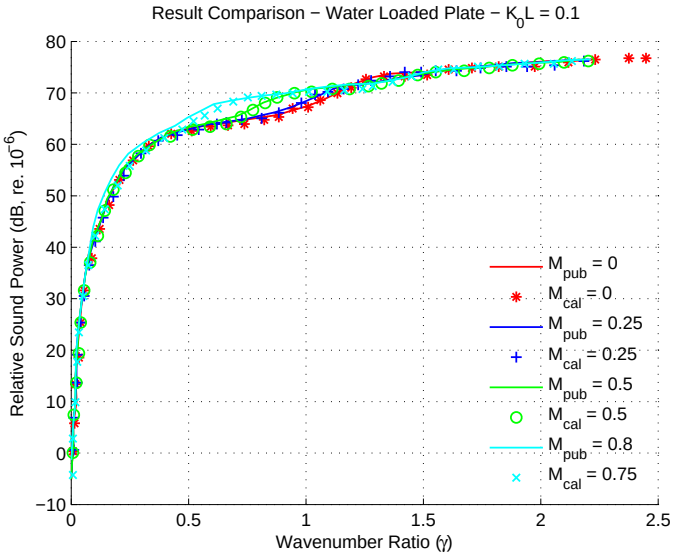

Fig. 5.5 Comparison of published and obtained results for a range of M values; $K_0L = 2\pi$, in water.

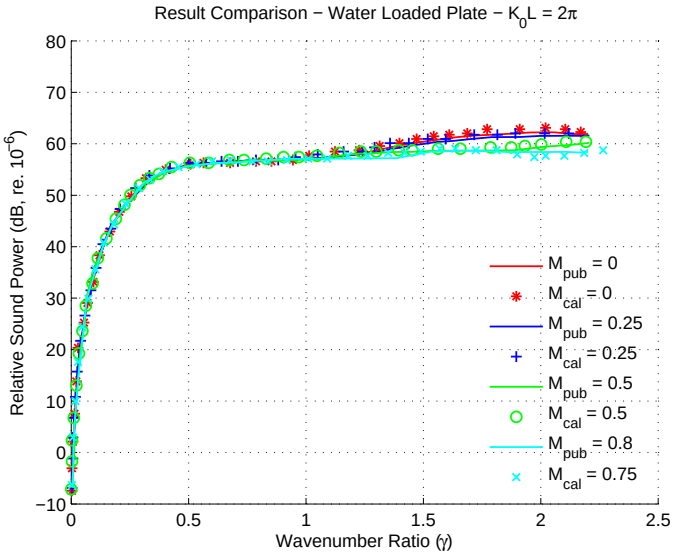

Fig. 5.6 Comparison of published and obtained results for a range of M values; $K_0L = 2\pi$, in water.

5.3 Flowchart

The flow chart for the numerical calculation of sound power generated by a moving load on a beam or a plate as discussed in chapters 2 and 3 is as shown in Figure 5.7. The broad steps that need to be followed to undertake the calculations are:

1. Input the values of the variable constants.
2. For a fixed value of K_0L, calculate the values of the variables, E, D and I.
3. Calculate the total sound power for a range of $0 < \gamma < 2.2$ by integrating it over the range of ζ_1 to ζ_2.
4. Plot graphs for the results obtained.
5. Iterate the steps 3 and 4 above over a range of Mach number ($0 < M < 0.9$).

5.4 Parameters used

In sections 5.5 and 5.6, the numerical analysis of the beam models using a Timoshenko beam, a Rayleigh beam, a Shear beam and an Euler-Bernoulli beam is undertaken. Equation (2.19) obtained in chapter 2 is numerically evaluated to calculate the sound power generated by a moving load on these beams. The material of the beams is considered to be steel. The beam is assumed to float on water. The basic geometrical and material parameters used in sections 5.5 and 5.6 are given in Table 5.1.

Table 5.1: Material Parameters - Beam

$E = 20 \times 10^{10}$	N/m^2
$\rho_v = 7800$	kg/m^3
$h = 2.54 \times 10^{-2}$	m
$\nu = 0.3$	
$\kappa^2 = 0.85$	
For water	

$C_0 = 1481$ m/s

$\rho_0 = 1000$ kg/m^3

5.5 Various Beam Type

5.5.1 Introduction

The investigation of the problem is undertaken to study of the effect of shear effect and rotatory inertia on the total radiated sound power by different beam types. The external force strength (f_0) is assumed to be of unit magnitude. By varying the values of parameters M and K_0L, the total sound power is computed and then plotted against the wave number ratio (γ) or non-dimensional frequency in the frequency range of 0.01 to 2.2. The value of η is taken as 0.01 as found in Ungar (1988).

Figures 5.8 to 5.13 show the effect of various beam types. Since the difference in the total sound power by various beam types is not of a very high magnitude, the Euler-Bernoulli is considered as the reference and difference of total sound power with respect to the Euler-Bernoulli beam is calculated and plotted. The percentage difference in the total sound power is shown in Figures 5.14 to 5.25.

5.5.2 Discussion

In Figures 5.8 to 5.13, one can see four distinct frequency ranges: the very low frequency region ($\gamma < 0.1$); the low frequency region ($0.1 < \gamma < 1.0$); the frequency region near coincidence ($\gamma \sim 1.0$); and the frequency region above coincidence ($\gamma > 1.0$). In the very low frequency region and in the region above coincidence frequency, the sound powers radiated show no discernible difference. It is hence the low frequency region and the region near coincidence which is of concern to us and needs to be discussed. It may be observed that there are no peaks in the sound power curves as obtained in light fluids.

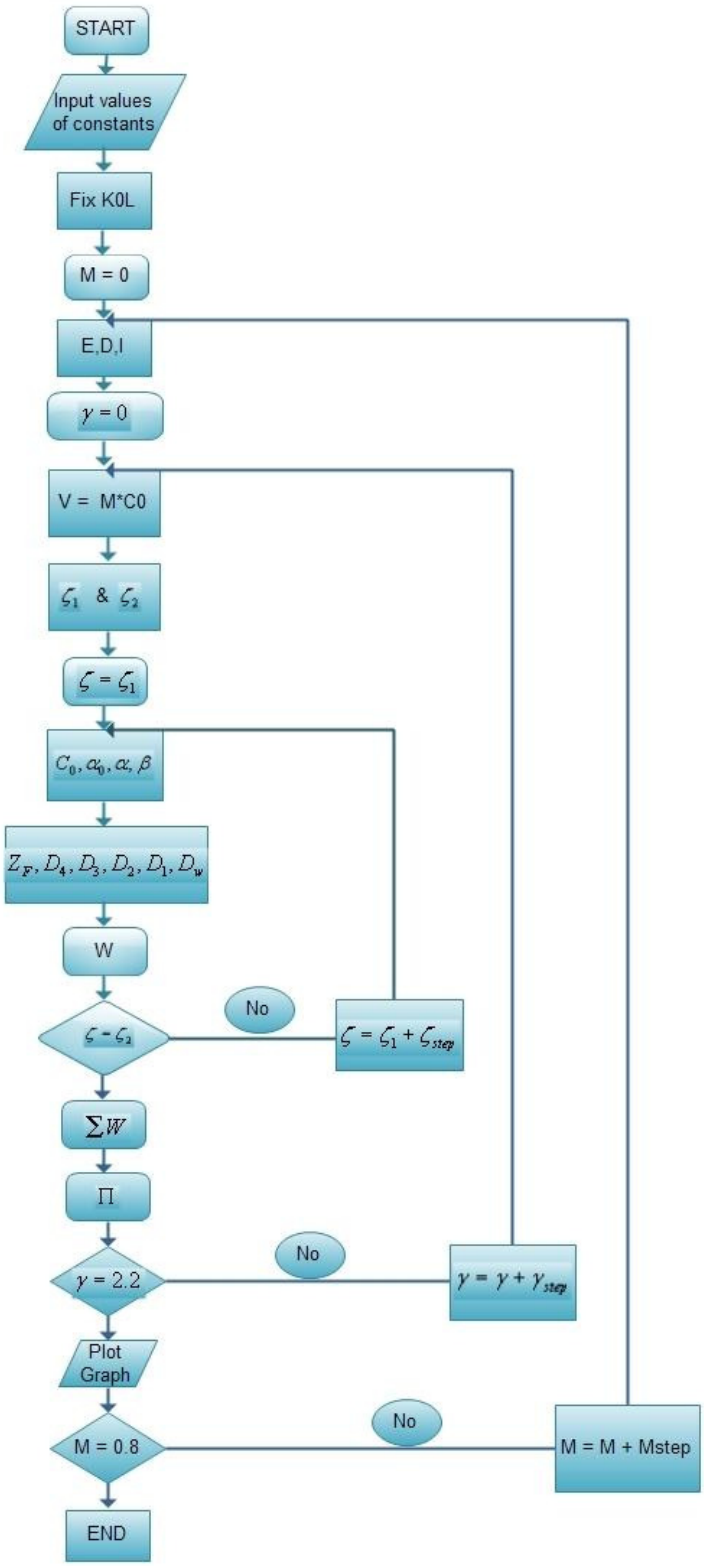

Fig. 5.7 Flow chart for Numerical analysis in MATLAB

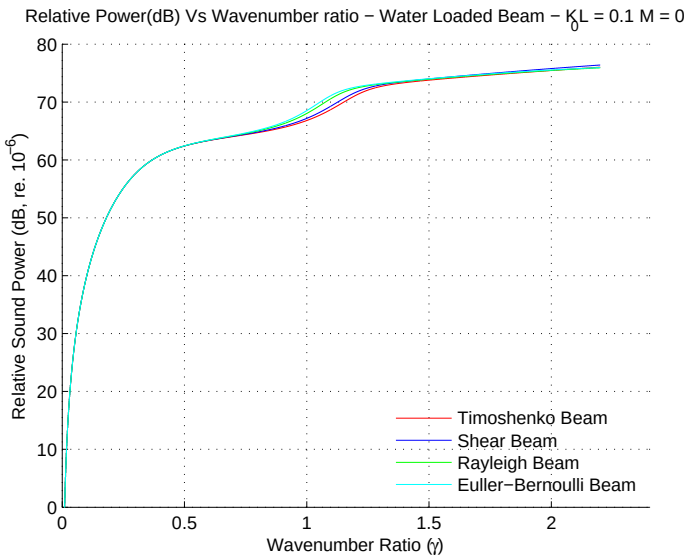

Fig. 5.8 Relative sound power v/s wavenumber ratio for **various beam types**; $M = 0$; $K_0L = 0.1$

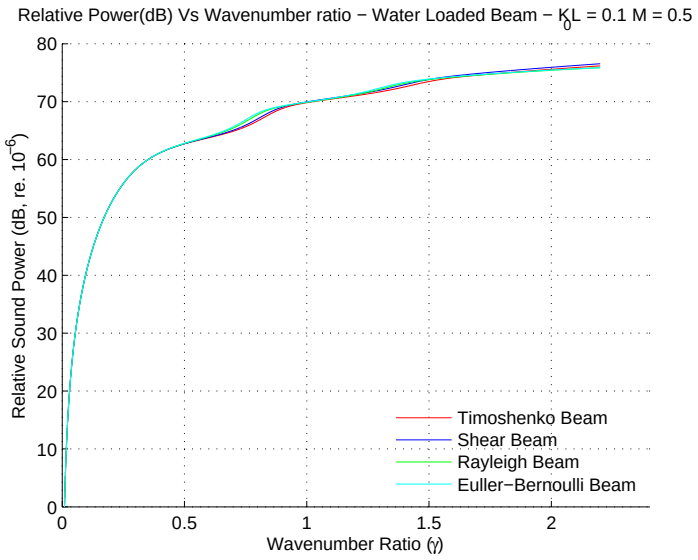

Fig. 5.9 Relative sound power v/s wavenumber ratio for **various beam types**; $M = 0.5$; $K_0L = 0.1$

The essential lack of peaks for a dense medium like water is due to the proportion of the structural energy converted to acoustic energy. This is larger for dense media, leading to the draining of the radiation energy faster from the structure thus disallowing peak formation. This results in larger effective damping. Figures 5.8 and 5.9 are for acoustic length 0.1 and Figures 5.10 and 5.11 are for an acoustic length of 2π.

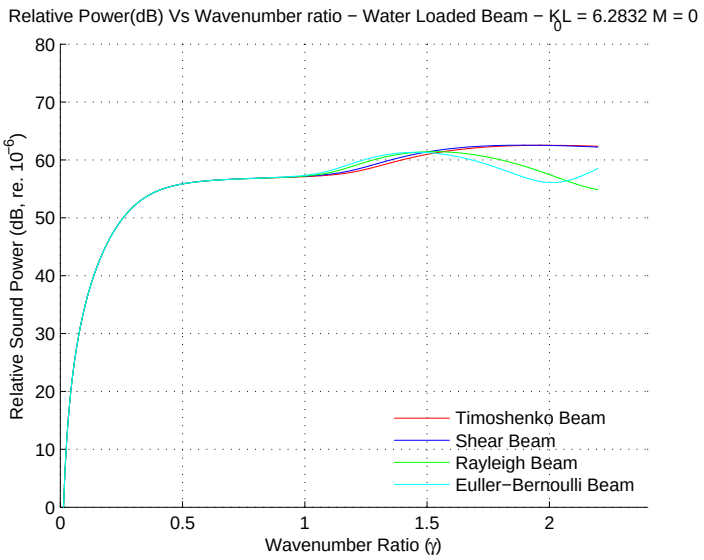

Fig. 5.10 Relative sound power v/s wavenumber ratio for **various beam types**; $M = 0$; $K_0L = 2\pi$

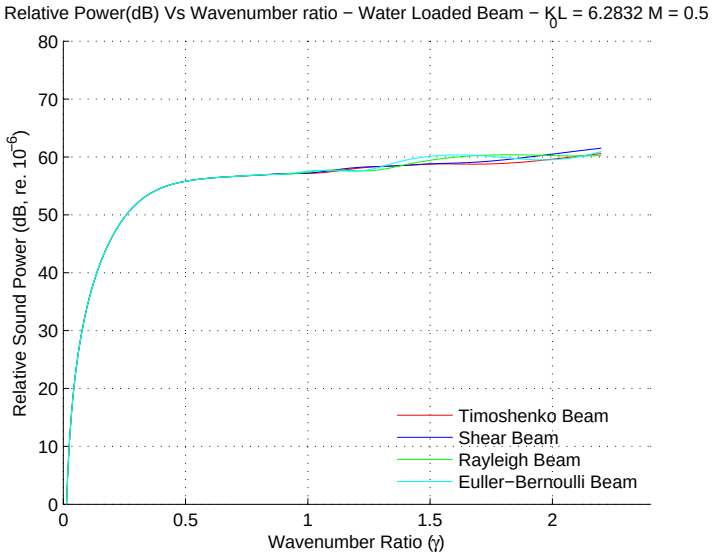

Fig. 5.11 Relative sound power v/s wavenumber ratio for **various beam types**; $M = 0.5$; $K_0L = 2\pi$

5.5.2.1 Static Load

Figures 5.8 and 5.10 are for Mach number, $M = 0$, which indicates a condition of static load. As expected, the sound radiation from the Timoshenko beam is the least while that of the Euler-Bernoulli beam is a maximum. The effect of Shear beam is greater than Rayleigh beam though within the bounds of Timoshenko beam and Euler-Bernoulli beam. This effect is as expected due to terms of contribution involved in the beams.

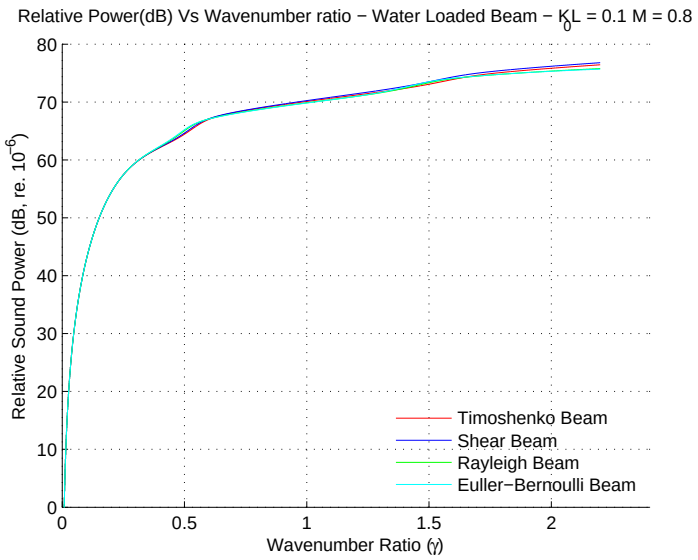

Fig. 5.12 Relative sound power v/s wavenumber ratio for **various beam types**; $M = 0.8$; $K_0L = 0.1$

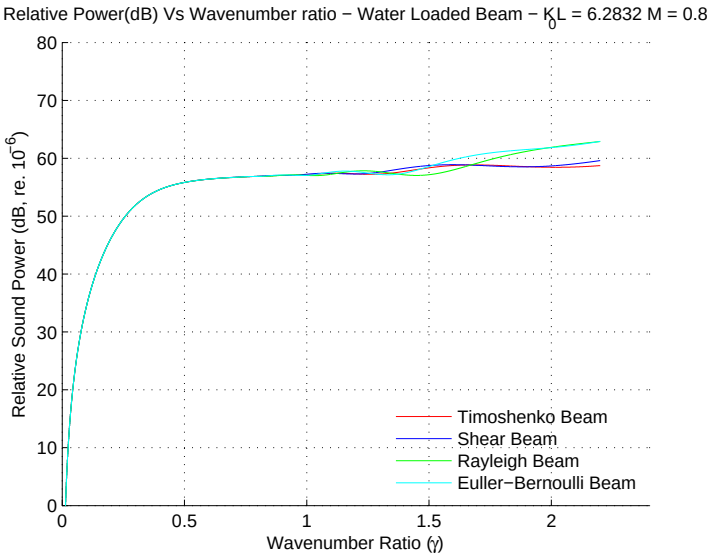

Fig. 5.13 Relative sound power v/s wavenumber ratio for **various beam types**; $M = 0.8$; $K_0L = 2\pi$

One notices that for the shear beam, the contributing element over the Euler-Bernoulli beam is $-\frac{\bar{E}I\rho_v}{\kappa^2\bar{G}}\frac{\partial^4 u(x,t)}{\partial x^2\partial t^2}$ which is added on the LHS and $-\frac{\bar{E}I}{\kappa^2\bar{G}h}\frac{\partial^2}{\partial x^2}$ on the RHS. With the values of κ^2 limited to 0.85 for beams, the contribution of the term shall be greater than 1 thus reducing the net magnitude of the beam impedance Z_m while increasing Z_F. This results in a reduced sound output when compared with the sound produced by a Euler-Bernoulli beam. On the other hand, for the Rayleigh beam, the contribution is by the

term $-\rho_v I \frac{\partial^4 u(x,t)}{\partial x^2 \partial t^2}$ which reduces the structural impedance Z_m. The Rayleigh beam has no effect on the Z_F but since the magnitude of the lowering term on Z_m is large, the net acoustic output is lesser than both the Euler-Bernoulli and the Shear beam. This effect is reversed for frequency regime above coincidence. If we see Equation (2.19), W is proportional to $\frac{Z_F}{D_2}$, while $D \propto -D_2$. For higher values of γ, for the shear beam, Z_F increases, while D reduces because of increase in D_2, thus reducing W. Similarly for the Rayleigh beam Z_F remains unchanged while D reduces due to increase of D_2. However $D_{2SB} > D_{2RB}$ and $Z_{FSB} > Z_{FRB}$ thus the sound power from Shear beam is greater than that obtained from a Rayleigh beam. For Euler-Bernoulli beam $D_{BE} > D_{RE}$ since $D_{2BE} < D_{2RB}$ and $Z_{FBE} = Z_{FRB} = 1$ resulting into increased power from Euler-Bernoulli beam as compared to Rayleigh beam.

5.5.2.2 Moving Load

With the load moving, i.e $M > 0$, and the acoustic length being the same, an overall increase in the sound power is observed as seen in Figures 5.8, 5.9 and 5.12 for $K_0L = 0.1$ and Figures 5.10, 5.11 and 5.13 for $K_0L = 2\pi$. Mathematically, as M increases α increases, thus increasing D_2 which leads to reduced D and hence increased sound power. Physically this is as expected, since with increased speed, the resulting sound is known to increase. However this trend is seen to be reversed for increased frequency the logic being the same as discussed for $M = 0$. It is clear that the increased acoustic length (K_0L) reduces the sound power level over the entire frequency range. This can be attributed to the fact that the total applied force strength is kept constant.

5.5.2.3 Analysis as percentage difference

In order to analyse the nature of the change in power of various beam types, we reorganise the results as a percentage difference. Since the Euler-Bernoulli beam gives maximum power, we use it as a base value and differences with respect to the values of sound power for Euler-Bernoulli beam are plotted for various beam types. It may be noticed that we have **two varying parameters** namely M and K_0L. We shall try and understand the

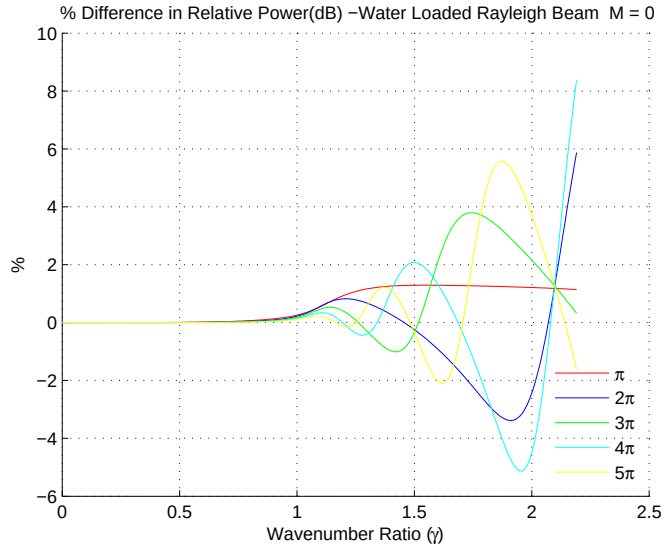

Fig. 5.14 % Difference in Relative sound power (Rayleigh beam); $K_0L = n\pi$; $M = 0$

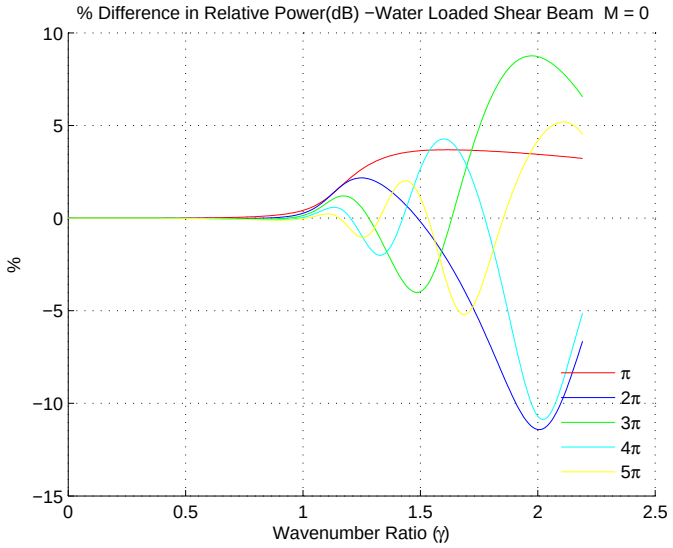

Fig. 5.15 % Difference in Relative sound power (Shear beam); $K_0L = n\pi$; $M = 0$

contribution of each while varying the other variable.

Variation of K_0L: It is interesting to note that if incase K_0L is an integer multiple of π, then the trend of the difference of the total sound power is different than that observed for K_0L being otherwise. The variations observed for the beam types is shown in Figures 5.14, 5.15, 5.16, for the Rayleigh beam, Shear beam and Timoshenko beam

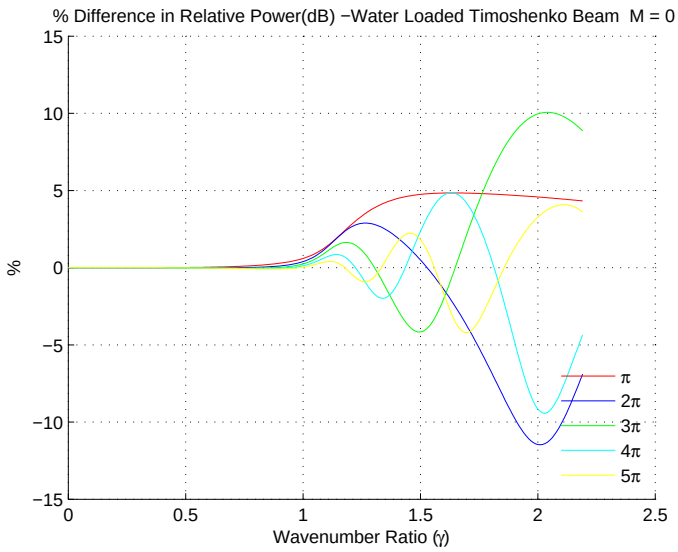

Fig. 5.16 % Difference in Relative sound power (Timoshenko beam); $K_0L = n\pi$; $M = 0$

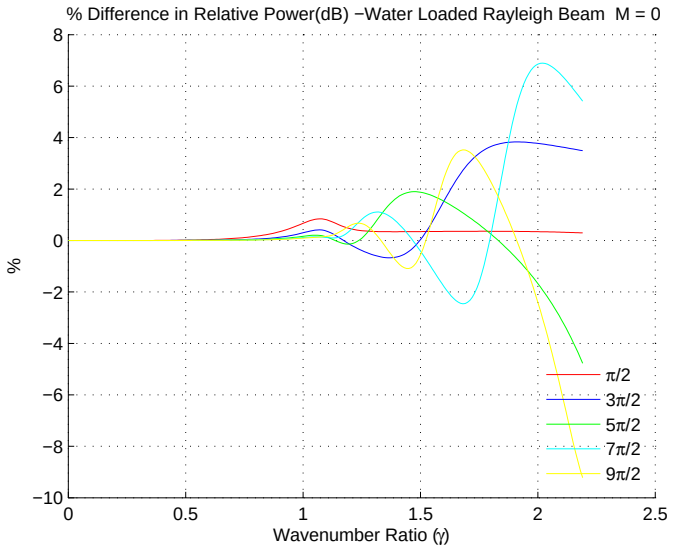

Fig. 5.17 % Difference in Relative sound power (Rayleigh beam); $K_0L = (2n-1)\frac{\pi}{2}$; $M = 0$

for $K_0L = n\pi$ respectively while Figures 5.17, 5.18, 5.19 respectively, are for $K_0L = (2n-1)\pi$. It is observed that the difference of sound power commences after coincidence if K_0L is an integral multiple of π and at half of coincidence when it is otherwise. The variation of the percentage difference is however consistence in its trend. For K_0L being an integral multiple of π, $(n-1)$ half modes are visible, where n is the integral multiple of π. However n number of half modes are seen when K_0L is a non integral multiple

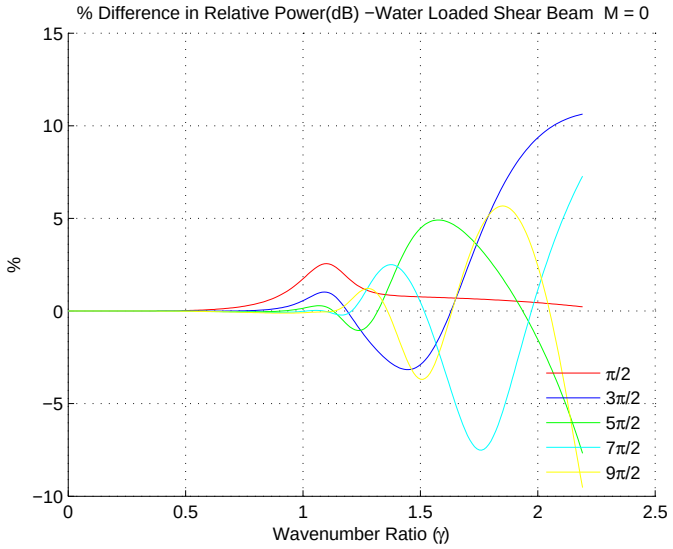

Fig. 5.18 % Difference in Relative sound power (Shear beam); $K_0L = (2n-1)\frac{\pi}{2}$; $M = 0$

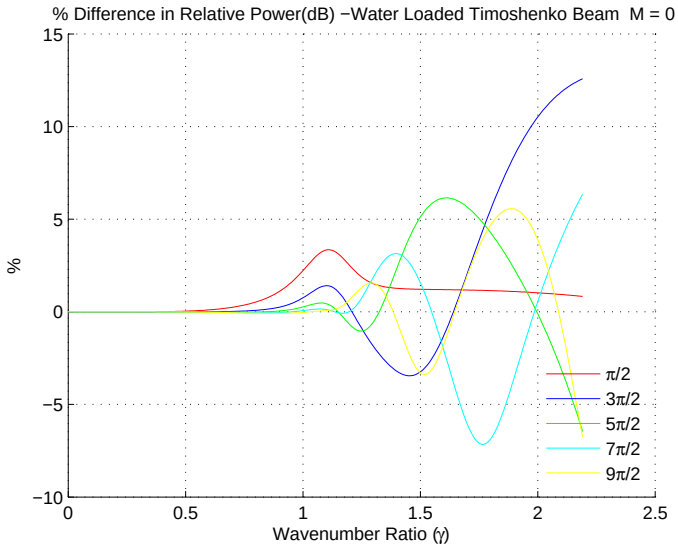

Fig. 5.19 % Difference in Relative sound power (Timoshenko beam); $K_0L = (2n-1)\frac{\pi}{2}$; $M = 0$

of π. The reasoning for this is that the beam responds preferentially at $\zeta = K_B$, the free bending wavenumber, which is the spatial scale of the propagating or the energy bearing portion of the beam's response at frequency ω. Height of the peak is controlled by the damping present in the structure. Physically, the amount of power radiated is determined by how much energy is available in the force spectrum at the structural / acoustic response wavenumber. When this wave number corresponds to an integral

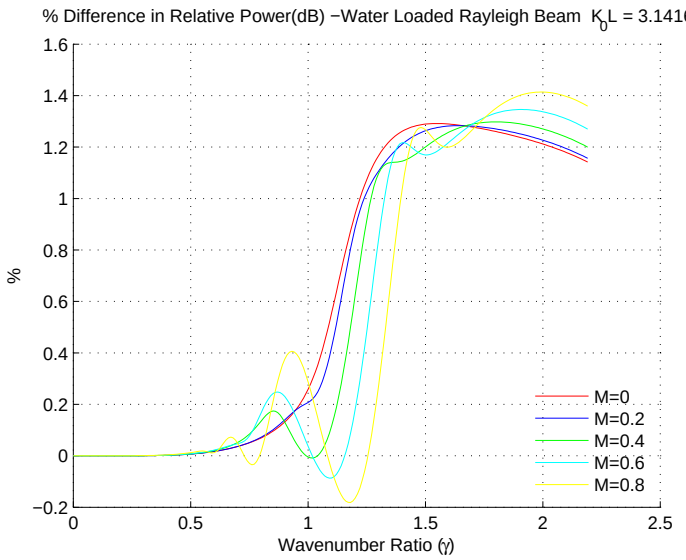

Fig. 5.20 % Difference in Relative sound power (Rayleigh beam); $K_0L = n\pi$; varying M

multiple of $\frac{n\pi}{L}$, there is no energy available in the free spectrum for the conversion to acoustic radiation. These wavenumbers of vanishing energy may be related to wavelength as

$$\zeta = \frac{2\pi}{\lambda} = \frac{n\pi}{L} \Rightarrow \lambda = \frac{2L}{n}$$

Variation of M: The effect of varying M displays the Doppler shift of the difference curves as the speed increases. The overall pattern that emerges when K_0L is an integral multiple of π and when the value of K_0L is not an integral multiple of π is worth noticing as seen in Figures 5.20, 5.21 and 5.22 for integral multiples of π and Figures 5.23, 5.24 and 5.25 for non-integral multiples of π. Special attention may be given to the packing of the values at the critical frequency and the convergence of the data at high wave number ratios.

5.5.3 Conclusion

Effect of shear effect and rotatory inertia on radiated sound power from beams subjected to moving loads has been analysed. It is concluded that a Timoshenko beam gives the least sound radiation power when compared to the other beam types. The correction for shear effect and rotatory inertia yield results within 4-5 % more accurate than classical

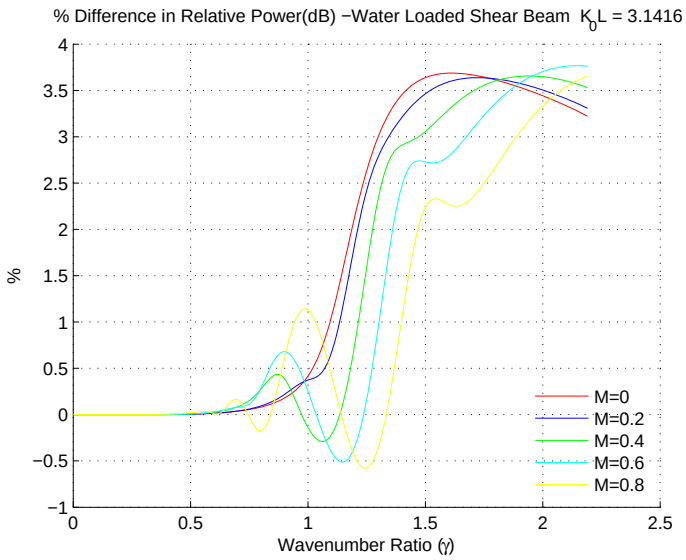

Fig. 5.21 % Difference in Relative sound power (Shear beam); $K_0L = n\pi$; varying M

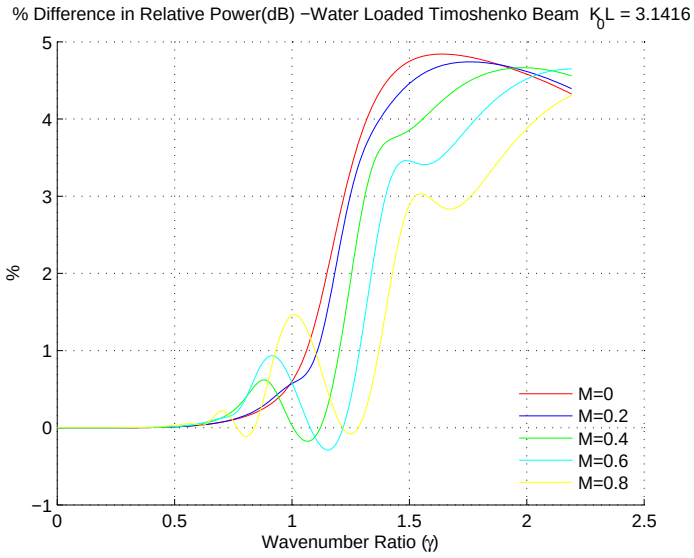

Fig. 5.22 % Difference in Relative sound power (Timoshenko beam); $K_0L = n\pi$; varying M

beam theory. The nature of the curves with varying K_0L is dependent on K_0L being an integral multiple of π or otherwise. For varying M, the Doppler shift of the curves is observed for increasing M. The overall pattern that emerges when K_0L is an integral multiple of π and when the value of K_0L is not an integral multiple of π is worth noticing. Special attention may be given to the packing of the values at the critical frequency and the convergence of the data at high wave number ratios.

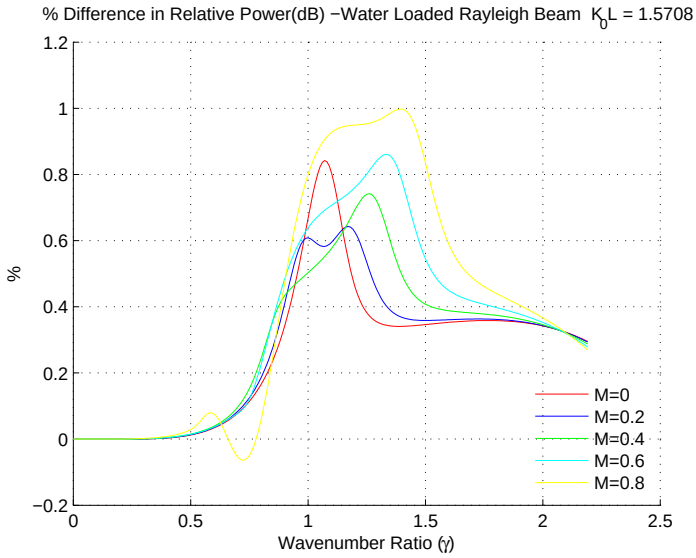

Fig. 5.23 % Difference in Relative sound power (Rayleigh beam); $K_0L = (2n-1)\frac{\pi}{2}$; varying M

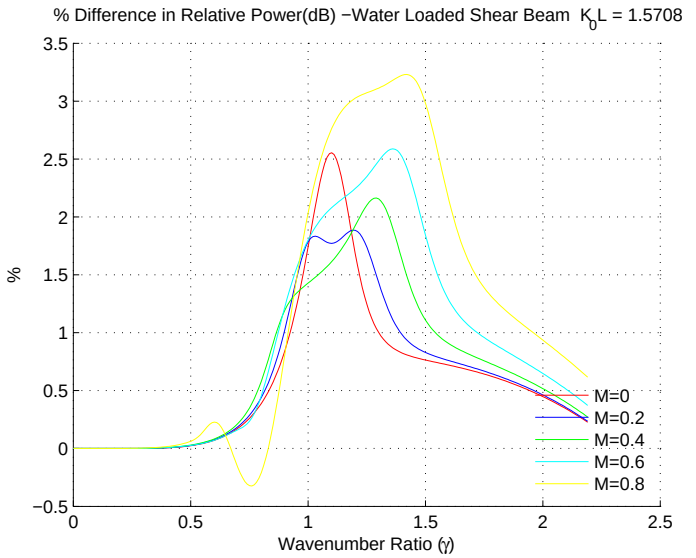

Fig. 5.24 % Difference in Relative sound power (Shear beam); $K_0L = (2n-1)\frac{\pi}{2}$; varying M

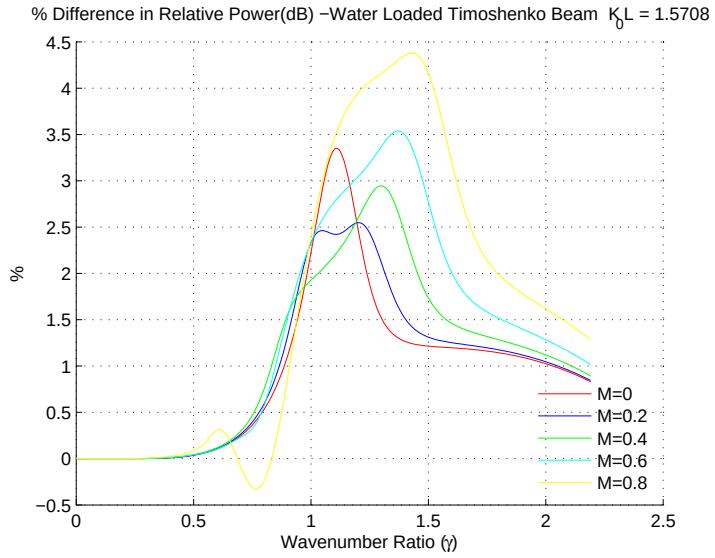

Fig. 5.25 % Difference in Relative sound power (Timoshenko beam); $K_0L = (2n-1)\frac{\pi}{2}$; varying M

5.6 Effect of Loss Factor

5.6.1 Introduction

It is well known that all solid materials are characterised by both elastic and damping properties. The elasticity of a material is exhibited by the fact that the action of a stress is accompanied by a strain while damping is the ability of a material to dissipate vibration energy into heat. Usually, damping is characterised by the loss factor, often denoted by η, and which is defined as the ratio of lost energy to the vibratory reversible energy during one cycle of vibration. Due to its importance in noise, and in the prevention of fatigue in structural elements, the study of damping in materials has been given some attention. We use a "constant loss factor" model for the damping mechanism.

The need to analyse the effect of loss factor arises because increased vibrational levels due to reduced damping (hence reduced loss factor) lead directly to increased sound radiation. In this section, a Timoshenko beam defined by Equation (2.19) is numerically evaluated for the case of a steel beam immersed in water for η varying as $0.9, 0.1, 0.01, 0.001, 0$. The results so obtained are shown in Figures 5.26 to 5.29.

5.6.2 Discussion

As explained in section 5.5.2, one can see four distinct frequency ranges: the very low frequency region ($\gamma < 0.1$); the low frequency region ($0.1 < \gamma < 1.0$); the frequency region near coincidence ($\gamma \sim 1.0$); and the frequency region above coincidence ($\gamma > 1.0$). Since the sound powers radiated show no discernible difference in the very low frequency region and in the region above coincidence frequency, we need to pay attention to the low frequency region and the region near coincidence. The effect of reduced loss factor as increased sound radiation is seen in the Figures 5.26 to 5.29. In this analysis one observes that the curves have the same basic shape as was seen for the case without damping. As the structural damping decreases, the amount of steady-state vibrational energy in the beam increases. This results into the shifting up of the curves by an amount which is

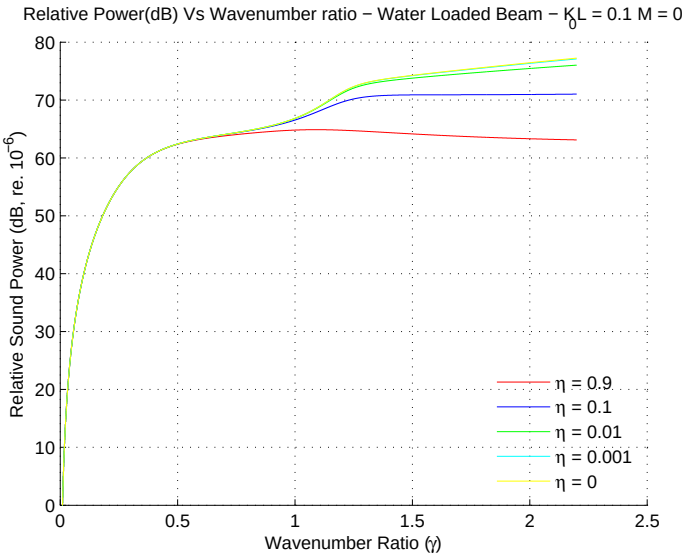

Fig. 5.26 Relative sound power v/s wavenumber ratio for **varying** η; $K_0L = 0.1$

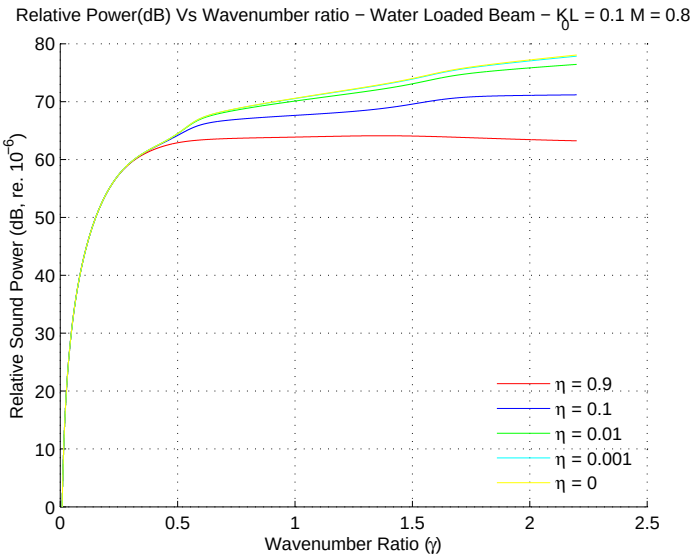

Fig. 5.27 Relative sound power v/s wavenumber ratio for **varying** η; $K_0L = 0.1$

directly proportional to the change in the loss factor.

Near the coincidence frequency, if the structural loss is large enough ($\eta \sim 0.1$), the damping provided by the material exceeds the damping provided by the fluid loading and there is significant difference between the two power curves as seen in Figures 5.26

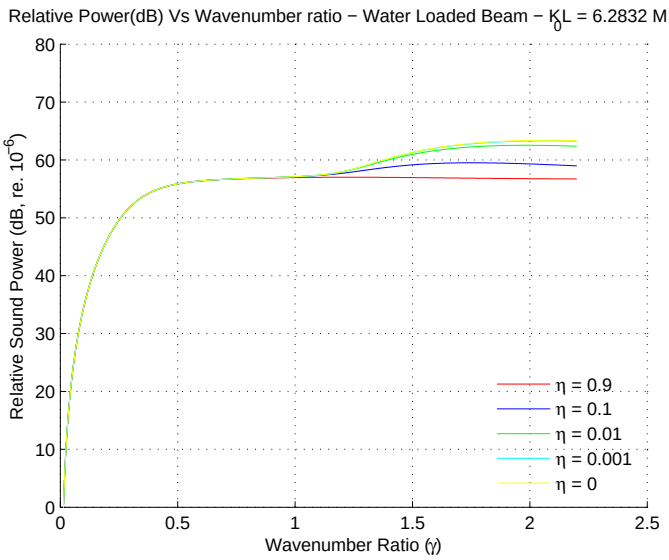

Fig. 5.28 Relative sound power v/s wavenumber ratio for **varying** η; $K_0L = 2\pi$

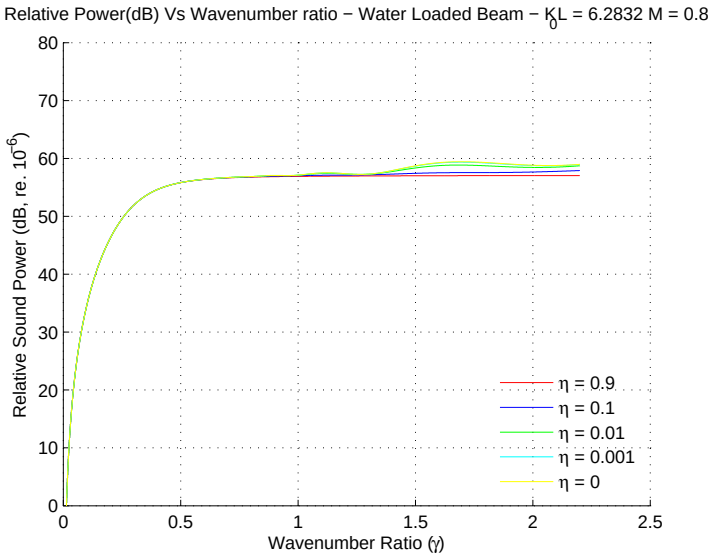

Fig. 5.29 Relative sound power v/s wavenumber ratio for **varying** η; $K_0L = 2\pi$

to 5.29. If the loss factor is small, then the damping effects reduce and the sound power level significantly increases. This shows that the damping effect cannot be neglected while looking at the sound power generated by a beam.

5.6.3 Conclusion

Effect of loss factor on radiated sound power from beams subjected to moving loads has been analysed. It is observed that as the structural damping decreases, vibrational levels increase thus causing an increase in the sound power. The shift of the curves with increasing loss factor is however found to be proportional to the change in the loss factor.

5.7 Floating Airport

5.7.1 Introduction

In this section we investigate and evaluate the total radiated sound power from a floating airport due to the landing / taking off of an airplane. The floating airport is modeled as a Timoshenko-Mindlin plate and the landing/ taking off of an airplane modeled as a moving uniformly distributed line force. The numerical analysis has been undertaken by calculating the total sound power for different structural materials to understand the effect of the material on the sound power radiated due to the landing / taking off of an airplane. The geometrical and material parameters used for the numerical analysis of a floating airport are given in Table 5.2.

Table 5.2: Material Parameters - Floating Airport

For Steel	
$E = 20 \times 10^{10}$	N/m^2
$\rho_v = 7800$	kg/m^3
$D = 560$	KNm
For Aluminium	
$E = 7.1 \times 10^{10}$	N/m^2
$\rho_v = 2700$	kg/m^3
$D = 237$	KNm
$h = 2.54 \times 10^{-2}$	m
$\nu = 0.3$	
$\kappa^2 = 0.85$	
For water	
$C_0 = 1481$	m/s
$\rho_0 = 1000$	kg/m^3

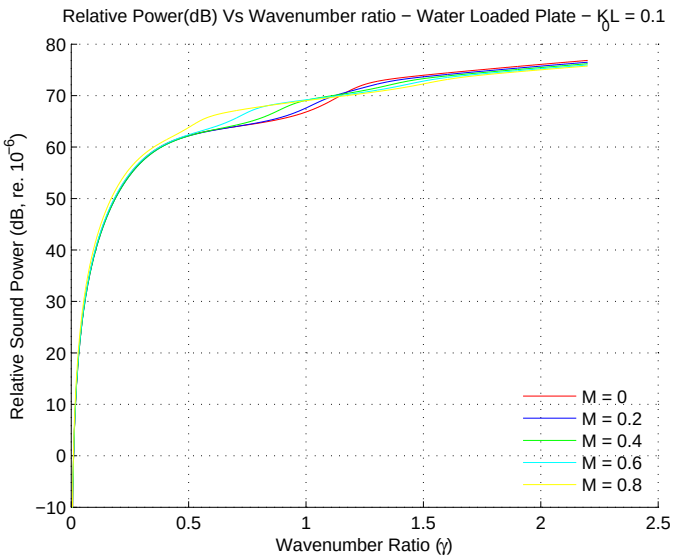

Fig. 5.30 Relative sound power v/s wavenumber ratio for **Steel** with various $K_0L = 0.1$

The external force strength (f_0) is assumed to be of unit magnitude. By varying the values of parameters M and K_0L, the sound power is computed and then plotted against the wave number ratio (γ) or nondimensional frequency.

The sound power has been calculated for $K_0L = 0$ and 2π in the frequency range $0.01 < \gamma < 2.2$. The results so obtained for steel plate are shown in Figures 5.30 and 5.31. The sound variation by an Aluminium plate is shown in Figures 5.32 and 5.33.

5.7.2 Discussion

The sound power generated by the moving load on a Timoshenko-Mindlin plate model made of steel can be viewed in Figures 5.30 and 5.31. With increased speed, the sound power generated increases, though marginally. However increased acoustic length K_0L reduces the sound power level over the entire frequency range. This effect is expected since the total applied force strength is kept constant. No pronounced peak is noticed in the sound power curves. This is attributed to the fact that denser mediums like water drain the energy faster from the structure disallowing the formation of the peak. One can see four distinct frequency ranges: the very low frequency region ($\gamma < 0.1$); the low

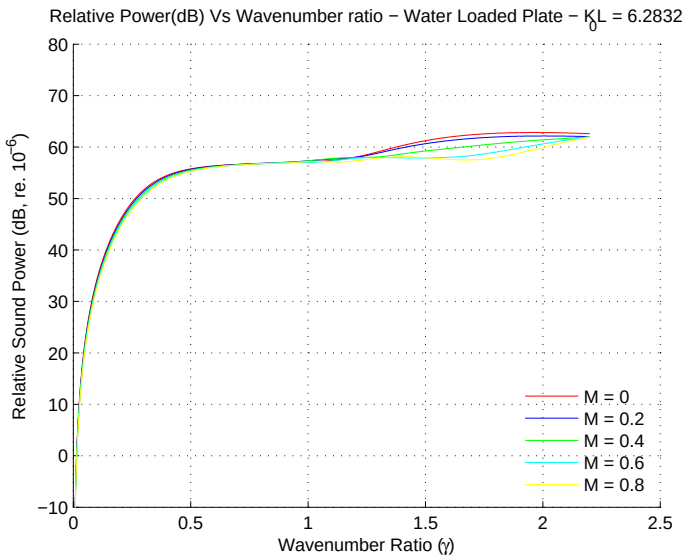

Fig. 5.31 Relative sound power v/s wavenumber ratio for **Steel** with various $K_0L = 2\pi$

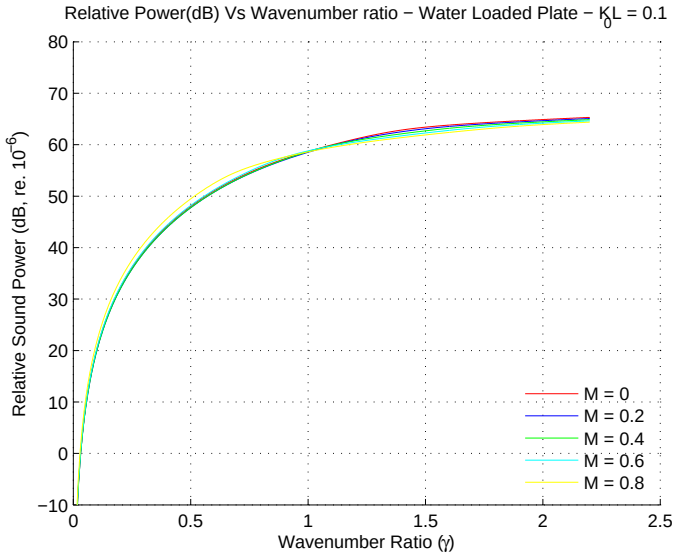

Fig. 5.32 Relative sound power v/s wavenumber ratio for **Aluminium** with various $K_0L = 0.1$

frequency region ($0.1 < \gamma < 1.0$); the frequency region near coincidence ($\gamma \sim 1.0$); and the frequency region above coincidence ($\gamma > 1.0$). In the very low frequency region and in the region above coincidence frequency, the sound powers radiated show no discernible difference. It is the low frequency region and the region near coincidence which are of significance.

Figures 5.32 and 5.33 show the sound power generated by a moving load on a

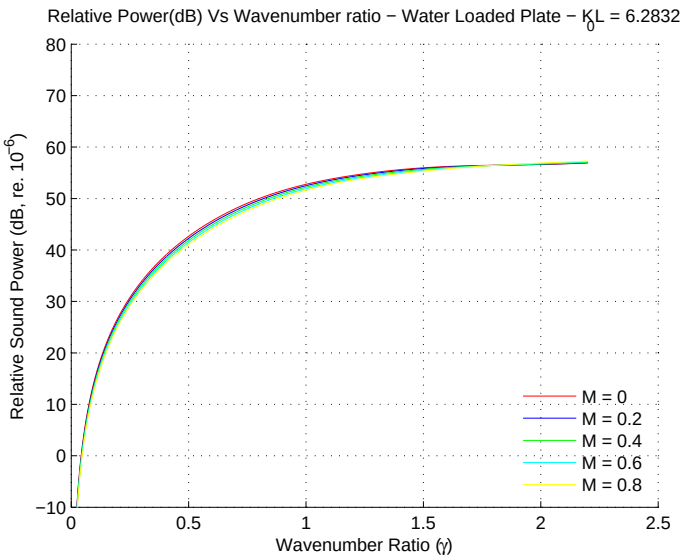

Fig. 5.33 Relative sound power v/s wavenumber ratio for **Aluminium** with various $K_0L = 2\pi$

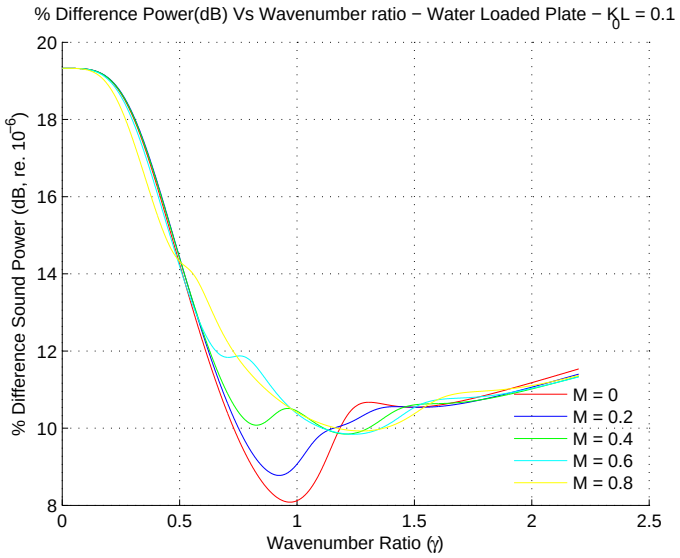

Fig. 5.34 % difference in sound power between Steel and Al. structures;$K_0L = 0.1$

Timoshenko-Mindlin plate made of Aluminium. As expected the sound produced from an Aluminium structure is lesser than that from a steel structure for all acoustic lengths. The difference of the acoustic power is however very large at low frequencies which reduces and then increases again as seen in Figures 5.34 to 5.36. The same trend is noticed for higher values of K_0L. What is interesting to note that the differences tend to converge for varying convective speed of loading at higher frequencies as noted by Keltie and Peng

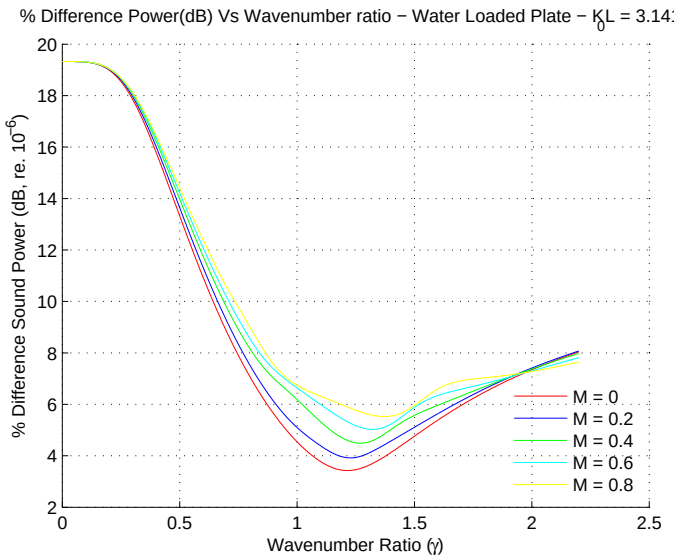

Fig. 5.35 % difference in sound power between Steel and Aluminium structures $K_0L = \pi$

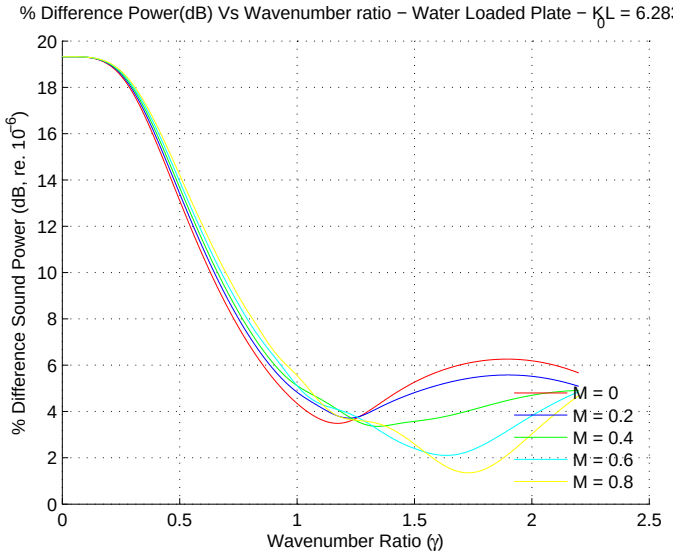

Fig. 5.36 % difference in sound power between Steel and Aluminium structures $K_0L = 2\pi$

(1988).

5.7.3 Conclusion

Sound produced by an airplane landing / taking off from a floating runway has been investigated for different structural materials. The entire analysis is carried out assuming a

one dimensional plate in lieu of a three dimensional runway with time varying harmonic loading. The sound generated at various speeds of convective loading has been calculated and as expected an increase in sound is observed with increasing Mach number. The overall sound generated reduces with an increased acoustic length K_0L over the entire frequency range. No pronounced peaks are observed in the sound power curves due to the denser medium of water wherein the energy drain is faster disallowing peak formation. Changing of structural material from steel to aluminium has a similar effect, however the difference of sound power from different speeds of convective loadings is seen to converge at higher frequencies.

For a floating airport the relationship between the frequency and the non-dimensional frequency (γ) is as given in Table 5.3. When analyzing the sound produced by the floating airport due to a landing / taking off of an airplane in conjunction with the hearing curves for the select teleost fishes as given in Figure 1.1, one notices that the low frequency region ($0 < \gamma < 1.0$) is what is of concern with respect to the marine life and is an area of concern in our study. One can thus infer that the sound power produced by the landing / taking off of an airplane from a floating airport has a direct co-relation to the hearing threshold of the fishes.

Table 5.3: Freq. relation with γ (for Floating Airport)

Parameter								
γ	0.2	0.4	0.8	1.0	1.4	1.8	2.0	2.2
ω	$2,500$	$10,000$	$40,000$	$62,500$	122500	$202,500$	250000	$302,500$
$Freq\ (Hz)$	398	$1,592$	$6,369$	$9,952$	$19,506$	$32,245$	$39,809$	$48,169$

It is thus concluded that the effect of sound produced by an aircraft landing / takeoff on a floating airport needs to be factored into while undertaking the design of a VLFS to be used as a floating airport for safer marine environment.

5.8 Floating Airport subjected to a Mean Flow

5.8.1 Introduction

Conventional Mega-Floats are set up in relatively calm water behind islands or breakwaters. This limitation has disallowed Mega-Floats to demonstrate primary cost performance. To extend their versatility, devices are being developed / studied to widen the range of potential setup sites .

In the present study the investigation of a floating airport subjected to the landing / taking off of an airplane and a mean flow is undertaken and the total radiated sound power is evaluated. The parameters used for the numerical analysis of a floating airport are given in Table 5.2. The mean flow velocity is taken as varying between $-10m/s$ to $10m/s$. The magnitude of this current is governed by **both the natural currents and those created by man due to discharge** of effluent and waste into the oceans. In actual the maximum surface current is that of Gulf stream at $2.5m/s$ followed by the Agulhas current at $2m/s$. One may argue to say that the magnitude of these currents is so low that the resultant effects shall be negligible, which is as observed in the present study. However effect of mean flow when considered in conjunction with other factors such as inplane loading etc., cannot be neglected when calculating the sound power generated by a moving load.

Recent discussions of having a floating airport in UK positioned in the river Thames which has a tidal rise and fall of 7 m (23 ft) leading to effective currents of 4.5 knots ($2.3m/s$) are indicative that study of "current" is essential.

In this section, Equation (3.34) is numerically evaluated for the case of a one dimensional steel plate (beam) immersed in water. The external force strength (f_0) is assumed to be of unit magnitude. By varying the values of parameters M and K_0L, the sound power is computed and then plotted against the wave number ratio (γ) or non-dimensional frequency. The sound power has been calculated for $K_0L = 0.1$ and 2π in the frequency

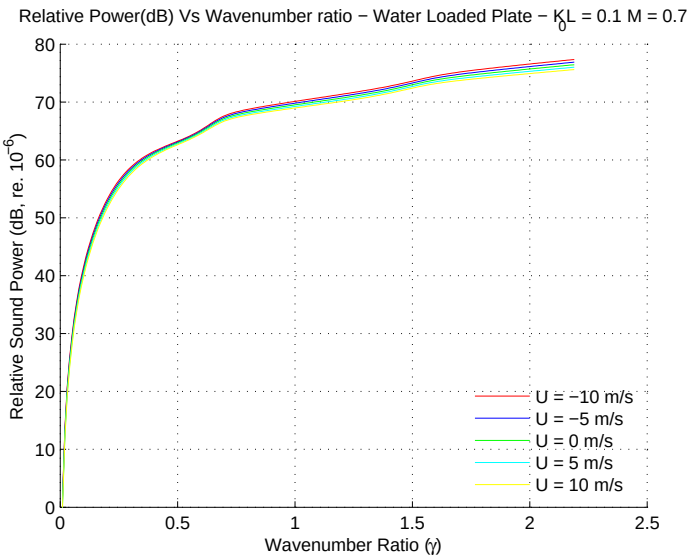

Fig. 5.37 Relative sound power v/s wavenumber ratio **with current**; varying K_0L

range $0.01 < \gamma < 2.2$. Figures 5.37 and 5.38 shows the effect on steel structures of varying current for $M = 0.7$ and the same combination of $K_0L = 0.1$ and 2π.

5.8.2 Discussion

Figures 5.37 and 5.38 shows the effect of the presence of current on the sound radiation for $M = 0.7$. The nature of the curves remain the same as that without current. The curves show a proportional shift due to the presence of current. The minus (-) current indicates direction of the current opposite to the direction of the subsonic moving force. The net effect is an increased Mach number and hence a shift of the curve upwards as was observed in Figures 5.30 and 5.31. The shift however is not very large. It may be noted that a high value of the current which makes the modified Mach number greater than 1 is not permissible since the calculations are valid for the subsonic speed domain.

Since the variations due to the presence of current is not predominantly visible in Figures 5.37 and 5.38, we replot the figure as a difference curve with $U = 0$ as the reference to get Figures 5.39 to 5.50. Figure 5.37 and 5.38 are for fixed M with varying K_0L. Figures 5.39 to 5.41 are for non-integral multiples of π and Figures 5.45 to 5.47 are for integral multiples of π for $M = 0.01$. Similarly Figures 5.42 to 5.44 are for non-integral multiples of π and Figures 5.48 to 5.50 are for integral multiples of π for

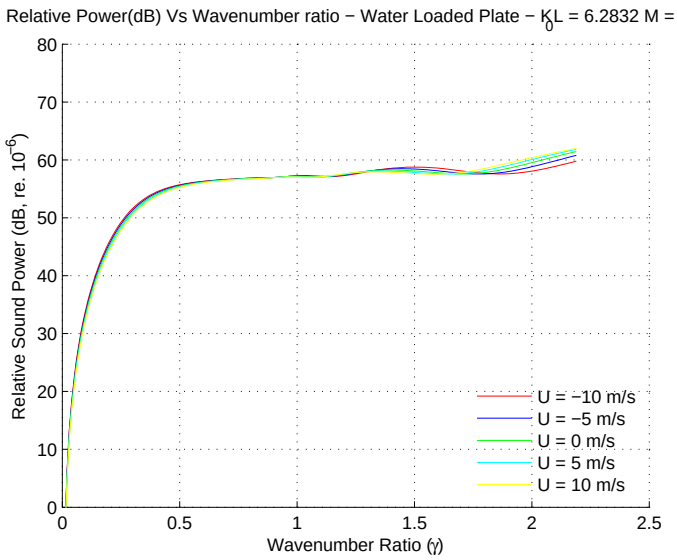

Fig. 5.38 Relative sound power v/s wavenumber ratio **with current**; varying K_0L

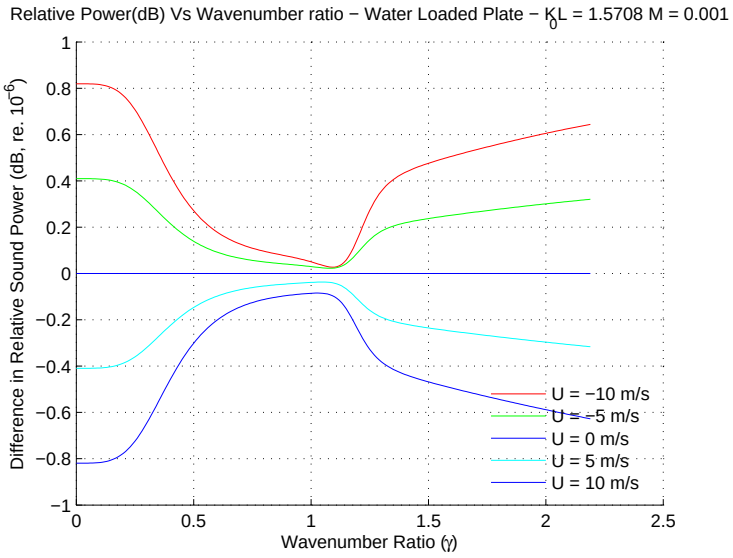

Fig. 5.39 Difference in Relative sound power for **current**; $M = 0.001$; $K_0L = \pi/2$

$M = 0.7$. It is interesting to note that the trend of curves of integral multiples and non-integral multiples is different, but consistent. The variation due to convective speed of loading is increased magnitudes for increased U while the curve trends remain to be the same. It is noted that for non-integral multiples of π, for every step increase of $\pi/2$, there is an added node with the magnitude of the previous nodes being reduced. For integral multiples of π, for every step increase of π, there are two added nodes, again

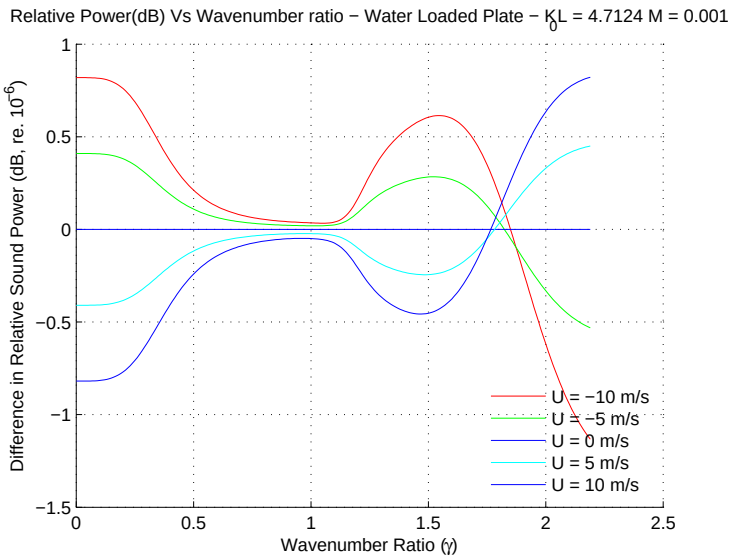

Fig. 5.40 Difference in Relative sound power for **current**; $M = 0.001$; $K_0L = 3\pi/2$

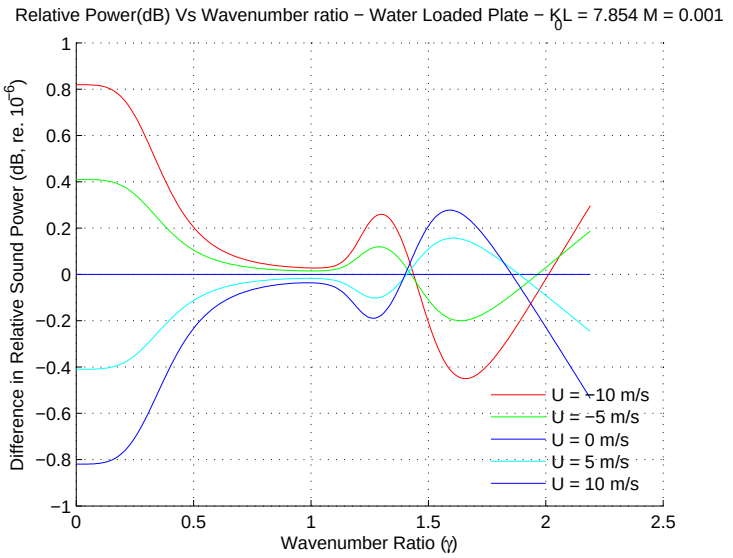

Fig. 5.41 Difference in Relative sound power for **current**; $M = 0.001$; $K_0L = 5\pi/2$

the previous nodes being reduced in magnitude. It may also be noted that the relative difference of sound power due to presence of mean flow is limited to 1 dB which may be considered to be negligible if considered in isolation but when considered in conjunction with other variables, it may be considered to be of a large magnitude.

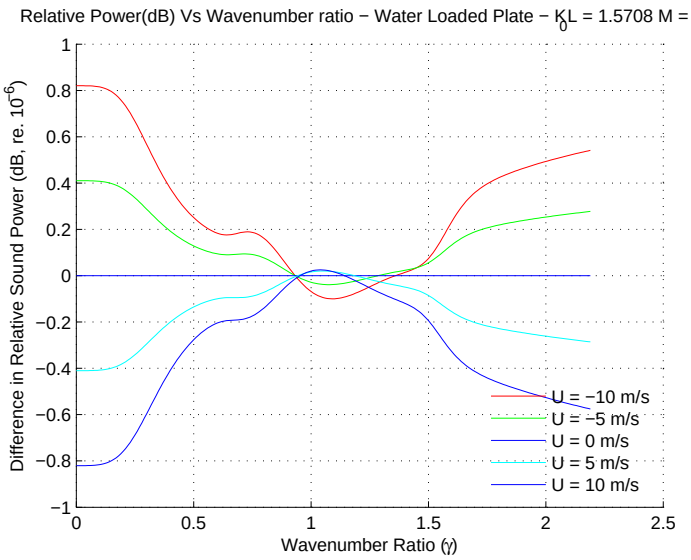

Fig. 5.42 Difference in Relative sound power for **current**; $M = 0.7$; $K_0L = \pi/2$

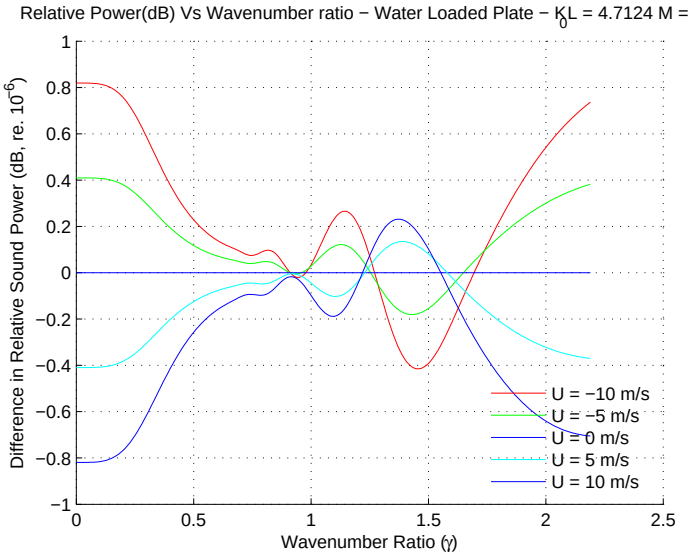

Fig. 5.43 Difference in Relative sound power for **current**; $M = 0.7$; $K_0L = 3\pi/2$

5.8.3 Conclusion

Sound produced by an airplane landing / taking off from a floating runway has been investigated in the presence of a mean flow on a floating steel runway. The entire analysis is carried out assuming a one dimensional plate in lieu of a three dimensional runway with time varying loading. The sound generated at various speeds of convective loading has been calculated and as expected an increase in sound is observed with an increasing

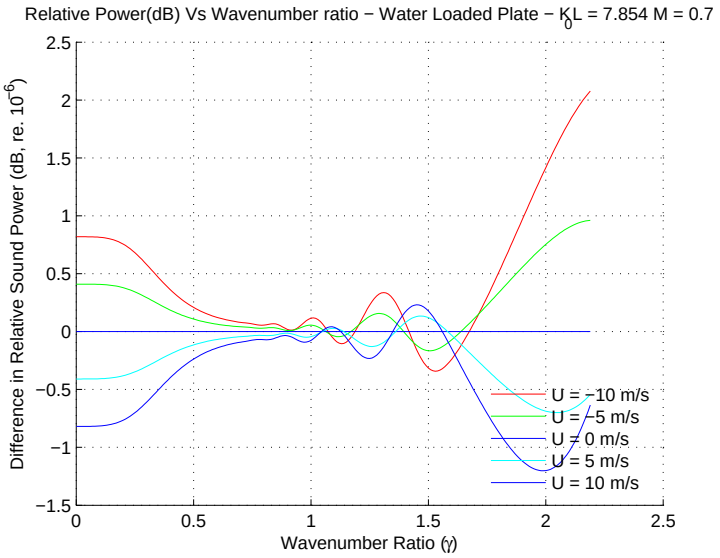

Fig. 5.44 Difference in Relative sound power for **current**; $M = 0.7$; $K_0L = 5\pi/2$

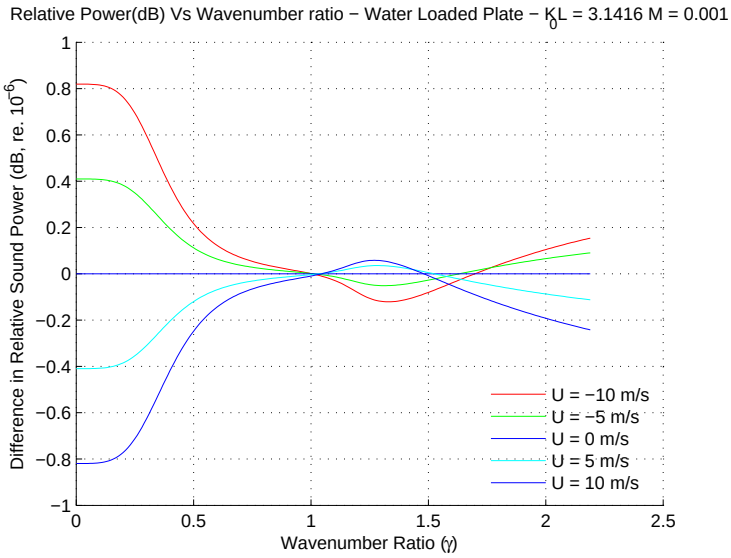

Fig. 5.45 Difference in Relative sound power for **current**; $M = 0.001$; $K_0L = \pi$

mean flow. The overall sound generated reduces with an increased acoustic length K_0L over the entire frequency range. No pronounced peaks are observed in the sound power curves due to the denser medium of water wherein the energy drain is faster disallowing peak formation. The presence of current does not alter the sound produced prominently and the change is seen to be in the range of 1dB. On analysing the difference of sound power with current a unique trend of curves is observed for acoustic lengths of integral

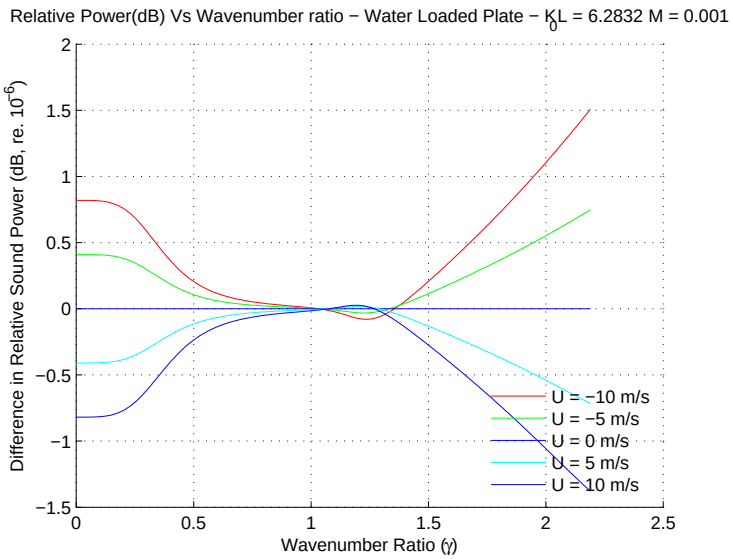

Fig. 5.46 Difference in Relative sound power for **current**; $M = 0.001$; $K_0L = 2\pi$

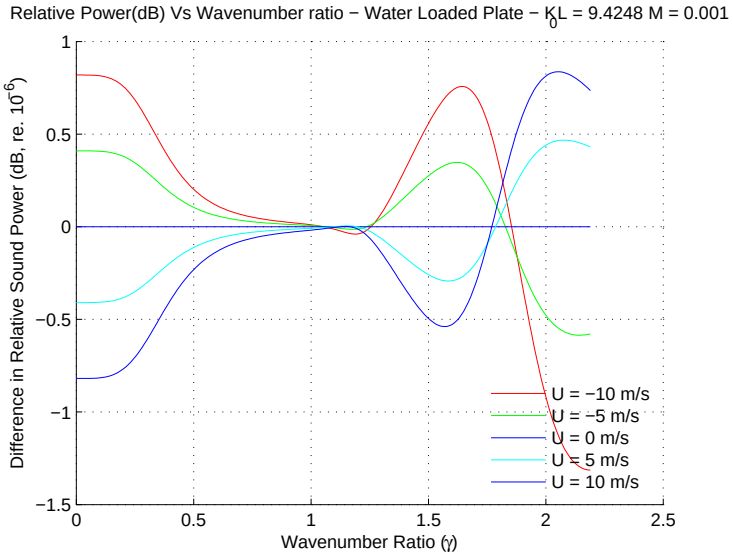

Fig. 5.47 Difference in Relative sound power for **current**; $M = 0.001$; $K_0L = 3\pi$

and non-integral multiples of π. The *inter se* trend however remains consistent.

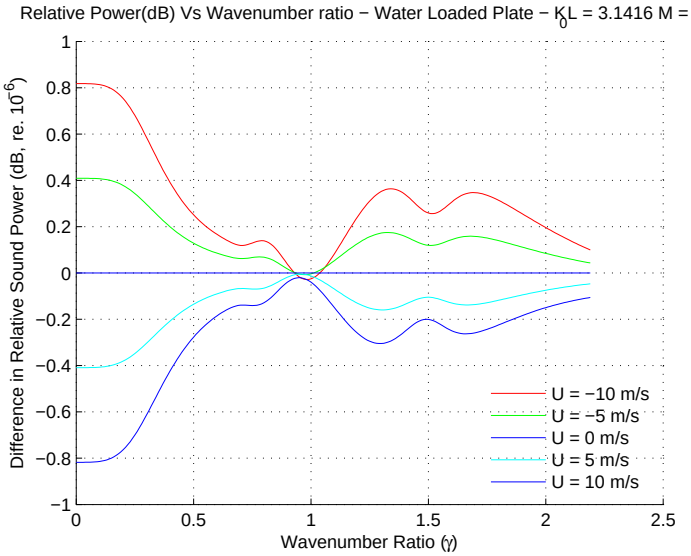

Fig. 5.48 Difference in Relative sound power for **current**; $M = 0.7$; $K_0L = \pi$

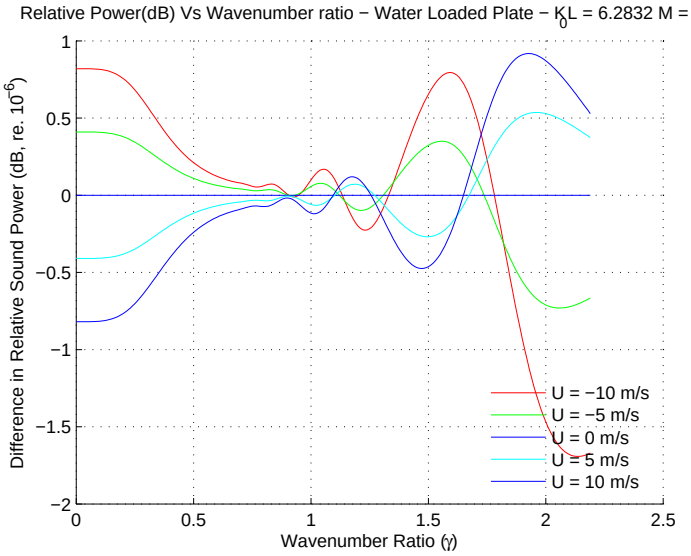

Fig. 5.49 Difference in Relative sound power for **current**; $M = 0.7$; $K_0L = 2\pi$

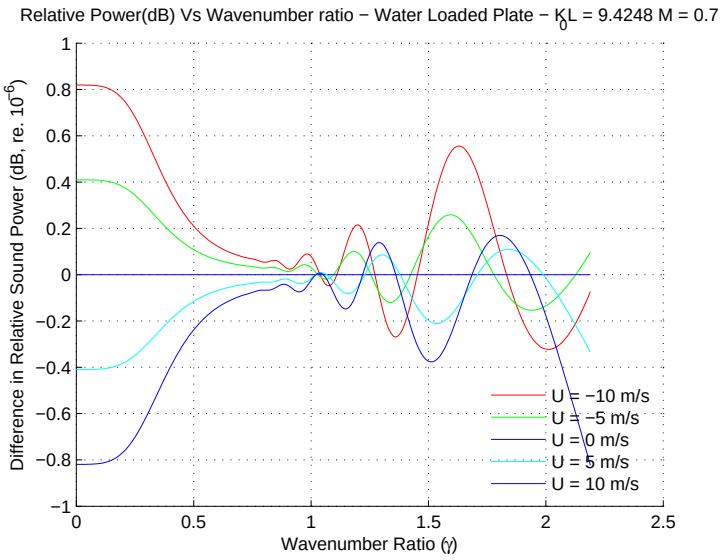

Fig. 5.50 Difference in Relative sound power for **current**; $M = 0.7$; $K_0 L = 3\pi$

5.9 Floating Airport subjected to Inplane Loading

5.9.1 Introduction

The effect of inplane loading on a floating airport is undertaken by evaluating the total radiated sound power for an inplane loaded Timoshenko-Mindlin plate. Equation (3.34) is numerically evaluated for the case of a steel beam floating on water. Geometrical and material parameters used in this section are given in Table 5.2. With a typical weight of a fully loaded Boeing-747-400 at 7767 KN (as available from the BOEING webpage) which acts as a compressive load on the deck of the floating airport, the compressive (Q) and tensile (T) load are varied between 5 MN to 200 MN. The external force strength (f_0) is assumed to be of unit magnitude. By varying the values of parameters M and K_0L, the sound power is computed and then plotted versus the wave number ratio (γ) or non-dimensional frequency. The sound power has been calculated for $K_0L = 0.1$ and 2π in the frequency range $0.01 < \gamma < 2.2$. The results so obtained for compressive loading are shown in Figures 5.51 and 5.52 and that for tensile loading in Figures 5.55 and 5.56.

5.9.2 Discussion

The sound power generated by the moving load on a one dimensional Timoshenko-Mindlin plate subjected to compressive inplane loading can be seen in Figures 5.51 and 5.52. With increased speed, there is a marginal decrease in the sound power generated, while an increased acoustic length K_0L reduces the sound power level over the entire frequency range. This occurs since the total applied force strength remains a constant. Due to a denser medium, like water, wherein energy drain is faster, no pronounced peaks are noticed.

With increasing compressive loading the sound power from the structure decreases as seen in Figures 5.51 and 5.52. The tensile loading on the other hand shows a corresponding increase in the sound power magnitude. The increase of the acoustic power is however not very large over the entire range of frequency as seen in Figures 5.53 and 5.54 for compressive loading and Figures 5.57 and 5.58 for tensile loading. It may be noted

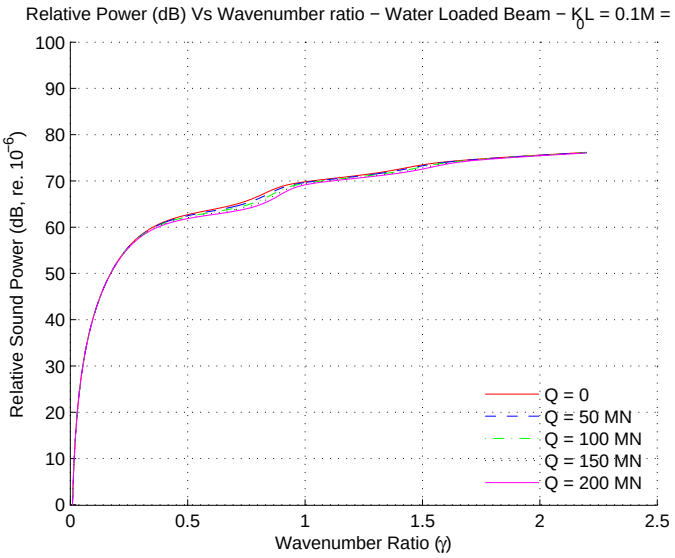

Fig. 5.51 Relative sound power v/s wavenumber ratio under Compressive Load; $M = 0.5$; $K_0L = 0.1$

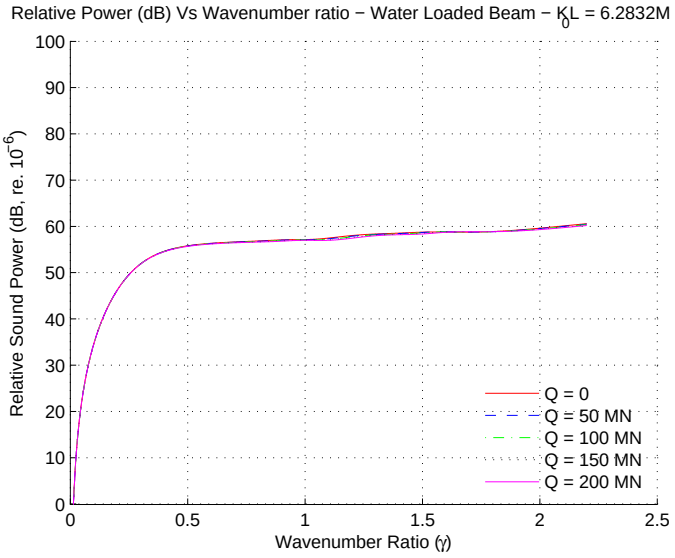

Fig. 5.52 Relative sound power v/s wavenumber ratio under Compressive Load; $M = 0.5$; $K_0L = 2\pi$

that the differences tend to converge for varying convective speed of loading at higher frequencies as noted by Keltie and Peng (1988).

5.9.3 Conclusion

The effect of inplane loading on total sound power generated by a one dimensional floating plate has been analysed. It is concluded that the effect of a **compressive** loading, is a

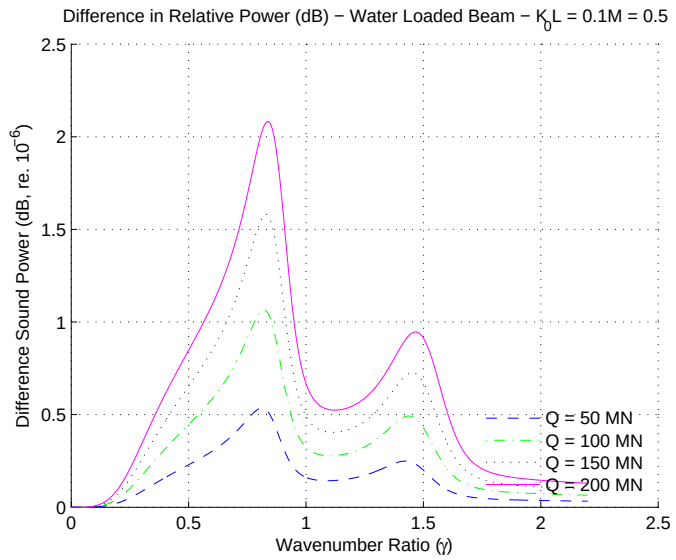

Fig. 5.53 % Difference for sound power v/s wavenumber ratio under Compressive Load; $M = 0.5$; $K_0L = 0.1$

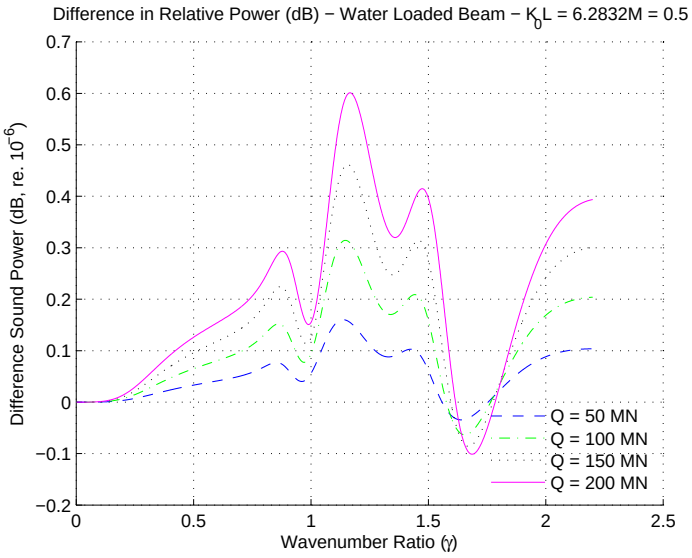

Fig. 5.54 % Difference for sound power v/s wavenumber ratio under Compressive Load; $M = 0.5$; $K_0L = 2\pi$

decreased sound power while an increased **tensile loading increases the sound power** of the floating structure, the change is however not very large over the entire range of frequency however cannot be neglected when treated with other components of loading. The observations so made are considered to be analogous to a guitar string which produces greater sound when tightened (under tensile loading) as compared to the dull sound it creates when relatively loose (under compressive loading). What is

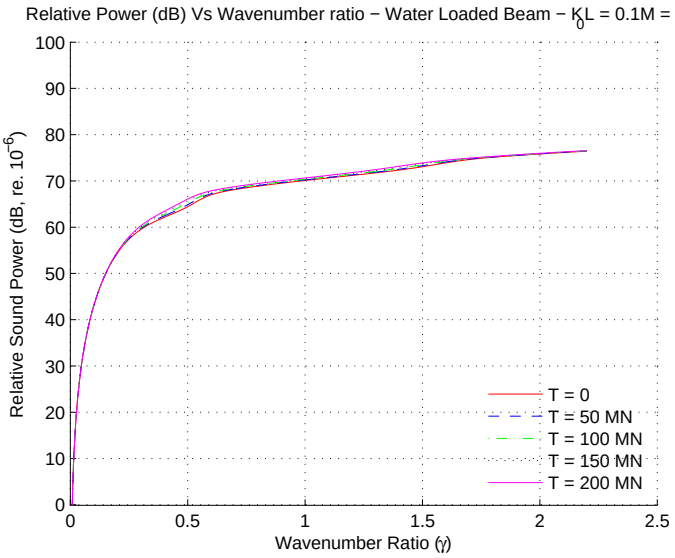

Fig. 5.55 Relative sound power v/s wavenumber ratio under Tensile Load; $M = 0.8$; $K_0L = 0.1$

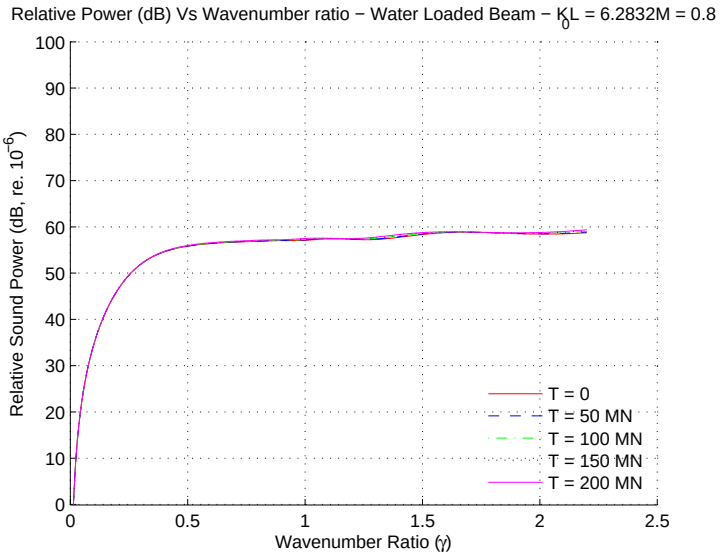

Fig. 5.56 Relative sound power v/s wavenumber ratio under Tensile Load; $M = 0.8$; $K_0L = 2\pi$

interesting to note is the difference tends to converge for varying convective speed of loading at higher frequencies as noted by Keltie and Peng (1988). For lower convective loading the wavenumber response peaks are approximately symmetrical and are identified as propagating flexural waves. With increased convective loading speed, the spectral response changes.

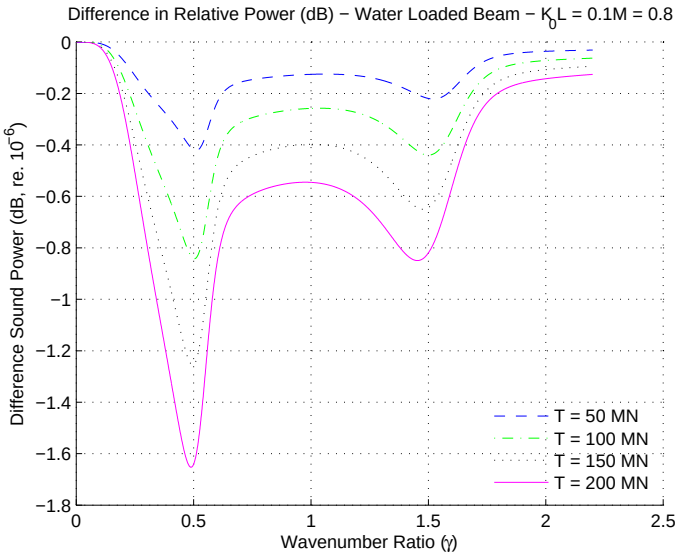

Fig. 5.57 % Difference for sound power v/s wavenumber ratio under Tensile Load; $M = 0.8$; $K_0L = 0.1$

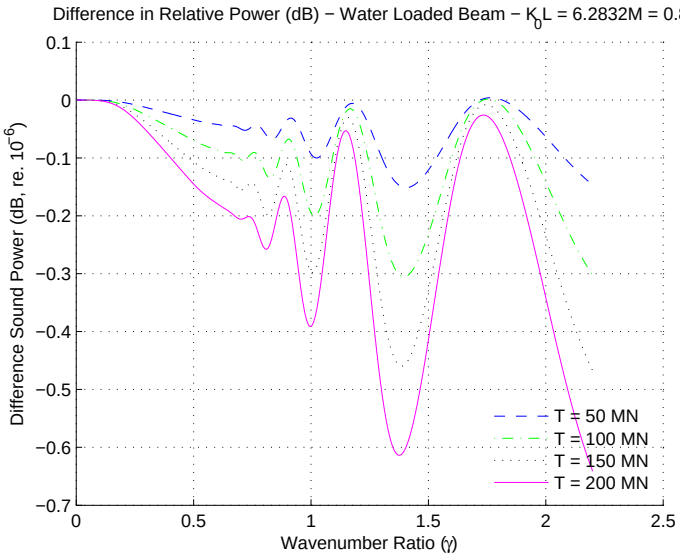

Fig. 5.58 % Difference for sound power v/s wavenumber ratio under Tensile Load; $M = 0.8$; $K_0L = 2\pi$

5.10 Structural Response of a Floating Airport

5.10.1 Introduction

The numerical investigation of the structural response of a floating airport subject to a moving load is discussed in this section. The investigation of the problem is undertaken by comparing the wavenumber response for a floating airport made of steel. The response is studied by analysing the response of a point loading and a distributed loading. In order to undertake the required investigation, Equation(3.13) is numerically evaluated for the case of a plate immersed in water. The properties of the floating airport model analysed are given in Table 5.2.

5.10.2 Discussion

The displacement of the idealized one dimensional floating airport is seen in Figures 5.59 and 5.60 for a distributed loading and a point loading respectively. In both the Figures 5.59 and 5.60, the large spectral responses of the fluid loaded flexural wavenumber are visible. These are seen as local peaks emanating the point of load application, indicated by $\zeta = 0$ from the $M = 0.1$ to 0.9. The presence of peak in the positive wavenumber is noticed, which represents the flexural wave that propagates in the same direction as the convected loading. With increased convected loading speed, the peak moves towards a larger value of wavenumber due to the Doppler effect. Similarly the negative peak represents the flexural wave for which the propagating direction is opposite to that of the convected loading. The wavenumber for this peak is found to be decreasing with increased convected loading thus indicating that the negative going wave may be supersonic. These sets of propagating positive going and negative going flexural waves can be noted in both the loading cases. The identification or pre-definition of the location of these peaks precisely can however not be done. It is further noticed that the local peak moves in a curvilinear path with increasing speed of the airplane (indicated by the increasing M). This local peak in turn gives the maximum deflection of the floating airport and is in concurrence with the results published by other researchers.

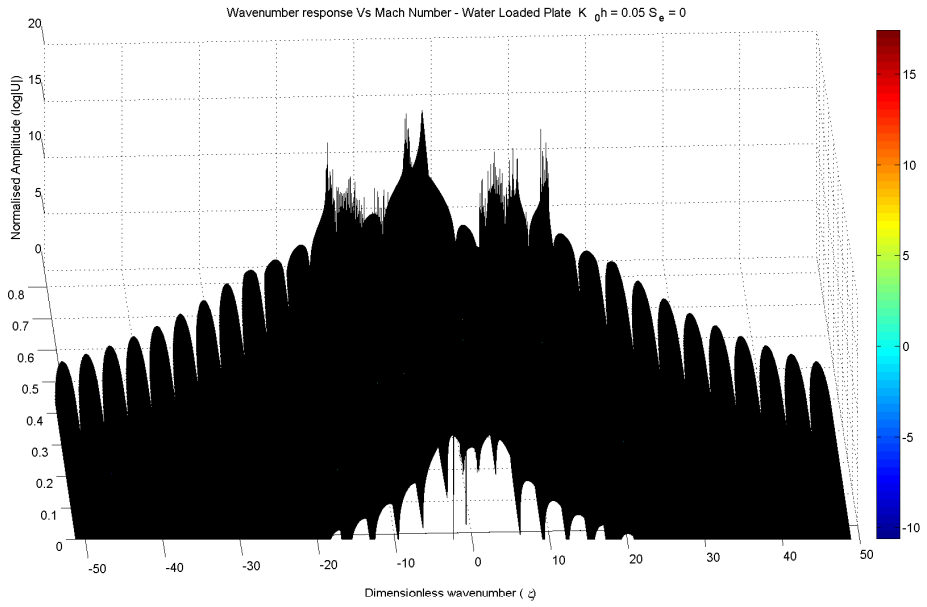

Fig. 5.59 Three Dimensional plot for Wavenumber response V/s Dimensionless Frequency; Distributed loading

To improve the understanding and visualization of the three dimensional plot, slice plots are presented in Figures 5.61 and 5.62 for both distributed loading and line loading respectively. For lower convective loading the structural response peaks are approximately symmetrical and are identified as propagating flexural waves. With increased convective loading speed, the spectral response changes as shown.

5.10.3 Conclusion

The structural response of a floating airport subjected to landing / taking off of an airplane has been analyzed. Since such problems are not conducive to physical modeling and experimental validation due to their size and speeds involved, numerical analysis is an excepted norm. However conventional means of using a three dimensional runway with time varying loads is extremely difficult and time consuming. The problem has been simplified by using a Timoshenko-Mindlin plate model. In developing the expression for the structural response, a Fourier transformation in space for the whole structure in wavenumber domain is utilized rather than using the wave propagation method to reduce

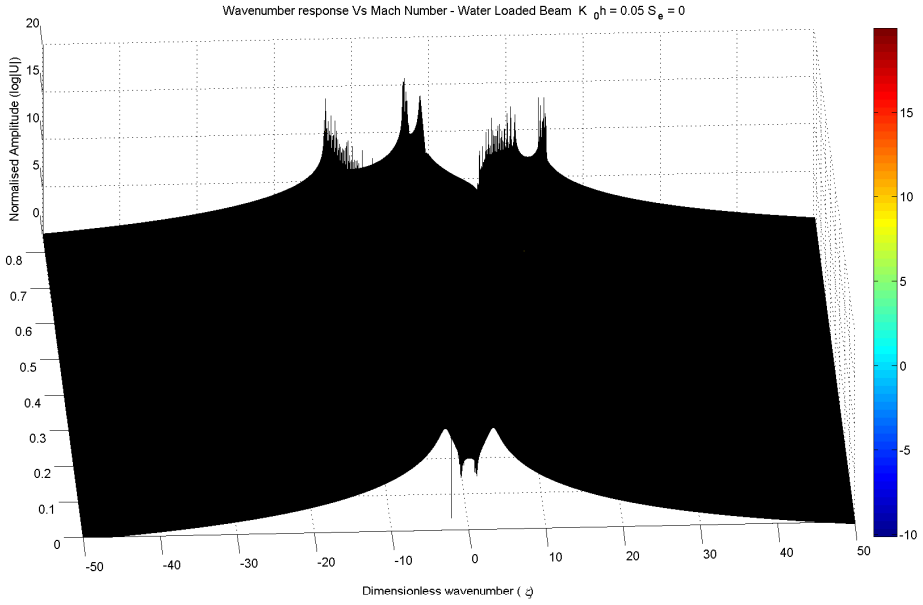

Fig. 5.60 Three Dimensional plot for Wavenumber response V/s Dimensionless Frequency; Point loading

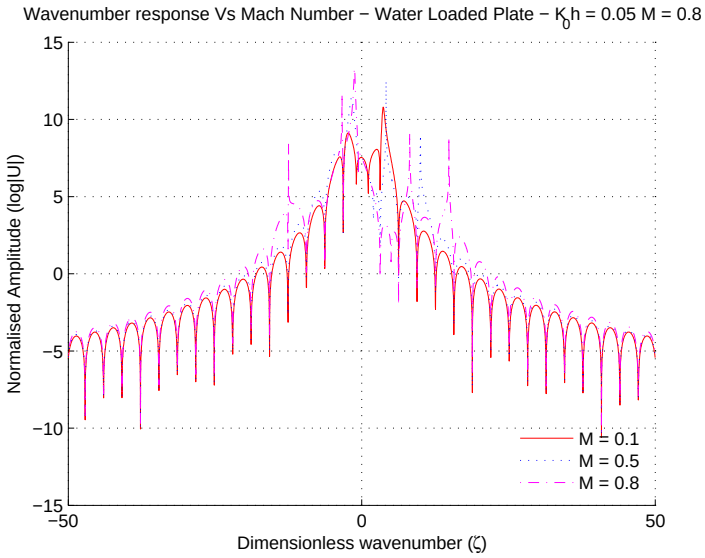

Fig. 5.61 Two Dimensional plot for Wavenumber response V/s Dimensionless Frequency; Distributed loading

the analysis to a substructure. One notices that

- Large spectral responses of the fluid loaded flexural wavenumber are visible when the wavenumber is plotted against the increasing speed of the airplane.
- The large spectral responses are seen as local peaks emanating from the point of

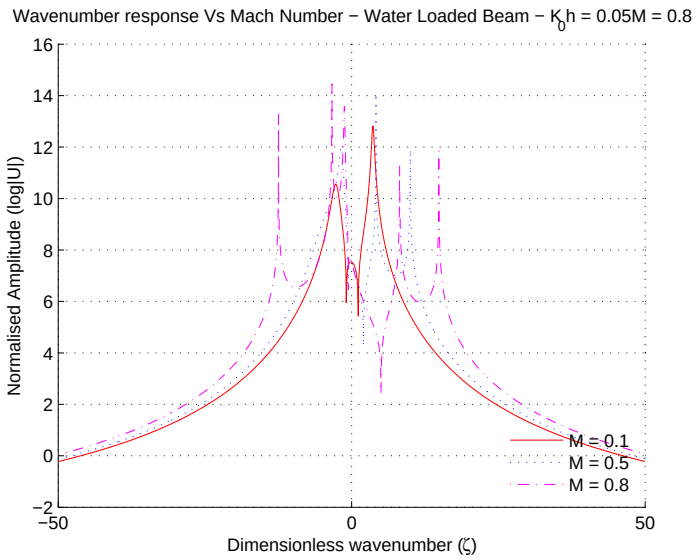

Fig. 5.62 Two Dimensional plot for Wavenumber response V/s Dimensionless Frequency; Point loading

load application and represent the flexural wave propagating in the same direction as the convected loading due to the Doppler Effect.

- Defining the location of these peaks precisely aprior is however not feasible.
- The local peak moves in a curvilinear path with increasing speed of the airplane.
- The results obtained are similar to those reported by other researchers in this field.

Chapter 6

Closure

6.1 Salient Feature of the Thesis

The present study provides a methodology for calculating of total sound power radiated due to a moving load on a floating platform (ship or airport). The ship has been modeled as a beam while the floating airport has been modeled as a one dimensional plate to simplify the formulation. The effect of external factors such as loss factor, mean flow, inplane loading on the total sound power radiated has been analyzed additionally. A GUI has been developed to undertake all the above analysis by varying the input parameters.

6.2 Contribution of the Thesis

The following are the contributions of this study:-

- An expression for **total sound power due to the presence of a moving load** on *Rayleigh beam*, *Shear beam* and *Euler-Bernoulli beam* has been developed. It is observed that the sound radiation from a Timoshenko beam is lower and increases with the Shear beam, Rayleigh beam to the Euler-Bernoulli beam in that order and is attributed to the inclusion or otherwise of the rotary and shear factors.

- The effect of **varying loss factor (structural damping)** on such floating beams has been evaluated. It is noticed that increased vibrational levels (due to structural damping) lead directly to increased sound radiation. It is interesting to note that the curves appear to have the same basic shape. As the structural damping decreases, the amount of steady-state vibrational energy in the beam increases. What is most interesting is that the curves shift up by an amount which is directly proportional to the change in the loss factor.

- The methodology has been extended to a floating airport and the **sound power generated by the landing / takeoff of airplanes** has been investigated. The concept of sound generated from the floating airport is important due to the effect the sound has on the ecology and the marine life below the airport.

- The floating airport has been evaluated for generated sound power in the **presence of a current** in the fluid along with the moving load. The relative difference of sound power due to the presence of mean flow is limited to 1dB, a small magnitude, however cannot be neglected when acting along with other types of loading.

- The **effect of inplane loading** in the sound power produced by a moving load on the structure has been analysed. The effect of increasing tensile loading shows an increased sound power from the structure while increased compressive loading shows reduced sound power.

- The **structural deflections** due to the moving load on a floating airport is studied. The effect of a point loading and distributed loading is considered to study this deflection.

- A **GUI** for undertaking the above analysis for both a ship model and a floating airport model has been developed for making the calculation procedure user friendly and speed up the user's work especially for non-technical people.

The study undertaken herein develops a methodology for understanding the total sound power produced by a floating structure, namely a ship modeled as a beam and a floating

airport modeled as a one dimensional plate due to moving loads. This study shall allow researchers to calculate sound produced by moving loads on such structures and hence reduce sound from such structures.

6.3 Brief Overview of the Research Work Pursued

The content of the thesis is divided into *six* chapters for ease of explanation and the problems investigated.

Chapter 1, gives a **basic introduction and the motivation** behind the present study. The available literature relevant to the present study is reviewed thoroughly followed by a brief introduction of the research work pursued in this thesis. The basic physical equations, boundary conditions associated with acoustic problems associated with fluids and moving loads and the preliminary mathematical tools relevant to the thesis are discussed.

In *Chapter 2*, the generalized expression for the total sound power due to a **moving load on a ship** (modeled as a beam) as given by Keltie and Peng (1988) is formulated in detail for the various beam types, viz. *Rayleigh beam*, *Shear beam* and the *Euler-Bernoulli beam*.

Studies of sound generated from **floating airfields** due to the traveling load of starting, landing or taxiing planes is a natural extension of the ship (modeled as a floating beam) studied in the previous chapter. A dynamic analysis of a three-dimensional runway with time varying loading during take-off however would be exceeding difficult. In *Chapter 3*, this analysis is made simpler by assuming that the runway behaves as a simple, infinitely long beam floating on water and supported by buoyancy. The model is assumed to be a one dimensional plate, described by the Timoshenko-Mindlin plate equation. The understanding of radiated sound power as established in chapter 2 has been extended to model a **floating airport**. The sound generated and platform response in frequency domain

by the landing / taking-off of an airplane from such an airport, which would be akin to a moving load, has been analysed in section 2 of the chapter. Acoustic analysis in the presence of a **mean flow or current** complicates the analysis of a floating airport by modifying the effect of the moving load. The effect of mean flow on the response of a fluid-loaded structure has been studied in Section 3. Even though a VLFS is structurally very long, the longitudinal strength does not play an important role in their design. The most severe type of loading for the bottom plate occurs when the structure is subjected to the combined action of uniformly distributed hydrostatic lateral loading and compression due to hogging. Similarly for the deck plate, maximum loading occurs when the structure is subjected to compression and tension due to sagging and hogging respectively. The inplane loading plays an important role for such structures during berthing, plate connections at ends, initial deformation and corrosion to name a few and hence needs to be accounted for. This effect of **inplane loading** has been studied in section 4 by extending the formulation developed in section 2.

Having developed the general expressions for the ship (in chapter 2) and floating airport (in chapter 3), one needs to validate the model. This is done by using the published results for a Timoshenko beam by Keltie and Peng (1988). Once the model has been validated, a **Graphical User Interface** for undertaking numerical calculations using these mathematical formulations is developed and discussed in *Chapter 4*. The GUI has been generated to make the calculation procedure user friendly and speed up the user's work especially for non-technical people.

The GUI developed in chapter 4 has been used to undertake **numerical analysis** to understand the total sound power radiated due to a moving load on a ship (modeled as a beam) and a floating airport (modeled as a plate) in *Chapter 5*. Using the **beam model** to represent the ship, we first analyse the total sound power produced by a Timoshenko beam, a Rayleigh beam, a Shear beam and an Euler-Bernoulli beam. We then compare them to understand which beam type produces the maximum sound power and the reasons associated with it in section 5.5. This is followed by the calculation and analysis of

the total sound power from a Timoshenko beam due to varying loss factor in section 5.6. Having analysed the beam model, the **plate model** is used to undertake the numerical analysis of the total sound power from a floating airport due to a landing / taking off of an airplane. The analysis is carried out for aluminium and steel and the **effect of the material** on the total sound power is studied in section 5.7. The same plate model is then extended by modifying the governing equation Equation (3.3) to Equation (3.21) to incorporate the **effect of mean flow** and the numerical results of the total sound power are obtained and analysed in section 5.8. Another extension is obtained by incorporating the **inplane loading** to the plate model to get Equation (3.35). This is analysed numerically next in section 5.9 to understand the effect of compressive and tensile inplane loads on the floating airport. The numerical analysis terminates with the **structural response** of the floating airport due to airplane landing / taking off modeled as a point and a harmonic moving load in section 5.10.

Finally, *Chapter 6*, **summarizes** the work done in the thesis followed by the future scope of research. Major contributions made in the thesis are also highlighted in this chapter.

Additional information used and derived is enumerated in the Appendices for clarity of the methods described in the chapters and as a starting point for future researchers working in this area.

- Appendix A : Time Averages of Products.
- Appendix B : Detailed derivation for the non-dimensionalized sound power.

6.4 Scope of Future Work

The study undertaken herein develops a methodology for understanding the total sound power produced by a floating platform due to moving loads. It hence allows development of procedures to reduce sound from structures. The following are the possible areas of

extension of this work

- The present analysis has been undertaken assuming a one dimensional plate for ease of formulation. The work can be extended to a two dimensional / three dimensional plate to model a floating airport.
- The structural material considered in the present study is isotropic. Further study could be undertaken for orthotropic material and cater for composite structures.
- The moving load type considered in the present study is a point / line load. More complicated loads such as platoon loads, circular loads, multiple loads etc. can be looked at to represent a variety of loads.
- This is an extremely difficult problem to tackle. What has been done as part of this thesis study is based on sound principles and are considered valuable as a first attempt to tackle a tough problem. However to validate these results the following may be considered as possible areas of extension of this work:
  - Laboratory testing with a scaled down model using relevant scaling laws and laws of similitude.
  - Field testing by deploying hydrophones around the floating platform, recording the acoustic pressure and comparing the results obtained with those recorded using these hydrophones.
  - Numerical modeling using other standard Finite Element packages (Abaqus/ Ansys etc).

6.5 Concluding remarks

6.5.1 Marine noise problem

Sound becomes noise when it is too loud, unexpected, contains unwanted tones (e.g. a whine, whistle, or hum), or is unpleasant. Sound only has to be unwanted for it to be noise, not necessarily just loud.

Acoustic pressure level takes into account the surroundings and the distance of the source as discussed in section 1.9.3. Available information in regards to the hearing curves for select fishes have been discussed in Figure 1.1 as a graph between frequency (Hz) and threshold (dB re 1 μ Pa). By calculating the acoustic power from a floating airport due to landing / taking off of an airplane one infers that the sound power produced by the landing / taking off of an airplane from a floating airport has a direct co-relation to the hearing threshold of the fishes and hence should be treated as a noise problem. Accordingly the effect of sound produced by the aircraft landing / taking off on a floating airport needs to be factored into while undertaking the design of such a floating airport for safer marine environment and hence the need for the present study.

6.5.2 Present study

We notice that the initial work of Keltie and Peng (1988) is for a harmonic line force moving along an infinite beam at a constant subsonic speed undertaken for a Timoshenko beam filled with an acoustic medium (water, air etc).

The present study may be considered as an extension of the work of Keltie and Peng (1988). The study is commenced by remodeling the Timoshenko beam as modeled by Keltie and Peng (1988) for validation of the model as discussed in section 5.2 (which can be considered as the only **similarity** between the two studies).

The study is then extended by modeling a ship as an Euler-Bernoulli, Rayleigh and Shear beam and comparing the results obtained to discuss the performance of the beam model in section 5.5. It is noticed that the Timoshenko model gives the least sound radiation power and is better when compared to other beam types in section 5.5.3.

The effect of the varying loss factor (structural damping) on sound radiation by floating beams has then been evaluated in section 5.6

This model has then been extended to a floating airport modeled as a one dimensional plate described by the Timoshenko-Mindlin plate in section 5.7. Since the plate can be one, two or three dimensional and since one dimensional plate has been studied here, the study of the two / three dimensional plate has been proposed as a likely extension of the study in section 6.4. Performance of the plate models can however be concluded once the study for two and three dimensional plate is undertaken.

The effect of presence of current and inplane loading on the one dimensional plate model has then been studied in section 5.8 and section 5.9 respectively.

Further structural deflections of the floating airport have been analyzed in section 5.10.

A GUI for undertaking the above studies for both a ship (beam model) and a floating airport (plate model) has been developed for making the calculation procedure more user friendly and speed up the user's work especially for non-technical people. This GUI has been discussed in *Chapter 4*.

6.5.3 Frequency Independent results

Results obtained in this study have been expressed as a wave number ratio (γ) against the total sound power (dB re 1 μ Pa), where wave number ratio (γ) is the ratio between the acoustic wave number (K_0) and the free bending wave number (K_B).

By doing so, the dependence on type of sound and structure have been removed hence making the results more versatile. If we were to make the results frequency dependent, then for varying structures, the analysis shall become more cumbersome.

Notwithstanding, for a floating airport with the structural parameters under reference, the relationship between the wave number ratio (γ), angular frequency (ω) and frequency (Hz) has been discussed in Table 5.3.

6.5.4 Conclusion

Effect of loss factor, shear effect and rotatory inertia on radiated sound power from a **ship** (modeled as a beam) subjected to a moving load has been investigated. It is concluded that a *Timoshenko beam* gives the least sound radiation power when compared to the other beam types. The correction for shear effect and rotatory inertia yield results within $4-5\%$ more accurate than classical beam theory. As the structural damping (loss factor) decreases, vibrational levels increase thus causing an increase in the sound vibrations. The shift of the curves are proportional to the change in the loss factor.

Sound produced by an airplane taking off from a floating **runway** has been investigated for different structural materials, presence of mean flow and inplane loading independently assuming a one-dimensional plate in lieu of a three dimensional runway with time varying loading. The sound generated at *various speeds of convective loading* has been calculated and as expected an increase in sound is observed with increasing Mach number. No pronounced peaks are observed in the sound power curves due to the denser medium of water wherein the energy drain is faster disallowing peak formation. *Changing of structural material* from steel to Aluminium has an effect of higher sound power from steel as compared to Aluminium. Presence of *current* does not alter the sound produced prominently and the change is seen to be in the range of 1dB. Though the need to study effect of mean flow (current) may be considered irrelevant in light of the fact that such structures are set up in relatively calm waters behind islands or breakwater, however recent interests to have a floating airport in River Thames, UK and studies to widen range of potential setup sites for VLFS emphasizes this need. With increasing compressive *inplane loading*, the sound power decreases while tensile inplane loading shows a corresponding increase in the sound power magnitude. The change though not very large over the entire range of frequency, cannot be neglected when treated with other components of loading. The observations so made are considered to be analogous to a guitar string which produces greater sound when tightened (under tensile loading) as compared to the dull sound it creates when relatively loose (under compressive loading).

When analyzing the **structural response** of a floating airport subjected to landing / taking off of an airplane, one notices that a number of large spectral responses are visible when the wave number is plotted against the increasing speed of the airplane. These large spectral responses are seen as local peaks emanating from the point of load application and represent the flexural wave propagating in the same direction as the convected loading due to the Doppler Effect with the local peak moving in a curvilinear path with increasing speed of the airplane. Defining the location of these peaks precisely a priori is however not feasible.

The **methodology** discussed herein provides the designer a simple tool for understanding the total sound power radiated from a floating structure subject to a moving load. Such a tool shall help in a better design of a VLFS for a safer marine environment.

References

Abu-Hilal, M. 2003 Forced vibration of Euler-Bernoulli beams by means of dynamic Green functions. *Journal of Sound and Vibration* **267**, 191–207.

Asanuma, K. and Wakui, H. 2012 Development of silent steel railway bridge equipped with floating ladder track and floating reinforced concrete deck. *Notes on Numerical Fluid Mechanics and Multidisciplinary Design* **118**, 211–219.

Au, F. T. K. and Wang, M. F. 2005 Sound radiation from forced vibration of rectangular orthotropic plates under moving loads. *Journal of Sound and Vibration* **281**, 1057–1075.

Bert, C. W., Wang, X. and Striz, A. G. 1994 Static and free vibrational analysis of beams and plates by differential quadrature method. *Acta Mechanica* **102**, 11–24.

Brazier-Smith, P. R. and Scott, J. F. 1984 Stability of fluid flow in the presence of a compliant surface. *Wave Motion* **6**, 547–560.

Bryan, G. H. 1891 On the Stability of a Plane Plate under Thrusts in its own Plane, with Applications to the "buckling" of the Sides of a Ship. *Proceedings of The London Mathematical Society* **s1-22**, 54–67.

Bulson, P. 1970 *The stability of flat plates*. London: Chatto and Windus.

Cebon, D. 1999 *Handbook of Vehicle Road Interaction*. Swets and Zeitlinger, London.

Cheng, C. C. 1999 Sound Radiation from Periodically spring-supported beams under the action of a convected uniform harmonic loading. *Journal of Sound and Vibration* **226**, 83–99.

Cheng, C. C., Kuo, C. P. and Yang, J. W. 2000 Wavenumber-Harmonic Analysis of a Periodically Supported Beam Under the Action of a Convected Loading. *Journal of Vibration and Acoustics* **122**.

Cheng, C. C., Kuo, C. P. and Yang, J. W. 2001 A note on the vibro-acoustic response of a periodically supported beam subjected to a travelling, time harmonic loading. *Journal of Sound and Vibration* **239**, 531–544.

Cray, B. A. 1994 Acoustic radiation from periodic and sectionally aperiodic rib-stiffened plates. *Journal of Acoustical Society of America* **95(1)**, 256–264.

Cremer, L., Heckl, M. and Ungar, E. E. 1988 *Structure-Borne Sound*. Springer Verlag, Berlin, 2^{nd} edition.

Crighton, D. G. 1972 Force and moment admittance of plates under arbitrary fluid loading. *Journal of Sound and Vibration* **20**, 209–218.

Crighton, D. G. 1977 Point admittance of an infinite thin elastic plate under fluid loading. *Journal of Sound and Vibration* **54**, 389–391.

Crighton, D. G. 1979 The free and forced waves on a fluid loaded elastic plate. *Journal of Sound and Vibration* **63**, 225–235.

Crighton, D. G. 1983 The Green function of an infinite, fluid loaded membrane. *Journal of Sound and Vibration* **86**, 411–433.

Crighton, D. G. and Innes, D. 1984 The Modes, Resonances and Forced Response of Elastic Structures under Heavy Fluid Loading. *Philosophical Transactions of the Royal Society of London. Series A, Mathematical and Physical Sciences* **312, No. 1521**, 295–341.

Crighton, D. G. and Oswell, J. E. 1991 Fluid loading with mean flow I, Response of an elastic plate to localized excitation. *Philos Trans. R . Soc. London A* **335**, 557–592.

Davys, J. W., Hosking, R. J. and Sneyd, A. D. 1985 Waves due to a steadily moving source on a floating ice plate. *Journal of Fluid Mechanics* **158**.

Dehestani, M., Mofid, M. and Vafai, A. 2009 Investigation of critical influential speed for moving mass problems on beams. *Applied Mathematical Modeling* **33**, 3885–3895.

Deng, X. and Sun, L. 2000 Dynamics of vehicle-pavement interaction. *Peoples Communication, Beijing* .

Endo, H. 2000 The behavior of a VLFS and an airplane during takeoff / landing run in wave condition. *Marine Structures* **13**, 477–491.

Endo, H. and Yago, K. 1999 Time-history response of a large floating structure subjected to a dynamic load (in Japanese). *Journal of The Society of Naval Architects of Japan* **186**, 369–376.

Esmailzadeh, E. and Ghorashi, M. 1994 Vibration analysis of Timoshenko beam subjected to a travelling mass. *American Society of Mechanical Engineers, Petroleum Division* pp. 64–233.

Esmailzadeh, E. and Jalili, N. 2003 Vehicle-passenger-structure interaction of uniform bridges traversed by moving vehicles. *Journal of Sound and Vibration* **260**, 611–635.

Fahy, F. and Gardonio, P. 2007 *Sound and Structural Vibration. Radiation, Transmission and Response*. Academic Press, Oxford, 2nd edition.

Fay, R. R. 1988 *Hearing in Vertebrates- A Psychophysics Databook*. Winnetka, Illinois-Hill-Fay Associates.

Feit, D. 1967 Pressure Radiated by a Point-Excited Elastic Plate. *Journal of The Acoustical Society of America* **40**, 1489–1494.

Fleischer, D. and Park, S. 2004 Plane hydroelastic beam vibrations due to uniformly moving one axle vehicle. *Journal of Sound and Vibration* **273** (3), 585 – 606.

Foda, M. A. and Abduljabbar, Z. 1994 A dynamic Green function formulation for the response of a beam structure to a moving mass. *Journal of Sound and Vibration* **210**, 295–306.

Frýba, L. 1999 *Vibration of Solids and Structures under Moving Loads*, , Vol. 59. Thomas Telford, London.

Gbadeyan, J. A. and Oni, S. T. 1994 Dynamic behavior of beams and rectangular plates under moving loads. *Journal of Sound and Vibration* **182**, 677–695.

Gutin, L. Y. 1965 Sound radiation from an infinite plate excited by a normal point force. *Sov. Phys. Acoust.* **10 (4)**, 369–371.

Hamada, R. 1981 Dynamic analysis of a beam under a moving force: A double Laplace transform solution. *Journal of Sound and Vibration* **74**, 221–233.

Heckl, M. 1985 Tire noise generation. *Seminar on Friction and Contact Noise* .

Henchi, K. and Fafard, M. 1997 Dynamic behavior of multi-span beams under moving loads. *Journal of Sound and Vibration* **199**, 33–50.

Holl, D. L. 1950 Dynamic loads on thin plates on elastic foundations. *Proceeding Symposium Applied Mathematics* **3**, 107–116.

Hosking, R. J. and Milinazzo, F. 2007 Floating ladder track response to a steadily moving load. *Mathematical Methods in The Applied Sciences* **30**, 1823–1841.

Hosking, R. J. and Milinazzo, F. 2012 Modelling the floating ladder track response to a moving load by an infinite Bernoulli-Euler beam on periodic flexible supports. *East Asian Journal on Applied Mathematics* **2(4)**, 285–308.

Ichikawa, M., Miyakawa, Y. and Matsuda, A. 2000 Vibration analysis of the continuous beam subjected to a moving mass. *Journal of Sound and Vibration* **230**, 493–506.

Jin, J. and Xing, J. 2007 Transient dynamic analysis of a floating beam water interaction system excited by the impact of a landing beam. *Journal of Sound and Vibration* **303(1-2)**, 371 – 390.

Ju, S., Lin, H.T.and Hsueh, H. and Wang, S. 2006 A simple finite element model for vibration analyses induced by moving vehicles. *Int. J. Numer. Methods Eng* **68**, 1232–1256.

Junger, M. C. and Feit, D. 1986 *Sound, Structures, and Their Interaction, 2nd edition*, , Vol. 82. MIT Press, Cambridge, MA.

Kargarnovin, M., Younesian, D., Thompson, D. and Jones, C. 2005 Response of beams on nonlinear viscoelastic foundations to harmonic moving loads. *Comput. Struct.* **83**, 1865–1877.

Kargarnovin, M. H. and Younesian, D. 2004 Dynamics of Timoshenko beams on Pasternak foundation under moving load. *Mech. Res. Commun* **31**, 713–723.

Kashiwagi, M. 2004 Transient responses of a VLFS during landing and take-off of an airplane. *Journal of Marine Science and Technology* **9**, 14–23.

Keltie, R. F. 1982 Analytical model of the truck tire vibration sound mechanism. *Journal of The Acoustical Society of America* **71(2)**, 359–367.

Keltie, R. F. and Peng, H. 1988 Sound radiation from beams under the action of moving line forces. *ASME Transactions Series E Journal of Applied Mechanics* **55**, 849–854.

Kidarsa, A., Scott, M. and Christopher, H. 2008 Analysis of moving loads using force-based finite elements. *Finite Elem. Anal. Des.* **44(4)**, 214–224.

Kim, B. S., Rhee, B. G. and Lee, T. K. 2006 An experimental study on sound radiation characteristics of radial tires for vehicles, due to excitation. *JSME International Journal* **49(C)**, 873–881.

Kim, C. W., Kawatani, M. and Kim, K. B. 2005 Three-dimensional dynamic analysis for bridge-vehicle interaction with roadway roughness. *Computer Structures* **83**, 1627–1645.

Kim, J. and Webster, W. 1998 The drag on an airplane taking off from a floating runway. *Journal of Marine Science and Technology* **3**, 76–81.

Kim, S. M. 2004 Vibration and stability of axial loaded beams on elastic foundation under moving harmonic loads. *Engineering Structures* **26**, 95–105.

Kropp, W. 2011 Sound radiation from a rolling tyre. *Proc. Svenska Mekanikdagar* .

Kropp, W., Sainiarz, P., Brick, H. and Beckenbaner, T. 2012 On the sound radiation of a rolling tyre. *Journal of Sound and Vibration* **33(8)**, 1789–1805.

Kyoung, J. H., Hong, S. Y. and Kim, B. W. 2006 FEM for time domain analysis of hydroelastic response of VLFS with fully nonlinear free-surface conditions. *International Journal of Offshore and Polar Engineering* **16(3)**, 168–174.

Ladich, F. and Popper, A. N. 2004 *In Evolution of the Vertebrate Auditory System*. Springer Handbook of Auditory Research.

Lee, D. H. and Choi, H. S. 2003 Transient hydroelastic response of Very Large Floating Structures by FE-BE Hybrid method. *Proceedings of the* 13^{th} *International Offshore and Polar Engineering Conference* pp. 100–105.

Lee, H. P. 1996 Dynamic response of a beam with a moving mass. *Journal of Sound and Vibration* **191**, 289–294.

Lee, H. P. 1998 Dynamic response of a Timoshenko beam on a Winkler foundation subjected to a moving mass. *Applied Acoustics* **55**, 203–215.

Lee, S. Y. and Yhim, S. S. 2004 Dynamic analysis of composite plates subjected to multi-moving loads based on a third order theory. *Int. J. Solids Struct* **41**, 4457–4472.

Li, Y., Qiang, S., Liao, H. and Xu, Y. 2005 Dynamics of wind rail vehicle bridge systems. *J. Wind Eng. Ind. Aerodyn* **93**, 483–507.

Liu, A. K. and Mollo-Christensen, E. 1988 Wave Propagation in a Solid Ice Pack. *Journal of Physical Oceanography* **18** (11), 1702–1712.

Liu-chao, Q. 2009 Modeling and simulation of transient responses of a flexible beam floating in finite depth water under moving loads. *Applied Mathematical Modelling* **33** (3), 1620 – 1632.

Liu-chao, Q. and Liu, H. 2007 Three-dimensional time-domain analysis of very large floating structures subjected to unsteady external loading. *Journal of Offshore Mechanics and Arctic Engineering* **129** (1), 21–28.

Livesley, R. 1953 Some notes on the mathematical theory of a loaded elastic plate resting on an elastic foundation. *Quarterly Journal Mech. Appl. Math* **6**, 32–44.

Maidanik, G. and Kerwin, Jr, E. M. 1966 Influence of Fluid Loading on the Radiation from Infinite Plates below the Critical Frequency. *Journal of The Acoustical Society of America* **40**, 1036–1038.

Manoach, E. 1993 Dynamic response of elastoplastic Mindlin plate by mode superposition method. *Journal of Sound and Vibration* **162**, 165–175.

Marchesiello, S., Fasana, A., Garibaldi, L. and Piombo, B. A. D. 1999 Dynamics of multi-span continuous straight bridges subjected to multi-degrees of freedom moving vehicle excitation. *Journal of Sound and Vibration* **224**, 541–561.

Mehri, B., Davar, A. and Rahmani, O. 2009 Dynamic green function solution of beams under a moving load with different boundary conditions. *Scientia Iranica* **16**, 273–279.

Michaltsos, G. T. 2002 Dynamic behavior of a single-span beam subjected to loads moving with variable speeds. *Journal of Sound and Vibration* **258**, 359–372.

Milinazzo, F., Shinbrot, M. and Evans, N. W. 1995 A mathematical analysis of the steady response of floating ice to the uniform motion of a rectangular load. *Journal of Fluid Mechanics* **287**, 173–197.

Mollo-Christensen, E. 1983*a* Edge waves as a cause of ice ride-up on shore. *Journal of Geophysical Research* **88**, 2967–2970.

Mollo-Christensen, E. 1983*b* Interactions Between Waves and Mean Drift in an Ice Pack. *Journal of Geophysical Research* **88**, 2971–2972.

Morley, L. S. D. 1962 Elastic plate with loads traveling at uniform velocity along the bounding surfaces. *Quart. J. Mech Appl. Math.* **15**, 194–213.

Morse, P. M. and Ingard, K. U. 1968 Theoretical Acoustics. *Princeton University Press* .

Nedwell, J. R., Edwards, B., Turnpenny, A. W. H. and Gordon, J. 2004 *Fish and marine mammal audiograms: A summary of available information.*, , Vol. Report 534. Subacoustech Ltd., Hamphire, UK.

Nowacki, W. 1963 *Dynamics of Elastic System*. John Wiley & Sons, Inc., New York,.

Ohmatsu, S. 1998 Numerical calculation of hydroelastic behavior of VLFS in time domain. *Proceedings of the* 2^{nd} *International Conference on Hydroelasticity in Marine Technology, Fukuoka* pp. 89–97.

Pierce, A. 1989 *Acoustics. Physical Principles and Applications*. Acoustical Society of America, New York, 2nd edition.

Piszczek, K. 1959 Possibility of dynamic stability loss under moving concentrated loads. *Arch. Mech. Stos.* **10**, 195–209.

Popper, A. N. 2003 Effects of anthropogenic sounds on fishes. *Fisheries* **28(10)**, 24–31.

Popper, A. N. 2008 Effects of Mid- and High-Frequency Sonars on Fish. *Tech. Rep.*. Naval Undersea Warfare Center Division, Newport, Rhode Island, Contract N66604-07M-6056.

Ranganath Nayak, P. 1970 Line Admittance of Infinite Isotropic Fluid-Loaded Plates. *Journal of The Acoustical Society of America* **47** (1B), 191–201.

Rayleigh, L. 1896 *The Theory of Sound (2 vols, second edition)*. MacMillan (reprinted 1945 by Dover).

Reismann, H. 1959 Dynamic response of elastic plates to moving loads. *Martin Company, Denver Colorado, Res. Report Number R-62-8* pp. 1–89.

Rossi, R. E., Gutierrez, R. H. and Laura, P. A. A. 2001 Forced vibrations of rectangular plates subjected to harmonic loading distributed over a rectangular subdomain. *Ocean Engineering* **28**, 1575–1584.

Schulkes, R. M. S. M., Hosking, R. J. and Sneyd, A. D. 1987 Waves due to a steadily moving source on a floating ice plate. part 2. *Journal of Fluid Mechanics* **180**, 297–318.

Schulkes, R. M. S. M. and Sneyd, A. D. 1988 Time-dependent response of floating ice to a steadily moving load. *Journal of Fluid Mechanics* **186**, 25–46.

Shadnam, M. R., Mofid, M. and Akin, J. E. 2001*a* On the dynamic response of rectangular plate with moving mass. *Thin-Walled Structures* **39**, 797–806.

Shadnam, M. R., Rofooei, F. R. and Mehri, B. 2001*b* Dynamics of nonlinear plates undermoving loads. *Mech. Res. Commun* **28**, 453–461.

Simsek, M. and Kocaturk, T. 2009 Nonlinear dynamic analysis of an eccentrically prestressed damped beam under a concentrated moving harmonic load. *J. Sound Vib.* **320**, 235–253.

Squire, V. A. 2007 Of ocean waves and sea-ice revisited. *Cold Regions Science and Technology* **49**, 110–133.

Sun, L. 1996 Experimental and theoretical analysis of dynamic vehicle loads and stochastic response of pavement systems under arbitrary moving loads. Ph.D. thesis, Southeast University, Nanjing, China.

Sun, L. 2001 Dynamic displacement response of beam-type structures to moving line loads. *Journal of Sound and Vibration* **38**, 8869–8878.

Sun, L. and Greenberg, B. 2000 Dynamic response of linear systems to moving stochastic sources. *Journal of Sound and Vibration* **229(4)**, 957–972.

Takabatake, H. 1998 Dynamic analysis of rectangular plates with stepped thickness subjected tomoving loads including additional mass. *Journal of Sound and Vibration* **213**, 829–842.

Timoshenko, S. P. and Gere, J. M. 2010 *Theory of Elastic Stability*. McGraw-Hill.

Ting, E. C., Genin, J. and Ginsberg, J. H. 1974 A general algorithm for moving mass problems. *Journal of Sound and Vibration* **33**, 49–58.

Ungar, E. E. 1988 *Noise and vibration control, Chapter 14*. Institute of Noise Control Engineering.

Visweswara Rao, G. 2000 Linear dynamics of an elastic beam under moving loads. *Journal of Vibration and Acoustics* **122**, 285–289.

Wang, K., Hosking, R. J. and Milinazzo, F. 2004 Time-dependent response of a floating viscoelastic plate to an impulsively started moving load. *Journal of Fluid Mechanics* **521**, 295–317.

Wang, R. 1998 Random vibration of multi-span Timoshenko beam due to a moving load. *Journal of Sound and Vibration* **213**, 127–138.

Watanabe, E. and Utsunomiya, T. 1996 Transient response analysis of a VLFS at airplane landing. *Proceedings of the* 2^{nd} *International Workshop on Very Large Floating Structures, Hayama* pp. 243–247.

Willis, R. ***et al.*** 1851 Preliminary Essay to the Appendix B: Experiments for Determining the Effects Produced by Causing Weights to Travel over Bars with Different Velocities. *In: GREY G. et al.: Report of the Commissioners Appointed to Inquire into the Application of Iron to Railway Structures. W. Clowes and So s London 1849. Reprinted in: BARLOW P.: Treatise on the Strength of Timber, Cast Iron and Malleable Iron. London (1851)* .

Wilson, G. P. 2004 Rail system noise and vibration control. *Proceedings of Acoustics* .

Wu, J. 2005 Dynamic analysis of an inclined beam due to moving loads. *J. Sound Vib.* **288**, 107–133.

Wu, J. J., Whittaker, A. R. and Cartmell, M. P. 2001 Dynamic responses of structures to moving bodies using combined finite element and analytical methods. *Int. Journal of Mechanical Sciences* **3**, 5–2579.

Wu, S. F. and Maestrello, L. 1995 Response of a finite baffled plate subject to turbulent and mean flow excitations. *AIAA* **33**, 12–19.

Wu, S. F. and Zhu, J. 1995 Sound radiation from two semi-infinite dissimilar plates subject to a harmonic line force excitation in mean flow. Part I. Theory. *Journal of The Acoustical Society of America* **97**, 2709–2723.

Yagiz, N. and Sakman, L. E. 2006 Vibrations of a rectangular bridge as an isotropic plate under a traveling full vehicle model. *Journal of Vibration Control* **12**, 83–98.

Yanmeni Wayou, A., Tchoukuegno, R. and Woafo, P. 2004 Nonlinear dynamics of an elastic beam under moving loads. *J. Sound Vib.* **273**, 1101–1108.

Yeung, R. W. and Kim, J. W. 1998 Structural drag and deformation of a moving load on a floating plate. *Proceedings of the 2nd International Conference on Hydroelasticity in Marine Technology, Fukuoka* pp. 77–88.

Yeung, R. W. and Kim, J. W. 2000 Effects of a translating load on a floating plate structural drag and plate deformations. *Journal of Fluids and Structures* **14**, 993–1011.

Yoshimura, T., Hino, J. and Anantharayana, N. 1986 Vibration analysis of a non-linear beam subjected to moving loads by using the galerkin method. *Journal of Sound and Vibration* **104**, 179–186.

Younesian, D., Kargarnovin, M., Thompson, D. and Jones, C. 2006 Parametrically excited vibration of a timoshenko beam on random viscoelastic foundation subjected to a harmonic moving load. *Nonlinear Dyn* **45**, 75–93.

Yuan, J., Zhu, Y. and Wu, M. 2009 Vibration characteristics and effectiveness of floating slab track system. *Journal of Computer* **4(12)**.

Yufeng, Q. and Qibai, H. 2009 Effect of the moving force on the radiated sound from rectangular plates with elastic support. *Adv. Studies Theor. Phys.* **3(9)**, 333–352.

Zhu, X. Q. and Law, S. S. 2000 Identification of vehicle axle loads from bridge dynamic responses. *Journal of Sound and Vibration* **236**, 705–724.

Zibdeh, H. S. and Juma, H. S. 1999 Dynamic response of a rotating beam subjected to a random moving load. *Journal of Sound and Vibration* **223**, 741–758.

Appendix A

Time Averages of Products

A.1 Introduction

When dealing with waves of constant frequency, one often makes use of averages over a wave period of the product of two quantities that oscillate with the same frequency. Before further discussion it is convenient to introduce the basic theory involved in the time averages of products.

A.2 Time Averages of Products

Let

$$p = Re(\hat{p}e^{-j\omega t}) \tag{A.1}$$

and

$$v = Re(\hat{v}e^{-j\omega t}) \tag{A.2}$$

be two such quantities. Then the time average of their product is

$$[p(t)v(t)]_{av} = |\hat{p}||\hat{v}|[cos(\omega t - \phi_p)cos(\omega t - \phi_t)]_{av} \tag{A.3}$$

where ϕ_p and ϕ_v are phases of $\hat{p}$ and $\hat{v}$ respectively. The trigonometric identity

$$cos(A)cos(B) = \frac{1}{2}[cos(A+B) + cos(A-B)] \tag{A.4}$$

with appropriate identifications for A and B, yields a term which averages out to zero and a term which is independent of time. Thus one has

$$[p(t)v(t)]_{av} = \frac{1}{2}|\hat{p}||\hat{v}|cos(\phi_p - \phi_v) \tag{A.5}$$

or, equivalently

$$[p(t)v(t)]_{av} = \frac{1}{2}|\hat{p}||\hat{v}|Re(e^{i(\phi_p - \phi_v)}) \tag{A.6}$$

which in turn can be written

$$[p(t)v(t)]_{av} = \frac{1}{2}Re(\hat{p}\hat{v}^*) \tag{A.7}$$

The asterisk here denotes the complex conjugate. Because the real part of a complex conjugate is the same as the real part of the original complex number, it is immaterial whether one takes the complex conjugate of $\hat{p}$ or $\hat{v}$, but one takes the complex conjugate of only one.

A.3 Time Averaged Sound Intensity

Surface sound intensity distribution is integrated over the surface of the structure to seek the sound power generated by the structure. By using the definition, of time averaged sound intensity as given by Morse and Ingard (1968), the time averaged surface sound intensity distribution, $\bar{I}(x)$ is given as

$$\bar{I} = \frac{1}{T}\int_0^T \overline{PV}dt \tag{A.8}$$

Using Equation (A.7) the time averaged surface sound intensity distribution is given as

$$\bar{I} = \frac{1}{2}Re[P\dot{U}^*(\xi, t)] \tag{A.9}$$

where P is the sound pressure on the beam / plate surface, $\dot{U}^*(\xi, t)$ is the beam / plate surface velocity of conjugation. Hence

$$\dot{U}(\xi, t) = \frac{dU(\xi)}{dt} = j(\omega + \xi V)U(\xi) \tag{A.10}$$

In order to find the total acoustic power (Π), the surface acoustic intensity distribution Equation (A.9) needs to be integrated over the infinite length of the beam /plate as

$$\Pi = \int_{-\infty}^{\infty} \frac{1}{2} Re[P(\xi, y = 0, t)\dot{U}^*(\xi, t)]d\xi \tag{A.11}$$

In this respect, sound power per unit width is calculated in the area of wave number to get

$$\Pi = \int_{-\infty}^{\infty} \frac{1}{4\pi} Re[P(\xi, y = 0, t)U^*(\xi, t)]d\xi \tag{A.12}$$

Upon substituting the reduced sound pressure equation i.e Equation (3.10) and calculating the surface velocity using Equation (A.10), the sound power radiated per unit width of the beam /plate is given as

$$\Pi = \frac{1}{4\pi} Re\left[\int_{-\infty}^{\infty} j\frac{\rho_0(\omega + \xi V)^2}{K_y} U(\xi) j(\omega + \xi V)U^*(\xi)d\xi\right] \tag{A.13}$$

This can be simplified as

$$\Pi = \frac{\rho_0}{4\pi} Re\left[\int_{-\infty}^{\infty} \frac{(\omega + \xi V)^3}{K_y} |U(\xi)|^2 d\xi\right] \tag{A.14}$$

Limiting the study to subsonic motion of the moving load, the limits within which K_y is real is given by

$$\xi_1 = \frac{-K_0}{1 + M} \leq \xi \leq \xi_2 = \frac{K_0}{1 - M} \tag{A.15}$$

This allows us to rewrite the expression for the sound power as

$$\mathbf{\Pi} = \frac{\boldsymbol{\rho_0}}{\mathbf{4\pi}} \mathbf{Re}\left[\int_{\boldsymbol{\xi_1}}^{\boldsymbol{\xi_2}} \frac{(\boldsymbol{\omega} + \boldsymbol{\xi}\mathbf{V})^{\mathbf{3}}}{\mathbf{K_y}} |\mathbf{U}(\boldsymbol{\xi})|^{\mathbf{2}} \mathbf{d}\boldsymbol{\xi}\right] \tag{A.16}$$

This completes the formulation of an expression for the total acoustic power for varying beam / plate types subjected to a moving load.

Appendix B

Nondimensionalization

B.1 Introduction

In engineering results obtained from the use of empirical results provide data which is often difficult to present in a readable form. Even from graphs it may be difficult to interpret this data. Dimensional analysis provides a strategy for choosing relevant data and how it should be presented. This is a useful technique in all experimentally based areas of engineering. If it is possible to identify the factors involved in a physical situation, dimensional analysis can form a relationship between them. The resulting expressions may not at first sight appear rigorous but these qualitative results converted to quantitative forms can be used to obtain any unknown factors from experimental analysis.

Nondimensionalization is the partial or full removal of units from an equation involving physical quantities by a suitable substitution of variables. This technique can simplify and parameterize problems where measured units are involved. It is closely related to dimensional analysis. In some physical systems, the term scaling is used interchangeably with nondimensionalization, in order to suggest that certain quantities are better measured relative to some appropriate unit. These units refer to quantities intrinsic to the system, rather than units such as SI units.

Nondimensionalization is not the same as converting extensive quantities in an equation to intensive quantities, since the latter procedure results in variables that still carry units. Nondimensionalization can also recover characteristic properties of a system. For example, if a system has an intrinsic resonance frequency, length, or time constant, nondimensionalization can recover these values. The technique is especially useful for systems

that can be described by differential equations. One important use is in the analysis of control systems. One of the simplest characteristic units is the doubling time of a system experiencing exponential growth, or conversely the half-life of a system experiencing exponential decay; a more natural pair of characteristic units is mean age/mean lifetime, which correspond to base "e" rather than base "2".

B.2 Nondimensionalization steps

To nondimensionalize a system of equations, one must do the following:

- Identify all the independent and dependent variables;
- Replace each of them with a quantity scaled relative to a characteristic unit of measure to be determined;
- Divide through by the coefficient of the highest order polynomial or derivative term;
- Choose judiciously the definition of the characteristic unit for each variable so that the coefficients of as many terms as possible become 1;
- Rewrite the system of equations in terms of their new dimensionless quantities.

The last three steps are usually specific to the problem where nondimensionalization is applied. However, almost all systems require the first two steps to be performed.

B.3 Nondimensionalization

The expression for the total acoustic power for varying beam types subjected to a moving load as obtained at Equation (A.16) is

$$\Pi = \frac{\rho_0}{4\pi} Re\left[\int_{\xi_1}^{\xi_2} \frac{(\omega + \xi V)^3}{K_y} |U(\xi)|^2 d\xi\right] \tag{B.1}$$

Rewriting Equation (B.1) explicitly we get

$$\Pi = \frac{\rho_0}{4\pi} Re\left[\int_{\xi_1}^{\xi_2} \frac{(\omega + \xi V)^3}{K_y} \left|\frac{Z_F F(\xi)}{Z_m + Z_F Z_a}\right|^2 d\xi\right] \tag{B.2}$$

To nondimensionalise we use the following nondimensional parameters

$$Wavenumber\ variable\ (\zeta) = \frac{Wavenumber\ variable\ (\xi)}{Acoustic\ wavenumber\ (K_0)} \tag{B.3}$$

$$Free\ bending\ wavenumber\ (K_B) = \left[\frac{12\rho_v\omega^2}{Eh^2}\right]^{\frac{1}{4}} \tag{B.4}$$

$$Wavenumber\ ratio\ (\gamma) = \frac{K_0}{K_B} \tag{B.5}$$

$$Longitudinal\ wave\ speed\ (C_L) = \sqrt{\frac{E}{\rho_v}} \tag{B.6}$$

$$Fluid\ loading\ parameter\ (\alpha_0) = \frac{\rho_0 C_L}{\sqrt{12}\ \rho_v C_0} \tag{B.7}$$

$$Power\ per\ unit\ width\ (W) = \frac{4\pi\omega(\rho_v h)^2}{\rho_0 f_0^2}\Pi \tag{B.8}$$

$$Displacement\ of\ plate\ (U_s(\zeta)) = \frac{E}{f_0 h}U_s(\xi) \tag{B.9}$$

$$Strength\ of\ external\ force\ (F(\zeta)) = \frac{F(\xi)}{f_0} \tag{B.10}$$

Hence using Equation (B.20) we get

$$d\xi = K_0 d\zeta$$

and $(\omega + \xi V)$ can we re-written as

$$\begin{aligned}(\omega + \xi V) &= (K_0 C_0 + K_0 \zeta M C_0) \\ &= K_0 C_0 (1 + M\zeta)\end{aligned}$$

Similarly K_y can be re-written as

$$\begin{aligned}K_y &= \sqrt{(K_0 + M\xi)^2 - \xi^2} \\ &= \sqrt{(K_0 + MK_0\zeta)^2 - (K_0\zeta)^2} \\ &= K_0\sqrt{(1 + M\zeta)^2 - \zeta^2}\end{aligned}$$

Introducing new nondimensionalised constants as $\alpha = (1 + M\zeta)$ and $\beta = \sqrt{\alpha^2 - \zeta^2}$ thus

$$K_y = K_0\beta \tag{B.11}$$

B.3.1 Parameter Z_F

The parameter Z_F is given by

$$Z_F = 1 + \frac{\bar{E}I}{\kappa^2 \bar{G}h}\xi^2 - \frac{\rho_v h^2}{12\kappa^2 \bar{G}}(\omega + \xi V)^2 \qquad \ldots \quad Timoshenko\,beam$$

$$Z_F = 1 \qquad \ldots \quad Rayleigh\,beam$$

$$Z_F = 1 + \frac{\bar{E}I}{\kappa^2 \bar{G}h}\xi^2 \qquad \ldots \quad Shear\,beam$$

$$Z_F = 1 \qquad \ldots \quad Euler - Bernoulli\,beam$$

The nondimensional parameter (Z_F) for Timoshenko beam is given by

$$\begin{aligned}
Z_F &= 1 + \frac{\bar{E}I}{\kappa^2 \bar{G}h}\xi^2 - \frac{\rho_v h^2}{12\kappa^2 \bar{G}}(\omega + \xi V)^2 \\
&= 1 + \frac{E(i+\eta j)2(1+\nu)I}{\kappa^2 E(1+\eta j)h}(K_0\zeta)^2 - \frac{\rho_v h^2 2(1+\nu)}{12\kappa^2 E(1+\eta j)}(\omega + \xi V)^2 \\
&= 1 + \frac{2(1+\nu)h^3}{12\kappa^2 h}(K_0\zeta)^2 - \frac{\rho_v h^2 2(1+\nu)}{12\kappa^2 E(1+\eta j)}\left[C_0(\frac{\omega}{C_0} + \frac{K_0}{C_0}\zeta V)\right]^2 \\
&= 1 + \frac{h^2 2(1+\nu)}{12\kappa^2}(K_0\zeta)^2 - \frac{h^2 2(1+\nu)}{12\kappa^2}\frac{\rho_v}{E(1+\eta j)}\left[C_0(K_0 + K_0\zeta M)\right]^2 \\
&= 1 + \frac{h^2 2(1+\nu)}{12\kappa^2}(K_0\zeta)^2 - \frac{h^2 2(1+\nu)}{12\kappa^2}\frac{1}{(1+\eta j)}\left(\frac{C_0}{C_L}\right)^2\left[K_0(1+\zeta M)\right]^2
\end{aligned}$$

Thus

$$Z_F = 1 + \frac{h^2(1+\nu)}{6\kappa^2}\left[(K_0\zeta)^2 - \frac{1}{(1+\eta j)}\left(\frac{C_0}{C_L}\right)^2(K_0\alpha)^2\right] \tag{B.12}$$

But

$$\begin{aligned}
\gamma^4 &= \left[\frac{K_0}{K_B}\right]^4 \\
&= K_0^4\frac{Eh^2}{12\rho_v\omega^2} = \frac{h^2}{12}(\frac{E}{\rho_v})(\frac{K_0^2}{\omega^2})K_0^2 \\
&= \frac{h^2}{12}C_L^2\frac{1}{C_0^2}K_0^2
\end{aligned}$$

Thus

$$\gamma^4 = \frac{h^2}{12}K_0^2\frac{C_L^2}{C_0^2} \tag{B.13}$$

Using Equation (B.19) in Equation (B.12) we get

$$Z_F = 1 + \frac{2(1+\nu)}{\kappa^2}\gamma^4(\frac{C_0}{C_L})^2\left[(\zeta)^2 - \frac{1}{(1+\eta j)}\left(\frac{C_0}{C_L}\right)^2(\alpha)^2\right]$$

B.3.2 The acoustic impedance operator(Z_a)

The acoustic impedance operator is dependent on the acoustic pressure and does not get effected by the change of the geometry / material being analysed. Hence for *Timoshenko beam*, *Rayleigh beam*, *Shear beam*, *Euler-Bernoulli beam* or *Timoshenko-Mindlin plate*, Z_a remains the same and is given by

$$Z_a = j\rho_0\frac{(\omega+\xi V)^2}{K_y}$$

and the nondimensional acoustic impedance operator is given by

$$Z_a = j\rho_0\frac{K_0^2C_0^2(1+M\zeta)^2}{K_0\sqrt{(1+M\zeta)^2-\zeta^2}} = j\rho_0\frac{K_0C_0^2(1+M\zeta)^2}{\sqrt{(1+M\zeta)^2-\zeta^2}} \tag{B.14}$$

Thus Equation (B.14) reduces to

$$\begin{aligned}
Z_a &= j\rho_0\frac{K_0C_0^2\alpha^2}{\beta} \\
&= j\frac{\rho_0h\omega^2}{\beta}\frac{K_0K_B^2C_0^2\alpha^2}{K_B^2h\omega^2} \\
&= j\frac{\rho_0h\omega^2}{\beta}\frac{K_0\alpha^2}{K_B^2h}\frac{K_B^2C_0^2}{K_0^2C_0^2} \\
&= j\frac{\rho_0h\omega^2}{\beta}\frac{\alpha^2}{\gamma^2}\frac{\sqrt{Eh^2}K_0}{\sqrt{12\rho_v\omega^2}h} \\
&= j\frac{\rho_0h\omega^2}{\beta}\frac{\alpha^2}{\gamma^2}\frac{1}{\sqrt{12}}\sqrt{\frac{E}{\rho_v}}\frac{1}{C_0} \\
&= j\frac{\rho_vh\omega^2}{\beta}\frac{\alpha^2}{\gamma^2}\frac{\rho_0}{\rho_v\sqrt{12}}\frac{C_L}{C_0} \\
&= j\rho_vh\omega^2\frac{\alpha_0\alpha^2}{\beta\gamma^2}
\end{aligned}$$

which can be rewritten as

$$Z_a = j\frac{\rho_vh\omega^2}{\beta}\frac{D_4}{Z_F} \tag{B.15}$$

B.3.3 The plate impedance operator(Z_m)

As discussed previously Z_m changes with the material and the geometry of the structure. For various structures discussed herein Z_m is given as

$$Z_m = \bar{E}I\xi^4 - \rho_v h(\omega+\xi V)^2 - \xi^2\rho_v I\left(1+\frac{\bar{E}}{\kappa^2\bar{G}}\right)(\omega+\xi V)^2 + \rho_v I\frac{\rho_v}{\kappa^2\bar{G}}(\omega+\xi V)^4$$

$$\ldots \quad Timoshenko\ beam$$

$$Z_m = \bar{E}I\xi^4 - \rho_v h(\omega+\xi V)^2 - \xi^2\rho_v I(\omega+\xi V)^2 \qquad \ldots \quad Rayleigh\ beam$$

$$Z_m = \bar{E}I\xi^4 - \rho_v h(\omega+\xi V)^2 - \xi^2\frac{\bar{E}I\rho_v}{\kappa^2\bar{G}}(\omega+\xi V)^2 \qquad \ldots \quad Shear\ beam$$

$$Z_m = \bar{E}I\xi^4 - \rho_v h(\omega+\xi V)^2 \qquad \ldots \quad Euler-Bernoulli\ beam$$

Nondimensionalising for Timoshenko beam gives

$$\begin{aligned}
Z_m &= E(1+\eta j)\frac{h^3}{12}(K_0\zeta)^4 - \rho_v h(K_0C_0\alpha)^2 \\
&\quad - (K_0\zeta)^2\rho_v\frac{h^3}{12}\left(1+\frac{E(1+\eta j)2(1+\nu)}{\kappa^2E(1+\eta j)}\right)(K_0C_0\alpha)^2 + \rho_v\frac{h^3}{12}\frac{2(1+\nu)\rho_v}{\kappa^2E(1+\eta j)}(\omega\alpha)^4 \\
&= E(1+\eta j)\frac{h^3}{12}K_B^4\left(\frac{K_0}{K_B}\right)^4\zeta^4 - \rho_v h(\omega\alpha)^2 - \rho_v\frac{h^3}{12}(K_0\zeta)^2\left(1+\frac{2(1+\nu)}{\kappa^2}\right)(\omega\alpha)^2 \\
&\quad + \rho_v\frac{h^3}{12}\frac{2(1+\nu)}{\kappa^2(1+\eta j)}\frac{\rho_v}{E}(\omega\alpha)^4 \\
&= E(1+\eta j)\frac{h^3}{12}\frac{12\rho_v\omega^2}{Eh^2}(\gamma)^4\zeta^4 - \rho_v h(\omega\alpha)^2 - \rho_v h\frac{\rho_v\omega^2}{EK_B^4}(K_0\zeta)^2\left(1+\frac{2(1+\nu)}{\kappa^2}\right)(\omega\alpha)^2 \\
&\quad + \rho_v h\frac{\rho_v\omega^2}{EK_B^4}\frac{2(1+\nu)}{\kappa^2(1+\eta j)}\frac{1}{C_L^2}(\omega\alpha)^4 \\
&= \rho_v h\omega^2\left[(1+\eta j)\gamma^4\zeta^4 - \alpha^2\left(1+\frac{K_0^4}{K_B^4}\frac{C_0^2}{C_L^2}\zeta^2\left[1+\frac{2(1+\nu)}{\kappa^2}\right]\right)\right. \\
&\quad \left. + (\frac{K_0}{K_B})^4\frac{2(1+\nu)}{\kappa^2(1+\eta j)}\frac{1}{C_L^4}(C_0\alpha)^4\right] \\
&= \rho_v h\omega^2\left[\underbrace{(1+\eta j)\gamma^4\zeta^4}_{D_1} - \underbrace{\alpha^2\left(1+\gamma^4(\frac{C_0}{C_L})^2\zeta^2\left[1+\frac{2(1+\nu)}{\kappa^2}\right]\right)}_{D_2} + \underbrace{\gamma^4\frac{2(1+\nu)}{\kappa^2(1+\eta j)}(\frac{C_0}{C_L})^4\alpha^4}_{D_3}\right]
\end{aligned}$$

$$Z_m = \rho_v h\omega^2(D_1 - D_2 + D_3) \tag{B.16}$$

where the expression for D_1, D_2, D_3, D_4 and Z_F vary based on the type of the beam as under

(a) *Timoshenko beam*:

$$Z_F = 1 + \frac{2(1+\nu)\gamma^4}{\kappa^2}\left(\frac{C_0}{C_L}\right)^2\left[\zeta^2 - \frac{1}{1+\eta j}\left(\frac{C_0}{C_L}\right)^2\alpha^2\right]$$

$$D_1 = \gamma^4\zeta^4(1+\eta j)$$

$$D_2 = \alpha^2\left[1 + [1 + \frac{2(1+\nu)}{\kappa^2}]\gamma^4\zeta^2\left(\frac{C_0}{C_L}\right)^2\right]$$

$$D_3 = \frac{2(1+\nu)}{\kappa^2(1+\eta j)}\alpha^4\gamma^4\left(\frac{C_0}{C_L}\right)^4$$

$$D_4 = Z_F\frac{\alpha_0\alpha^2}{\gamma^2}$$

(b) *Rayleigh beam*:

$$Z_F = 1$$

$$D_1 = \gamma^4\zeta^4(1+\eta j)$$

$$D_2 = \alpha^2\left[1 + \gamma^4\zeta^2\left(\frac{C_0}{C_L}\right)^2\right]$$

$$D_3 = 0$$

$$D_4 = Z_F\frac{\alpha_0\alpha^2}{\gamma^2}$$

(c) *Shear beam*:

$$Z_F = 1 + \frac{2(1+\nu)\gamma^4}{\kappa^2}\left(\frac{C_0}{C_L}\right)^2\zeta^2$$

$$D_1 = \gamma^4\zeta^4(1+\eta j)$$

$$D_2 = \alpha^2\left[1 + \frac{2(1+\nu)}{\kappa^2}\gamma^4\zeta^2\left(\frac{C_0}{C_L}\right)^2\right]$$

$$D_3 = 0$$

$$D_4 = Z_F\frac{\alpha_0\alpha^2}{\gamma^2}$$

(d) *Euler-Bernoulli beam*:

$$Z_F = 1$$

$$D_1 = \gamma^4\zeta^4(1+\eta j)$$

$$D_2 = \alpha^2$$

$$D_3 = 0$$

$$D_4 = Z_F \frac{\alpha_0 \alpha^2}{\gamma^2}$$

B.3.4 The Force Parameter

If f_0 is the strength of external force per unit width, $H(x)$ the Heavyside step function, and $\delta(x - Vt)$ a Delta function, the moving force may be expressed as a **uniform distributed line force** by

$$f(x,t) = \frac{f_0}{2L}[H(x - Vt + L) - H(x - Vt - L)]e^{j\omega t}$$

which after taking a spatial transformation gives the force as

$$\begin{aligned} \tilde{f}(\xi,t) &= f_0 \frac{sin(\xi L)}{\xi L} e^{j(\omega + \xi V)t} \\ &= F(\xi) e^{j(\omega + \xi V)t} \end{aligned}$$

On nondimensionalising we get

$$F(\zeta) = \frac{sin(K_0 \zeta L)}{K_0 \zeta L} \tag{B.17}$$

If the force is expressed as a **point force** then

$$f(x,t) = f_0 e^{j\omega t} \delta(x - Vt)$$

and the nondimensionalised force is given as

$$F(\zeta) = 1 \tag{B.18}$$

B.3.5 Power per unit length

Knowing the nondimensionalised expressions for $F(\xi)$, Z_F, Z_m and Z_a, we begin simplifying Equation (B.2). Hence

$$\begin{aligned} Z_m + Z_F Z_a &= \rho_v h\omega^2(D_1 - D_2 + D_3) + Z_F j\frac{\rho_v h\omega^2}{\beta}\frac{D_4}{Z_F} \\ &= \rho_v h\omega^2\left[D_1 - D_2 + D_3 + \frac{jD_4}{\beta}\right] \\ &= \frac{\rho_v h\omega^2}{\beta}\left[\beta(D_1 - D_2 + D_3) + jD_4\right] \end{aligned}$$

Hence

$$Z_m + Z_F Z_a = \frac{\rho_v h\omega^2}{\beta} D \tag{B.19}$$

Using Equations (B.8) and (B.2) gives

$$\begin{aligned} W &= \frac{4\pi\omega(\rho_v h)^2}{\rho_0 f_0^2}\frac{\rho_0}{4\pi} Re\left[\int_{\xi_1}^{\xi_2} \frac{(\omega + \xi V)^3}{K_y}\left|\frac{Z_F F(\xi)}{Z_m + Z_F Z_a}\right|^2 d\xi\right] \\ &= \frac{\omega(\rho_v h)^2}{f_0^2} Re\left[\int_{\xi_1}^{\xi_2} \frac{(\omega + \xi V)^3}{K_y}\left|\frac{Z_F F(\xi)}{Z_m + Z_F Z_a}\right|^2 d\xi\right] \end{aligned}$$

Substituting from Equations (B.19) and (B.11), we get

$$\begin{aligned} W &= \frac{\omega(\rho_v h)^2}{f_0^2} Re\left[\int_{\zeta_1}^{\zeta_2} \frac{(K_0 C_0 + K_0\zeta M C_0)^3}{K_0\beta}\left|Z_F F(\xi)\right|^2\left|\frac{1}{Z_m + Z_F Z_a}\right|^2 K_0 d\zeta\right] \\ &= \frac{\omega(\rho_v h)^2}{f_0^2} Re\left[\int_{\zeta_1}^{\zeta_2} \omega^3\frac{\alpha^3}{\beta}\left|Z_F F(\xi)\right|^2\left|\frac{\beta}{\rho_v h\omega^2 D}\right|^2 d\zeta\right] \\ &= \frac{1}{f_0^2} Re\left[\int_{\zeta_1}^{\zeta_2} \alpha^3\beta\left|Z_F F(\xi)\right|^2\left|\frac{1}{D}\right|^2 d\zeta\right] \end{aligned}$$

For a uniformly distributed line force the dimensionless radiated sound can be expressed as

$$\mathbf{W} = \int_{\boldsymbol{\zeta_1}}^{\boldsymbol{\zeta_2}} \boldsymbol{\alpha^3\beta}\left|\mathbf{Z_F}\frac{\mathbf{sin}(\boldsymbol{\zeta}\mathbf{K_0 L})}{\boldsymbol{\zeta}\mathbf{K_0 L}}\right|^{\mathbf{2}} |\mathbf{D}|^{\mathbf{-2}}\mathbf{d}\boldsymbol{\zeta} \tag{B.20}$$

where

$$D = \beta(D_1 - D_2 + D_3) + jD_4$$

Author's Resume

Commander Nitin Agarwala is a qualified Naval Architect from the Cochin University of Science and Technology, Department of Ship Technology, XV^{th} batch. He was commissioned in the Indian Navy in 1993. He has done his diploma in Naval Construction from Indian Institute of Technology Delhi followed by a Post Graduation in Naval Architecture and Ocean Engineering from Indian Institute of Technology, Kharagpur. The Officer has served onboard naval ships, the Fabrication Departments of both the Naval Dockyards in various capacities and in the staff of the Headquarters Western Naval Command (Mumbai). He has been part of the faculty to the Department of Ship Technology, Cochin University of Science and Technology between 2007 and 2011. He is presently the Officer-in-charge of the Hull Inspection and Trials Unit at Vishakhapatnam.